

Development of a wet screw compressor model operating with NH₃-H₂O-CO₂

by

Dionne Agnes Willemien Gruijthuijsen

in partial fulfillment of the requirements for the degree of

Master of Science

in Mechanical Engineering

at the Delft University of Technology, to be defended publicly on Monday May 13, 2019 at 13:30.

Supervisors: Dr. ir. C.A. Infante Ferreira

Ir. V. Gudjonsdottir

Thesis committee: Prof. dr. ir. T.J.H. Vlugt

Dr. R. Delfos

An electronic version of this thesis is available at http://repository.tudelft.nl/.



SUMMARY

Energy consumption is still growing worldwide and due to the problems of global warming, sustainable developments become of more importance. Heat pumps are one of the technologies that can contribute to energy savings of industrial processes, for example by heat recovery from waste water streams. The focus of this research is to improve the performance of these heat pump systems.

The compression-resorption heat pump (CRHP) can be distinguished from a traditional vapor-compression heat pump (VCHP) by operating with non-azeotropic mixtures and an incomplete evaporation in the desorber. The working fluid enters the compressor as a two-phase mixture. This type of compression is known as wet compression. Several advantages of CRHPs compared to VCHPs have been reported due to the utilization of the temperature glide of the working fluid along the heat exchangers. A new mixture, NH_3 - H_2O - CO_2 , has been proposed in order to increase the performance of CRHPs even more. However, these advantages are based on the assumption that the wet compression process can reach isentropic efficiencies of at least 70 %. The aim of this research is to investigate the performance of NH_3 - H_2O - CO_2 during a wet compression process, and compare it with the performance when ammonia water is used. If the addition of CO_2 has disadvantageous effects on the compressor performance, the benefits of this new mixture in a CRHP system may disappear.

A wet compressor model operating with ammonia water has been developed in Matlab. This model can be adapted in order to operate with NH_3 - H_2O - CO_2 by modifying the thermodynamic part of the model. Several thermodynamic property models have been developed for NH_3 - H_2O - CO_2 and are implemented in the commercial software Aspen Plus. However, these property models are not available as Matlab executable functions. In order to implement the properties of NH_3 - H_2O - CO_2 in the Matlab model, tables containing the thermodynamic properties are generated from Aspen and interpolation is used to obtain the properties in between the tabulated values.

Before the model was extended for NH_3 - H_2O - CO_2 , the current model contained convergence problems for certain input conditions. Several modeling errors are solved, which made the model faster and more stable.

The model indicates improvements on the isentropic efficiency with NH₃-H₂O-CO₂ compared to ammonia water up to 3.5 % for vapor qualities higher than 0.45. During this comparison the pressure ratio, vapor quality and ammonia concentration are the same for both mixtures. For lower vapor qualities (q < 0.45), the isentropic efficiencies for NH₃-H₂O-CO₂ increase very rapidly. A vapor quality of 0.20 results in an isentropic efficiency of 94.56 % (14 % higher than for ammonia water), which is not expected to be correct. The problem seems to be related to the entropy calculations of the thermodynamic model in Aspen. The indicated power is used instead as a performance indicator, since the other output parameters of the model are comparable for both mixtures. It is observed that the indicated power for

iv Summary

 NH_3 - H_2O - CO_2 decreases compared to ammonia water operating at the same conditions. To compare the isentropic efficiencies of both mixtures the model with NH_3 - H_2O - CO_2 should be limited to higher vapor qualities.

The compressor model is used in the performance calculations of a CRHP cycle for several applications. First a CRHP cycle is considered with a heating and cooling requirement. Ammonia water in a CRHP is able to compete with the performances of many working fluids in a VCHP cycle for the same application. However, some working fluids, as DME isopentane, perform slightly better. NH_3 - H_2O - CO_2 performs worse than ammonia water because the temperature glide in the desorber does not fit well to the heat source. To omit this disadvantage, two applications are considered that only contain a heating requirement. When the isentropic efficiency is the same assumed value for both mixtures, and no compressor model is used, the COP for NH_3 - H_2O - CO_2 with 5 wt% CO_2 addition is around 1% higher than the COP of ammonia water. When the compressor model is included in the calculations, the COP increases with 4.1 %, due to a higher determined isentropic efficiency of the compressor. The produced heat in the resorber increases almost with 10 % for 5 wt% CO_2 addition.

In conclusion, the compressor model indicates improvements on the isentropic efficiency operating with NH_3 - H_2O - CO_2 compared to ammonia water within the model limitations. It depends on the type of applications whether NH_3 - H_2O - CO_2 is beneficial for the COP of the CRHP cycle. For heating applications, NH_3 - H_2O - CO_2 shows significant improvements in the COP compared to ammonia water, partly by higher expected isentropic efficiencies and larger amounts of produced heat in the resorber. Experimental validation of the compressor model is the next important step at this point. An experimental setup is built, however, some technical problems with the compressor caused a delay of performing these experiments. Especially at low vapor qualities the model with NH_3 - H_2O - CO_2 gives unexpected values and the model needs to be modified to what happens in reality.

ACKNOWLEDGMENTS

First of all I would like to thank my supervisor Dr. ir. C.A. Infante Ferreira and my daily supervisor Ir. V. Gudjonsdottir. Your guidance has been of great value to my thesis. Thank you Carlos, for your critical opinions and suggestions. I really appreciated your patience for my desire to wait for the experimental setup to be fixed. Thank you Vilborg, for being always available for questions and for thinking along with difficult problems that had to be encountered. It was really nice working with you and it is very unfortunate that we were not able to work on the experiments together. However, I am happy that the both of you supported me with redefining my thesis, such that I was still able to finish with a nice project.

Furthermore, I would like to thank the additional members of the exam committee, Prof. dr. ir. T.J.H. Vlugt and Dr. R. Delfos for putting effort in evaluating my work.

I would like to conclude with looking back on the past 7 years in Delft. I had the best of times during my studies at the TU Delft and the complete experience that comes with this. Delft will always feel like coming home. I got to meet many people that have become friends for life. I want to thank them all, for always being there and for all the fun moments we had. Furthermore, I will never forget the days and nights of spending time in TU Delft library, that finally brought me at this point of graduation. The support of my mother Lilian was indispensable during the past seven years. I am forever grateful to her. Thank you Pjotr, for the unforgettable moments during my final year in Delft and to your great support during some stressful moments of my thesis.

D.A.W Gruijthuijsen Delft, April 2019

NOMENCLATURE

Roman Symbols

A	Leakage area	$[m^2]$
a	Activity	[-]
C	Empirical factor in compressor power	[-]
C_p	Heat capacity	$[Jkg^{-1}K^{-1}]$
f	(partial) Fugacity	[Pa]
f^*	Pure component fugacity	[Pa]
G	Gibbs free energy	$[\mathcal{J}]$
Н	Enthalpy	[J]
h	Specific enthalpy	$[Jkg^{-1}]$
I	Current	[A]
l	Sealing line	[m]
m	Mass	[kg]
ṁ	Mass flow	$[kgs^{-1}]$
n	Rotation speed	[rpm]
P	Pressure	[Pa]
Ċ	Heat transfer rate	[W]
q	Vapor quality	[-]
S	Spline function	[-]
S	Entropy	$[JK^{-1}]$
S	Specific entropy	$[Jkg^{-1}K^{-1}]$
T	Temperature	[K]
U	Uncertainty	[-]
и	Flow velocity	$[ms^{-1}]$

viii Nomenclature

V	Voltage	[V]
V	Volume	$[m^3]$
υ	Specific volume	$[m^3kg^{-1}]$
\dot{W}	power	[W]
x	Concentration in mixture composition	$[molmol^{-1}]$
x	Liquid mole fraction	$[molmol^{-1}]$
y	Vapor mole fraction	$[molmol^{-1}]$
z_1	Number of lobes male rotor	[-]
Greek	Symbols	
γ	Activity coefficient	[-]
δ	Clearance height	[m]
ζ	Empirical flow coefficient	[-]
η	Efficiency	[-]
μ	Chemical potential	$[Jkg^{-1}]$
ρ	Density	$[kgm^{-3}]$
ϕ	Fugacity coefficient	[-]
ϕ	Rotation angle male rotor	[°]
ω	Angular speed male rotor	$[s^{-1}]$
Subsc	ripts	
avg	Average	
C	Cooling	
dis	Discharge	
down	Downstream pressure	
end	End value in the property table	
H	Heating	
high	High pressure level in CRHP	
i	Number of component in mixture	
in	Inlet	

NOMENCLATURE ix

ind Indicated

is Isentropic

low Low pressure level in CRHP

mech Mechanical

in Total mass flow

 \dot{m}_L Liquid mass flow

 \dot{m}_V Vapour mass flow

out Outlet

pinch Pinch point temperature

prop Property

real Real

sink Heat sink

source Heat source

start Start value in the property table

suc Suction

th Theoretical

tot Total

up Upstream pressure

vol Volume

Superscripts

0 Reference state

aq Aqueous

L Liquid

V Vapor

Abbreviations

COP Coefficient of performance

CRHP Compression-resorption heat pump

e-NRTL Electrolyte non-random two-liquid

NOMENCLATURE

EOS Equation of sate

HEX Heat exchanger

ILs Ionic liquids

MEX Matlab executable function

PC-SAFT Perturbed chain statistical associating fluid theory

PR Peng-Robinson equation of state

RK Redlich-Kwong equation of state

SLE Solid-liquid equilibrium

UNIQUAC Universal quasi-chemical

VBA Visual basic for applications

VCHP Vapor-compression heat pump

VLE Vapor-liquid equilibrium

CONTENTS

No	omen	nclature	vii
1		Heat pump systems	1 1 2 3 4 5
2	The	eoretical background	7
	2.1	Previous studies on compression-resorption heat pumps and wet compres-	
	2.2	sion	7 9 12 13
	2.3	2.2.2 Thermodynamic models of NH ₃ -H ₂ O-CO ₂	15 17
		2.3.1 Property calculations by a Matlab routine	17
		2.3.2 Linking Matlab to Aspen	18
		2.3.3 Fitting the properties to temperature and pressure	18
		2.3.4 Tables and interpolation methods	19
		2.3.5 Conclusion	20
3	The	eoretical model of wet compression	21
	3.1	The compressor model	22
		3.1.1 Geometry model	22
		3.1.2 Thermodynamic model	25
		3.1.3 Structure and implementation of the compressor model	26
		3.1.4 Sensitivity analysis of the compressor model	28
	3.2	The compressor model operating with $NH_3-H_2O-CO_2$	32
		3.2.1 Table layout and refinement	33
		3.2.2 Table generator	34
		3.2.3 Spline interpolation method	35 37
4	The	e compressor performance operating with NH ₃ -H ₂ O-CO ₂	41
4	4.1	Effect of pressure ratio	41
		Effect of vapor quality	42 44
	4.4	4.2.1 Model limitations	44
	4.3	Effect of CO ₂ concentration	53
	4.4	Conclusion	55
		,	55

xii Contents

5	The heat pump cycle performance 5.1 Performances of the compression-resorption heat pump cycle 5.2 Heating applications: Upgrading waste water streams with a CRHP	57 58 71
6	Experimental setup and preparations 6.1 Experimental Setup	83 83 85 86
7	Conclusions and Recommendations 7.1 Conclusions	89 89
A	Appendix	93
В	Appendix	95
C	Appendix	99
Bi	i <mark>bliography</mark> Bibliography	103 105

1

INTRODUCTION

Nowadays, the need for sustainable developments and energy supply have worldwide attention. Mankind consumes more and more energy and, still, the large part of that energy is utilized by fossil fuel combustion. The extensive consumption of fossil energy sources causes large emissions of greenhouse gases, especially CO_2 , that contribute greatly to global warming. The last few years have seen great developments of renewable energy systems, mainly based on solar and wind energy. Heat pump systems can contribute as well to saving of fossil energy sources. However, the integration of heat pump systems in industry is not yet widely applied. One of the main reasons for the limited usages of heat pump systems is the long payback periods [9]. The increase in energy costs and growing limitations on CO_2 emission, make heat pump systems become of more interest for industry. One way to make heat pumps more attractive and reduce the payback time is to improve the performances of heat pump systems.

1.1. HEAT PUMP SYSTEMS

A heat pump is a device that is able to transfer heat from a low temperature level to a high temperature level by using a thermodynamic cycle. The conventional heat pump system consists of four components: a compressor, condenser, evaporator and an expansion valve. The working fluid is transported in a closed cycle through these four components, where it absorbs heat in the evaporator from a heat source and releases heat in the condenser to a heat sink. The compressor serves as a pump to transport the working fluid around and compresses the fluid in order to increase the pressure and temperature. To accomplish this external work to the compressor is necessary. The traditional heat pump is also known as a vapor-compression heat pump (VCHP). A typical temperature-enthalpy diagram of such a heat pump cycle can be seen in Figure 1.1. In the condenser and the evaporator (from $2a \rightarrow 3$ and $4 \rightarrow 1$) the temperature of the working fluid stays constant during the phase transition.

The principle of a compression-resorption heat pump (CRHP) is exactly the same, however this type of heat pump has a resorber and desorber instead of a condenser and evaporator. The reason behind this difference is that the working fluid of a CRHP is a mixture instead of a pure fluid. In the case of a binary mixture, the two fluids have different boiling points and when the heat is absorbed or released in the desorber and resorber, the composition of the

2 1. Introduction

liquid and gas phases of the fluid changes. Thus, the resorber and desorber have still the same function as the condenser and evaporator but as it works with a mixture the phase transitions in the resorber and desorber are non-isothermal. Figure 1.1 shows on the right side the temperature-enthalpy diagram of a CRHP, where this temperature glide is clearly visible (from $2 \rightarrow 3$ and $4 \rightarrow 1$).

From this diagram it can be observed, as well, that the working fluid in the CRHP cycle is mainly operating in the two-phase regime, including during the compression process (from $1 \rightarrow 2$). Conventional compressors operate with the working fluid being in the gaseous phase. In this research a prototype compressor is considered that is able to operate within the two-phase regime. This type of compression is known as wet compression and is explained in further detail in the next chapter.

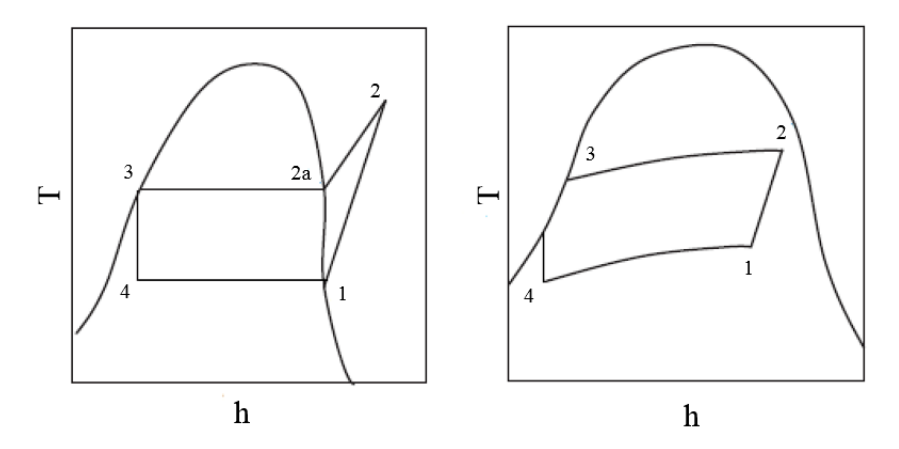


Figure 1.1: Typical temperature-enthalpy diagram for a VCHP (left) and a CRHP (right) [26].

1.2. HEAT PUMPS IN THE INDUSTRIAL FIELD

Heat pumps have been the topic for a large amount of applications in the industrial field. It has been observed that heat pumps can have a significant efficiency effect on the energetic performance of processes in industry [26]. Van de Bor and Infante Ferreira [26] considered two examples where a heat pump can be applied to a distillation column. A distillation column is characterized by very high energy requirements and can generate half of the operating cost of an industrial plant [27]. Distillation columns require a large heat input in the boiler and release a similar amount of heat in the condenser to the surrounding. By integrating heat pumps in distillation columns useful process heat can be recovered which reduces the use of primary energy and energy cost savings are obtained.

Within this research, the application of using a CRHP system in the recovery of low grade waste streams is considered. Many industrial plants contain separation processes, leaving waste water streams with temperatures around 45-60 °C [25]. These streams are no longer useful, because the temperatures are too high to be able to use it as cooling water but too low for the usage as heating water. Such a waste stream can be combined with a heat pump cycle, one part of the waste stream can be heated to temperatures above 100 °C and the other part is cooled down to temperatures below 20 °C. Therefore, the waste stream can be reused for the purpose of heating and/or cooling.

The attention of high temperature heat pumps for industrial processes is increasing as well [1]. Large application potentials have been recognized for heat sink temperatures of at least 80-90 °C. Especially CRHP are able to maintain high performances for large temperature glides in the heat sink or source.

In Figure 1.2 a schematic representation of the four components of the heat pump cycle can be seen, using a waste stream as the cold and hot utility. The waste stream is thereby divided into two separate streams. In the resorber the waste stream is absorbing heat from the working fluid of the heat pump, since the working fluid has a high pressure and temperature after the compression. In the desorber the waste stream is transferring heat to the working fluid and thus the waste stream is cooling down.

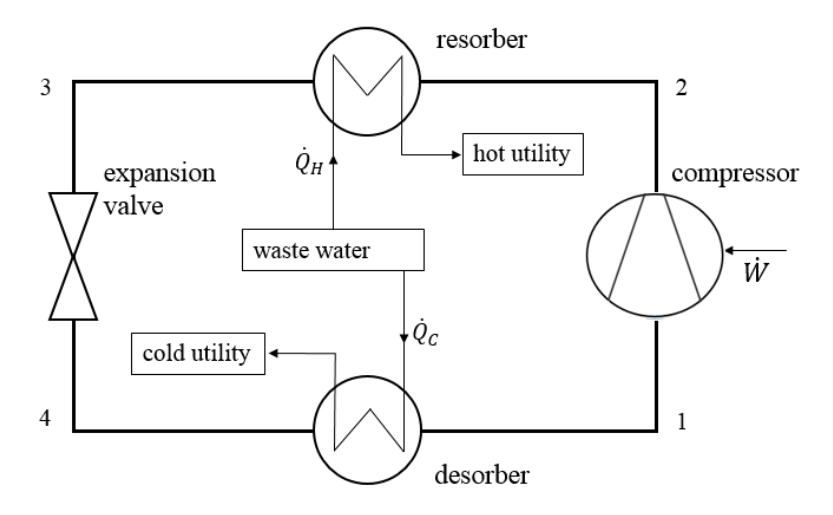


Figure 1.2: Heat recovery from a waste water stream using a heat pump cycle.

1.3. THESIS SCOPE AND OBJECTIVES

As mentioned earlier the large payback time of heat pump systems is still a major draw-back. One solution to make heat pumps more attractive for the industry is to improve the performance of heat pump systems, which is the focus of this study. A measure for the performance of a heat pump system is expressed as the ratio of heat delivered by the heat pump to the power required to deliver that heat [17], also known as the coefficient of performance (COP):

$$COP = \frac{\dot{Q}_H}{\dot{W}} \tag{1.1}$$

When a heat pump system achieves a COP of 3.5, it means that with one unit of consumed energy by the compressor 3.5 units of heat can be provided by the resorber. Thus by making the heat pump more efficient, the heat pump can deliver a larger amount of heat with the same amount of external work input. Typical values of the COP of operating heat pumps are in the range 3-4, which depends on many factors including the type of heat pump and the temperature difference between the hot and cold utilities. However, the temperature range wherein the heat pump needs to operate is limited by a particular application.

4 1. Introduction

The working fluid of the heat pump has influence on the COP of the system as well. CRHPs often operate with the binary mixture ammonia water as a working fluid [26]. Earlier studies have indicated that adding CO_2 to ammonia water may lead to positive effects on the performance when applied to compression-resorption cycles [22]. V. Gudjonsdottir et al. [9] investigated the impact of adding CO_2 to an ammonia water mixture in a CRHP. For the application, where a waste stream is heated from 60 to 105 ° C, a COP increase up to 5 % can be obtained with the addition of CO_2 . However, these values have been reached by assuming an isentropic efficiency for the compressor of 70 %. The isentropic efficiency of the compressor has a significant influence on the COP of a heat pump cycle. In this research a wet compression process is considered, which still contains many challenges. If an efficiency of at least 70 % is not reached there might be no advantage of using wet compression in a CRHP cycle compared to a traditional VCHP cycle [8].

In conclusion the overall goal of this project is to increase the performance of a CRHP cycle by investigating the benefits of a wet compression process with NH_3 - H_2O - CO_2 compared to an ammonia water working fluid. The aim is to reach an efficiency of the compressor of at least 70 % to make the wet CRHP cycle competitive with the VCHP cycle. In order to reach this goal, a wet compression model is developed to predict the performance of the compressor operating with NH_3 - H_2O - CO_2 for different operation conditions. A compressor model operating with ammonia water is already available. The following sub goals can be distinguished:

- Implement the thermodynamic property model of NH₃-H₂O-CO₂ into the current wet compressor model operating with ammonia water.
- Investigate the performance of the compressor operating with NH₃-H₂O-CO₂ with the compressor model for different operation conditions and compare the results with the compressor performance operating with ammonia water.
- Extend the results of the compressor model to the performance calculations of the heat pump cycle operating with NH₃-H₂O-CO₂ for several applications and compare the results with a heat pump cycle operating with ammonia water.
- Prepare an experimental setup for validation of the compressor model operating with ammonia water and NH₃-H₂O-CO₂.

1.4. APPROACH

The approach during this research is to start with a literature study. During this study the theoretical background needed for this topic is provided and previous research is being reviewed. In order to predict the performance of a compressor operating with NH_3 - H_2O - CO_2 , a model is developed in Matlab [16]. A wet compressor model operating with ammonia water has already been proposed [10]. This compressor model can be adapted to operate with NH_3 - H_2O - CO_2 .

1.5. REPORT OUTLINE 5

The solid base of such a process simulation is represented by the physical properties of the mixture. $NH_3-H_2O-CO_2$ has not previously been proposed and a Matlab compatible library containing these physical properties is not yet available. During the literature study several possibilities will be investigated for the implementation of the thermodynamic properties of $NH_3-H_2O-CO_2$.

The next step will be to implement the thermodynamic model of NH_3 - H_2O - CO_2 into the current compressor model. The model allows investigations of different operation conditions and the wet compression process with both mixtures can be compared. At last, this analysis should be extended to the prediction of the performance of the complete heat pump cycle. This is done by considering several industrial applications. The performances of the CRHPs are again compared for both mixtures. In previous studies on this topic, the isentropic efficiency was an assumed value during the heat pump cycle calculations. With the available compressor model the isentropic efficiency and indicated power can be determined for the specific working fluid and taken into account in the heat pump cycle calculation.

Originally, it was planned to validate the compressor model operating with ammonia water and NH₃-H₂O-CO₂ experimentally with a new compressor prototype, built for the purposes of this research. Due to many problems with the compressor these experiments are not yet carried out. However, several preparations have been done already in order to make this possible in the near future.

Finally, conclusions and recommendations are made on the performances of the wet compression process with NH_3 - H_2O - CO_2 determined by the model and the influence of these results on several heat pump applications.

1.5. REPORT OUTLINE

In the next chapter the literature review is presented. The chapter concludes on the most suitable method of implementing the thermodynamic property model of NH_3 - H_2O - CO_2 into the compressor model. Chapter 3 describes the current wet compressor model in more detail and presents the implementation of the modified thermodynamic model for the NH_3 - H_2O - CO_2 mixture. In Chapter 4 the results of the compressor model with NH_3 - H_2O - CO_2 are presented and compared with the results of the compressor operating with ammonia water. The effect of pressure ratio, vapor quality and addition of CO_2 are investigated in more extend. Chapter 5 shows the performance of the CRHP operating with both mixtures for several applications. In these heat pump cycle calculations the compressor model is included to determine the isentropic efficiency. The preparations of the experimental setup are outlined in Chapter 6. The report finishes with chapter 7, containing the conclusions and recommendations for further research and development steps.

THEORETICAL BACKGROUND

This chapter starts with a review on several studies that have been done on the topics of CRHPs and compression under wet conditions. Previous developed compressor models are combined in the development of the wet compression model used in this study and are shortly discussed. The section that follows, introduces different thermodynamic property models of the NH_3 - H_2O - CO_2 mixture. A short review is given about the thermodynamics of mixtures in general, in order to understand the way these models are developed. The final part of this chapter describes the possibilities for the implementation of the thermodynamic property model of the NH_3 - H_2O - CO_2 mixture in the wet compression model.

2.1. PREVIOUS STUDIES ON COMPRESSION-RESORPTION HEAT PUMPS AND WET COMPRESSION

In the introduction, Figure 1.1, the temperature-enthalpy diagram of a CRHP cycle showed that the working fluid during the compression process is located in the two-phase regime. However, conventional compressors operate with working fluids being in the gaseous state, also known as dry compression. Considering a CRHP cycle, the following alternatives are possible [12]. When the CRHP cycle is operating with a conventional compressor, a separator is placed after the desorber to separate the liquid from the vapor. The vapor part of the working fluid goes through a compressor and the liquid part is guided through a pump. This solution is called a recirculation cycle or Osenbrück cycle, visualized in Figure 2.1(a), and contains a dry compression process. The separate streams are combined again in the resorber. In the other case, the two-phase mixture is conveyed to the compressor without separation, Figure 2.1(b). The working fluid enters the compressor partly as a vapor and partly as a liquid and this cycle is referred to as a total wet compression cycle. An intermediate case exists that separates the liquid from the vapor, part of the liquid is pumped to the resorber and part of the liquid is injected into the compressor [30].

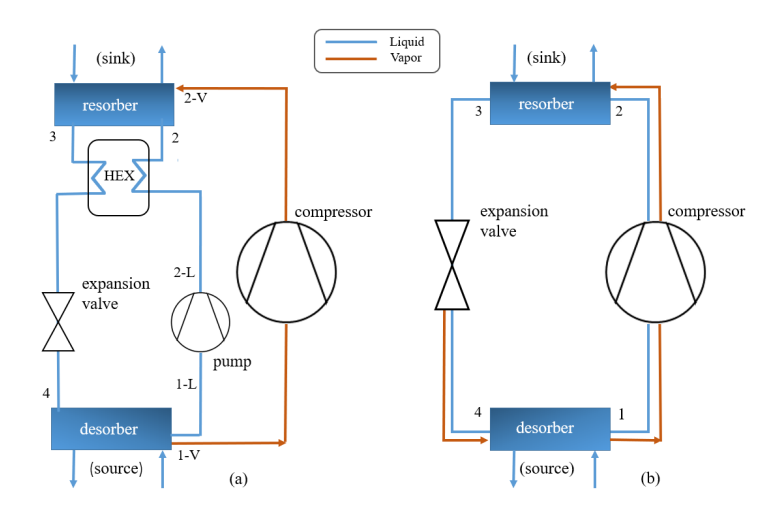


Figure 2.1: (a) CRHP with a recirculation cycle, (b) CRHP with a total wet compression cycle.

Itard [12] has studied under which conditions wet compression is effectively attractive and in which cases it is not. This was done by comparing the COPs of different dry and wet compression cycles with different working fluids, pure refrigerants and mixtures. First the cycles are considered to be ideal, i.e. isentropic expansion and isentropic compression. Second, the influence of irreversibilities are taken into account. It is concluded that the use of total wet compression is considered to be advantageous in particular for the use of mixtures, for pure refrigerants it has only few or no advantages. Considering non-azeotropic mixtures (e.g. ammonia water), an ideal version of a total wet compression cycle always leads to higher COP values than the recirculation cycle. When irreversibilities are considered, this advantage could be eliminated if ideal wet compression cannot reasonably be approached in the compressor or the isentropic efficiency is too low. In the case of a recirculation compression cycle, an extra internal heat exchanger, a pump and a separator are needed. All these components contain extra irreveribilities as well, which lowers the COP. In this current research, a CRHP with a total wet compression cycle is considered.

Previous studies investigated the potential of CRHP cycles over the conventional vapor-compression cycles and showed significant improvements on the performances of the heat pump cycles ([27], [26], [13]). CRHPs operate with non-azeotropic mixtures and the evaporation and condensation at a constant pressure is non-isothermal. Due to utilization of non-isothermal phase change processes the temperature profile of the working fluid fits better to the temperature profile of the heat source and sink, and improves the COP of the cycle [13]. Especially for industrial heating processes with large temperature glides the CRHPs allow energy performance gains of more than 20 % compared to VCHPs ([25],[9],[26]).

The application of low grade waste heat recovery was studied by van de Bor et al. [25]. The goal was to identify the potential of heat pumps and low temperature engines to reduce energy used in industry. The imposed application was the recovery of waste heat from spent cooling water, which is upgraded to heat or electricity. Different types of heat pumps, including CRHPs, are compared. The study focused on temperature levels of waste water around 45-60 °C, since large amounts of waste streams are rejected to the surroundings at these conditions. During the comparison of the heat pumps, the efficiency of the compres-

sor is assumed to be 70 %. With this assumption, van de Bor et al. concluded that CRHPs operating with ammonia water exhibit the best performance in the application of heating waste water streams from 60 °C to temperatures above 100 °C compared to the other alternatives.

van de Bor et al. [25] studied the influence of wet and dry compression on the performance of CRHPs as well. This research showed that for most cases the COP improves when moving from a dry to a wet compression system. Several disadvantages of the dry compression solution are indicated. In the case of dry compression temperatures at the compressor outlet can reach very high values, this can cause lubrication problems and result in high irreversibility losses. An additional problem is that some evaporated lubricant can be transported to the heat exchangers and can accumulate on the surfaces of the heat exchangers, which lowers the heat transfer. Both problems degrade the overall performance of the cycle. Compressors operating under wet conditions avoid superheating since the working fluid is in the two-phase regime.

van de Bor and Infante Ferreira [27] reported about the optimal performances of CRHP systems operating with ammonia water as working fluid. The performances of these heat pumps have been investigated numerically for 50 specific industrial cases. From the simulation it has been concluded that for optimal performance of the cycle, the vapor quality at the inlet for the resorber should be 100 % for all cases. The optimal ammonia concentration is depending on the temperature glide in the resorber and desorber and is for most cases in the range of 0-0.20 and 0.95-1 (mole/mole). Finally it is recommended to investigate the ability of compressors to operate in the wet regime. The results were based on an assumed isentropic efficiency of the compressor of 70 %. Still, limited results are available about wet compression and if these values actually can be reached.

In many of the studies about CRHPs, the advantages in the performance of the CRHP cycle are based on the assumption that the compressor is able to reach an isentropic efficiency of 70%. Still, a total wet compression cycle includes a complicated two-phase compression process and the development of such compressors is difficult. Wet compressor models have been developed to better understand the process and investigate the efficiencies that can be reached under wet compression conditions. Eventually, experiments are needed to validate these models.

2.1.1. WET COMPRESSION MODELS

Zaytsev [30] has performed experimental studies on wet compression-absorption cycles operating with ammonia water. For the specific requirements of wet compression cycles, Zaytsev discussed different compressor types and concluded that the screw compressor type is the most suitable type to handle liquid. This conclusion is based on the fact that screw compressors do not have thin blades or contain any valves that can be damaged by the liquid.

The screw compressor under wet compression conditions can be implemented in two ways: with and without liquid injection of the working fluid. In the case of liquid injection, part of the liquid is separated after the compressor and returned to the compressor at the suc-

tion or intermediate stages during the compression process. Due to the liquid injection the concentration of ammonia changes since the concentration of the injected liquid is often not the same as the concentration of the main flow. Before the liquid is injected into the compressor, it needs to be cooled. Otherwise, the injected liquid flashes when flowing through the injection valve. The additional vapor during the compression process requires additional power. In a heat pump cycle, the heat sink or source can be used to cool down the liquid injection. However, it requires extra heat exchangers in the heat pump cycle. The other possibility is to do the compression process without any liquid injection. The liquid is not separated after the desorber or after the compressor. The mixture enters the compressor in a two-phase state and is then directly compressed. The additional heat exchangers are for this case not necessary.

Several theoretical compressor models operating under wet compression conditions, with and without liquid injection, have been developed. A short overview of this type of models follows. During this research a compressor without liquid injection is considered, however, some elements of the models with liquid injection are used in the development of the compressor model that is used during this study.

WET COMPRESSOR MODELS WITH LIQUID INJECTION

Zaytsev and Infante Ferreira developed ([30],[31]) a twin screw compressor model operating under wet compression conditions for application in CRHPs. In this model an ammonia water mixture is used as the working fluid and it includes a liquid injection during the compression process. The model is divided roughly into two parts. The thermodynamic part is based on mass and energy conservation laws for a chosen control volume of the compressor. The derived conservation equations provide for the pressure, temperature and concentration of the mixture during the compression process. The second part is based on the geometry of the compressor. Therefore, Zaytsev analyzed the geometry of the compressor and the model requires accurate details regarding this geometry [31].

To validate the model, Zaytsev modified an existing twin screw compressor in order to satisfy the requirements of wet compression conditions. This compressor was implemented in a heat pump cycle and experimental data was collected. However, this first compressor prototype resulted in very low isentropic efficiencies. The liquid refrigerant that was injected into the suction cavity evaporated and reduced the volume of displaced vapor significantly. Zaytsev recommends that the liquid in the suction line should be separated and injected into the compressor cavities after they are disconnected from the suction port, i.e. at the start of the compression [30]. An additional reason for the low efficiency was due to over-dimensioned working clearances.

Infante Ferreira et al. [11] investigated a twin screw oil-free wet compressor for compression-absorption cycle with ammonia water as working fluid. The screw compressor model that was developed, is used to investigate the location of the liquid intake, injection angle and mass flow rate of the liquid on the performance of the compressor. In conclusion, the liquid injection location shows a significant effect on the performance of the compressor by the model and the experiments. The ideal location of the injection is at the start phase of the compression rather than at the suction, as Zaytsev recommended it[30]. The experiments show an increase in the isentropic efficiency from 10 to 35 % by changing the injection port location.

Chamoun et al. [3] modelled a twin screw compressor for high temperature heat pump applications using water as working fluid. In this model the geometry is simplified by analogy of the control volume in a screw compressor with a piston compressor. Based on a finite volume method, the compression zone is divided into N equal parts as function of the angular position of the male rotor. The governing equations are solved in each control volume in order to obtain the thermodynamic properties. This model describes the compression process in a more general way than the model of Zaytsev ([30],[31]), due to the fact that the model is less dependent on the exact geometry of the compressor.

Tian et al. [24] performed as well a numerical investigation on mass and heat transfer in an ammonia oil-free twin screw compressor with liquid injection. Tian proposed a heterogeneous thermodynamic model to study the phase transition of the wet compression process. The model was validated by using experimental data using a two-stage compression ammonia refining system. The isentropic efficiencies of the two compressors from the experiments were 75 % and 64 % respectively.

Tang [21] described the theory and the derived equations for computer aided design techniques of screw refrigeration compressors. Tang developed the volume curve of a twin screw compressor as a function of the rotation angle of the male rotor. Furthermore, Tang developed the theoretical shapes of the suction port and discharge port as a functions of the rotation angle of the male rotor. During this research Tang identified 6 leakage paths for a twin screw compressor and investigated where and how those leakages are occurring during the compression process.

WET COMPRESSOR MODELS WITHOUT LIQUID INJECTION

Gudjonsdottir et al. [8] developed a compressor model for a twin screw compressor operating with ammonia water without liquid injection. This model is developed for the purpose of theoretically predicting the performance of a new twin screw compressor prototype that is specifically designed for wet compression.

The compressor model is based on the proposed compressor model of Zaytsev ([30] [31]) consisting again of a geometry part and a thermodynamic part. The geometry part of Zaytsev's model is used, but adapted with the new compressor prototype in mind. The exact geometry of the new compressor prototype was not yet available during the development of the model, therefore, some geometrical characteristics of Zaytsev's compressor are still used in this model.

For the new compressor prototype liquid injection is no longer considered, as it was in the case of the compressor used by Zaytsev. Therefore, the concentration of ammonia does not change during the compression. For this reason the thermodynamic model had to be modified. In the mass and energy conservation equations the ammonia concentration is now taken as a constant value.

The working fluid enters the compressor as a two-phase fluid. The ideal vapor quality for the working fluid to enter the compressor is critical. Ideally, the outlet vapor quality is saturated vapor. However, when the working fluid goes into the superheated region the temperature rises quickly. This must be avoided, since the thermal expansion will damage the compressor. With a very low vapor quality, i.e. an excessive amount of liquid, the compressor can be damaged as well.

In the new compressor prototype the rotors are kept apart by timing gears. Therefore, no losses caused by friction need to be taken into account by the model. Finally, no labyrinth seal, a seal that lies between the discharge and suction side of the compressor, is present in the new prototype in contrast to Zaytsev's. The reason to remove this, was that the labyrinth seal caused additional leakages.

Due to the long computational time of the wet compressor model by Gudjonsdottir et al. [8], a new thesis research about wet compression modelling has been proposed. Guðmundsdóttir [10] has developed a wet compressor model, with an ammonia water mixture as working fluid, for the purpose of predicting the performance of the new compressor prototype in a quicker and more efficient way. The aim of this new model was mostly to improve the computational speed, and still preserve an accurate compressor model. During this research the work of Tian et al. [24], Tang [21], Chamoun et al. [3] and Zaytsev [30] have been studied in more detail and several aspects of their work is used in the present compressor model. The geometrical part is much more simplified. The main reason is that the model is being developed without access to the detailed geometry of the new compressor prototype. Accurate details regarding the geometry of the compressor is, therefore, left out in the model. The simpler solving strategy from Chamoun et al., by dividing the compressor zone in small sections, evaluating them separately and then adding them all together, is used to compute the governing equations derived by Zaytsev [30],[31]. Tang [21] describes a general method of approaching the geometry of a screw compressor and is used for this model. The volume, leakages, and port areas in Zaytsev's and Tang's compressor models seem to be comparable and related to the different sizes of the compressors they used in their studies [10]. Finally, the geometries of Zaytsev and Tang are used to scale the geometry close to the size of the new compressor prototype.

2.2. WET COMPRESSION WITH NH₃-H₂O-CO₂

In order to predict the performance of wet compression with NH_3 - H_2O - CO_2 , a model in Matlab [16] is developed. In the previous section it became clear that several wet compression models operating with ammonia water have already been developed. For the wet compressor prototype, which is being built for this study, two models have been developed operating with an ammonia water working fluid ([8], [10]). The model developed by Guðmundsdóttir [10] is used as a basis for this study and modified to operate with NH_3 - H_2O - CO_2 .

The geometric part of the model is not affected by the change of the mixture, as it is the same twin screw compressor that will be used. However, the thermodynamic properties of the new mixture are different and, therefore, the thermodynamic calculations in the model must be adapted.

The mixture ammonia water is widely used and there are many international databases for the ammonia water thermodynamic properties. The accuracy of these databases are widely accepted and validated by international researches including the property database REFPROP [14]. Rattner and Garimella [19] developed a fast and stable routine that approximates the thermodynamic properties for ammonia water mixtures in a Matlab compatible

library. The thermodynamic property routines developed in this study adopt the empirical EOS formulation of Ziegler and Trepp [32]. These developed routines achieve significant reductions in property evaluation times compared to existing property implementations in programs such as REFPROP.

With these available property routines, the thermodynamic properties of ammonia water can be directly implemented into a Matlab model. The compressor model operating with ammonia water, developed by Guðmundsdóttir [10], is using the Matlab routines of Rattner and Garimella due to the low computational time.

However, for the NH_3 - H_2O - CO_2 system, such a Matlab compatible library is not available yet. Proper calculations of the NH_3 - H_2O - CO_2 properties is a prerequisite for a wet compression simulation operating with this mixture. The NH_3 - H_2O - CO_2 system has been described in thermodynamic models ([4],[9],[18],[23]) and can be used for the purposes of this study.

2.2.1. THERMODYNAMICS OF MIXTURES ([17],[20])

Thermodynamic models are used to predict the chemical and physical equilibria for pure fluids or mixtures. In this study a mixture of three components is considered, which during the compression process will appear as a two-phase mixture. It is assumed that the liquid and vapor phases are in equilibrium during the compression. For a system to be in thermodynamic equilibrium the following must hold for phase I and phase II:

$$P^{\mathrm{I}} = P^{\mathrm{II}} \tag{2.1}$$

$$T^{\rm I} = T^{\rm II} \tag{2.2}$$

$$\mu_i^{\rm I} = \mu_i^{\rm II} \tag{2.3}$$

Where the P and T stand for pressure and temperature, which are both macroscopic properties and can be easily handled in the calculations. However, the chemical potential, μ , can not be expressed as an absolute quantity and always needs a reference state, μ^0 . In case of a mixture this equilibrium condition must hold for all components i. Thus, the more components present in the mixture, the more equilibrium conditions need to be solved and the more complicated the model becomes. Due to difficulty of relating chemical potential to better understandable physical properties (e.g. pressure), two other properties are used to describe chemical equilibria: namely the fugacity, f, and the activity, a. Equation 2.3 is then replaced by one of the following:

$$f_i^{\mathrm{I}} = f_i^{\mathrm{II}} \tag{2.4}$$

$$a_i^{\rm I} = a_i^{\rm II} \tag{2.5}$$

Again, these equilibrium conditions must hold for each component i in the mixture. Both properties account for the deviation of ideal behavior of chemical substances in a mixture. For a real gas mixture, the partial fugacity of component i is defined as the partial pressure of that component multiplied by a dimensionless partial fugacity coefficient, ϕ_i .

$$f_i = \phi_i \cdot P_i \tag{2.6}$$

For an ideal gas mixture, the partial fugacity and partial pressure are the same, such that the fugacity coefficient, ϕ_i , is one. The partial pressure is the total pressure, P, times the vapor mole fraction of the component, γ_i .

$$P_i = \gamma_i \cdot P \tag{2.7}$$

Dalton's law expresses that the sum of the partial pressures of the components in the ideal gas mixture are equal to the total pressure of the mixture. The partial fugacity of component i is described with the vapor mole fraction and the fugacity of pure vapor component i, f_i^* . This is known as the Lewis and Randall rule.

$$f_i = y_i \cdot f_i^* \tag{2.8}$$

The partial fugacity of component i in an ideal liquid mixture, is equal to the vapor fugacity of the pure component, f_i^* , multiplied by its mole fraction in the mixture. The vapor mole fraction in Eq. 2.8 is replaced by the liquid mole fraction, x_i , and is known as Raoult's law. In a dilute mixture, there is a difference in behavior of the solvent (the component with the larger mole fraction) and the solute component. The solvent is often described with Raoult's law and the solute obeys a different law, namely Henry's law. This law states that the mole fraction of the solute is proportional with the partial pressure of that component.

The thermodynamic activity is closely related to the fugacity and is determined by dividing the fugacity through a reference state fugacity, f_i^0 , at the same pressure. The reference state fugacity is often the pure component fugacity, f_i^* .

$$a_i = \frac{f_i}{f_i^0} \tag{2.9}$$

For gases, the activity is simply the fugacity divided by a reference pressure, the standard state, and is normally chosen to be 1 atmosphere or 1 bar. The activity is, therefore, mostly used to describe the liquid phase in mixtures. The activity can be defined again with a dimensionless quantity, the activity coefficient, γ . This coefficient accounts for the deviations from ideal behavior, just like the fugacity coefficient. For a non-ideal liquid mixture, the activity for component i is the liquid mole fraction, x_i , multiplied by the activity coefficient:

$$a_i = x_i \cdot \gamma_i \tag{2.10}$$

To build a thermodynamic model the chemical equilibrium processes need to be described, such as the vapor-liquid equilibrium (VLE). In liquid solutions, H_2O , CO_2 and NH_3 undergo partial dissociation and speciation which involve chemical equilibria and need to be described. Likewise, the precipitation of solids is described by the solid-liquid equilibrium (SLE). The enthalpy, heat of solution and the heat capacity are often described by the thermodynamic models as well.

For vapor-liquid equilibrium, Equation 2.4 can be written for component i, as follows:

$$y_i \phi_i^V P = a_i \cdot f_i^0 \tag{2.11}$$

The left hand side is describing the vapor phase of component i, where the partial fugacity coefficient is used. The left side is obtained by substituting Equation 2.7 into Equation 2.6.

The liquid phase is described by the activity on the right hand side of the equation. The right side is obtained with Equation 2.9. Then Equation 2.10 is substituted into the right hand side of Equation 2.11.

$$y_i \phi_i^V P = x_i \gamma_i f_i^0 \tag{2.12}$$

Where the reference state fugacity, f_i^0 , can be the fugacity of pure liquid component i, using Raoult's law. The solvent H_2O in NH_3 - H_2O - CO_2 mixture is often described by this law. For dilute components in the mixture, the reference state would be Henry's law constant, which is the case for NH_3 and CO_2 . Instead of using the chemical potentials of equation 2.3 the pressure, fugacity coefficients and activity coefficient can be used to compute chemical equilibrium.

For determining the vapor phase fugacities, an equation of state (EOS) is typically involved in these thermodynamic models. The simplest one is the ideal gas law, which describes the behavior of an ideal gas. Many EOS are available, for the existing thermodynamic models of the NH₃-H₂O-CO₂ system: Peng-Robinson (PR), Redlich-Kwong (RK) or PC-SAFT are EOS that have often been used.

The liquid phase activity coefficients are determined by the so called activity coefficient models, where again many model have been proposed. In prior studies for the $NH_3-H_2O-CO_2$ system, the activity coefficient models that are used, can be grouped into three categories for: (1) Pitzer model, (2) e-NRTL model and (3) extended UNIQUAC model [18].

2.2.2. THERMODYNAMIC MODELS OF $NH_3-H_2O-CO_2$

The important equilibria of the NH_3 - H_2O - CO_2 mixture are presented in Figure 2.2. An extensive amount of experimental data is available for the NH_3 - H_2O - CO_2 system. This data can be compiled and regressed in order to obtain the parameters in the EOS and in the activity coefficient models, to develop a thermodynamic property model for this system. Different thermodynamic models for the NH_3 - H_2O - CO_2 system have been developed and will be shortly reviewed.

$CO_{2}^{aq} \leftrightarrow CO_{2}^{V} \qquad NH_{3}^{aq} + H_{2}O \leftrightarrow NH_{4}^{+} + OH^{-} \qquad NH_{4}^{+} + HCO_{3}^{-} \leftrightarrow NH_{4}HCO_{3}^{S} \\ H_{2}O^{L} \leftrightarrow H_{2}O^{V} \qquad H_{2}O^{L} \leftrightarrow H_{2}O^{O} \leftrightarrow H_{2}COONH_{4}^{S} \\ HCO_{3}^{-} \leftrightarrow H^{+} + CO_{3}^{2-} \qquad 2NH_{4}^{+} + CO_{3}^{2-} + H_{2}O \leftrightarrow NH_{3}^{aq} \leftrightarrow NH_{3}^{V} \qquad H_{2}O^{L} \leftrightarrow OH^{-} + H^{+} \qquad (NH_{4})_{2}CO_{3} \cdot H_{2}O^{S}$	Vapor-liquid equilibria (VLE):	Speciation equilibria:	Solid-liquid equilibria (SLE):
$H_2O^L \leftrightarrow H_2O^V$ $HCO_3^- \leftrightarrow H^+ + CO_3^{2-}$ $2NH_4^+ + CO_3^{2-} + H_2O \leftrightarrow H_2O^S$	$CO_2^{aq} \leftrightarrow CO_2^{V}$	$NH_3^{aq} + H_2O \leftrightarrow NH_4^+ + OH^-$	$N{H_4}^+ + HCO_3^- \leftrightarrow N{H_4}HCO_3^S$
$HCO_3^- \leftrightarrow H^+ + CO_3^{2-}$ $2NH_4^+ + CO_3^{2-} + H_2O \leftrightarrow CO_3^+ + CO_3^- + H_2O^S$	$H_{-}O^{L} \leftrightarrow H_{-}O^{V}$	$H_2O^L + CO_2^{aq} \leftrightarrow HCO_3^- + H^+$	$NH_4^+ + NH_2COO^- \leftrightarrow NH_2COONH_4^S$
$NH_{3}^{aq} \leftrightarrow NH_{3}^{V}$ $H_{2}O^{L} \leftrightarrow OH^{-} + H^{+}$ $(NH_{4})_{2}CO_{3} \cdot H_{2}O^{3}$	1120 V 1120	$HCO_3^- \leftrightarrow H^+ + CO_3^{2-}$	
2	$\mathit{NH_3}^{aq} \leftrightarrow \mathit{NH_3}^{V}$	$H_2O^L \leftrightarrow OH^- + H^+$	$(NH_4)_2CO_3 \cdot H_2O^3$
$NH_3^{aq} + HCO_3^- \leftrightarrow H_2O^L$ $4NH_4^+ + CO_3^{2-} + 2HCO_3^- \leftrightarrow H_2COO^ (NH_4)_2CO_3 \cdot 2NH_4HCO_3^S$		3 3 2	

Figure 2.2: The NH₃-H₂O-CO₂ system.

The extended UNIQUAC model, developed by Thomsen and Rasmussen [23], takes all the chemical equilibria presented in Figure 2.2 into account. The activity coefficients for the liquid phase are described by the extended UNIQUAC activity coefficient model and for the vapor phase calculations the Soave-Redlich-Kwong EOS is used. Darde et al. [5] upgraded this model by increasing the number of experimental data points and extending the validity of the model for a higher temperature range.

Several thermodynamic models based on the e-NRTL activity coefficient model have been proposed as well. The commercial Aspen Plus software [2] includes a data package of the NH_3 - H_2O - CO_2 system using the e-NRTL method and the Redlich-Kwong EOS for the vapor phase. Darde et al. [4] compared a modified version of the e-NRTL model with the upgraded extended UNIQUAC model (both implemented in the Aspen plus software) and showed that in general, the extended UNIQUAC model appears to describe the experimental data more satisfactorily.

A further modified e-NRTL model has been proposed by Que and Chen [18], using the PC-SAFT EOS for the vapor phase calculations and using more experimental data for the regression of the model parameters. The model developed by Que and Chen is reported to be accurate for a wide range of pressures, temperatures and concentrations. For SLE at temperatures above 50 °C and high ammonia concentrations the model showed less satisfactory results. For ammonia concentrations up to 30 wt% and $\rm CO_2$ concentrations up to unity the model enables reliable results. The modified model of Que and Chen is available in the Aspen Plus package and widely used by researchers. One big drawback of the e-NRTL model is that from the SLE, only the formation of ammonium bicarbonate (NH₄HCO₃) is taken into account. However, the risk of other solid formations is present. For the application in the CRHP, all solid formation is undesirable since it can cause blockages.

Recently Gudjonsdottir et al. [9] made a comparison between the several e-NRTL models and the extented UNIQUAC model. In order to improve the model proposed by Que and Chen, a new fit based on their model has been developed as well. During the fitting procedure, the binary interaction parameters (in the activity coefficient model) of Chen and Que were used as initial values and refitted to additional experimental data. It should, therefore, provide better results for higher ammonia concentrations and it partly improves the problems with the SLE.

In conclusion, the model proposed by Que and Chen and the new fit are compatible with the extended UNIQUAC model [9]. As mentioned earlier, the model proposed by Que and Chen [18] is available in the Aspen Plus package. The new fit can be easily implemented in Aspen by changing the interaction parameters of Que and Chen to the values reported by Gudjonsdottir et al. [9]. This new fit can provide for the thermodynamic properties of the $NH_3-H_2O-CO_2$ system that are needed for the compressor model calculations. In the next chapters, when speaking of the thermodynamic property model of $NH_3-H_2O-CO_2$, it always refers to this new fit in Aspen Plus developed by Gudjonsdottir et al.

2.3. IMPLEMENTATION OF THE THERMODYNAMIC MODEL

The current wet compressor model is operating with an ammonia water working fluid. This mixture is already widely used and the properties can be found in thermodynamic databases, that are made available in Matlab compatible libraries. The ternary mixture, NH₃-H₂O-CO₂, has not previously been proposed for the application in CRHPs and such Matlab compatible routines are not available yet. The properties enthalpy and specific volume are needed as a function of temperature, pressure and composition of the mixture throughout the complete compression process calculation. The thermodynamic property model, developed by Gudjonsdottir et al. [9], can be used to compile these thermodynamic properties. To implement the properties into the compressor model four different methods are investigated. The following selection criteria are taken into account:

The properties must be determined with a high accuracy. Otherwise, the model is not useful in order to predict the real behavior of the mixture during the compression process.

The computational cost must be kept low in order to make quick analyzes of the behavior of the mixtures for different operating conditions in the compressor.

The model must be consistent. Table interpolation or curve fits of property data can result in thermodynamic inconsistency. This can lead to computational models that do not conserve mass and energy and yield to non physical results or numerical problems [19].

2.3.1. Property calculations by a Matlab routine

The thermodynamic property model of NH_3 - H_2O - CO_2 can be implemented into the compressor model as a Matlab executable function (MEX). Rattner and Garimella [19] have developed such a thermodynamic property routine for the ammonia water mixture. The approach proposed in their study can be applied to other fluid mixtures. However, in this study a ternary mixture is considered. By keeping the complexity of their program in mind and the fact that there is an addition of one more mixture component, makes this option too time consuming for the scope of this thesis.

Wang and Infante Ferreira[29] investigated absorption heat pump cycles with NH_3 -ionic liquids (ILs) working pairs. Wang developed a thermodynamic model of a single-effect absorption heat pump and investigated different NH_3 -ILs working pairs with this model. It was investigated if this thermodynamic model can be extended to the considered ternary mixture of this research. Again adding one more component to their model increases the number of variables and, therefore, the complexity of the model. After analyzing the work of Wang some other fundamental differences can be noted, which makes this model not applicable for the thermodynamic modeling of NH_3 - H_2O - CO_2 . Ionic liquids are known for their really high boiling points and due to this non-volatility, the equilibrium equations in the model can be simplified considerably. Only the NH_3 undergoes phase changes but the ILs can be assumed to remain in the liquid phase throughout the whole cycle. In case of NH_3 - H_2O - CO_2 , there are three components and each of them undergo phase changes. This makes the thermodynamic system far more complex. For these reasons this method is not further investigated.

2.3.2. LINKING MATLAB TO ASPEN

After some literature study it is found that Matlab and Aspen can be linked to each other using an intermediary software, for example Excel [7]. Visual Basics for Applications (VBA) is a programming language that is build into Excel and enables to automate application processes. This programming language can be used to communicate with the Aspen plus software and with the compressor model in Matlab. In terms of consistency, stability and accuracy this method can be an attractive option, since the thermodynamic property model in Aspen is used directly without for example interpolation.

However, the mass and energy conservation equations that contain the thermodynamic properties in the compressor model are discretized and solved in small displacement steps throughout the compression process. Due to this solving method the thermodynamic properties need to be determined many times. A test VBA function was made to get an idea of the usability of this method. However, the communication between the software was slow and the computational time of the compressor model would add up to days. For the compressor model this method is, therefore, not applicable. Later, when the complete heat pump cycle will be analyzed, this method can become useful because the working fluid only needs to be determined at a few state points throughout the heat pump cycle.

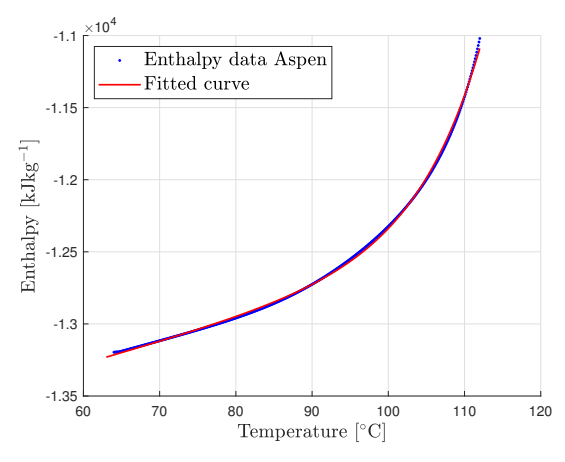
2.3.3. FITTING THE PROPERTIES TO TEMPERATURE AND PRESSURE

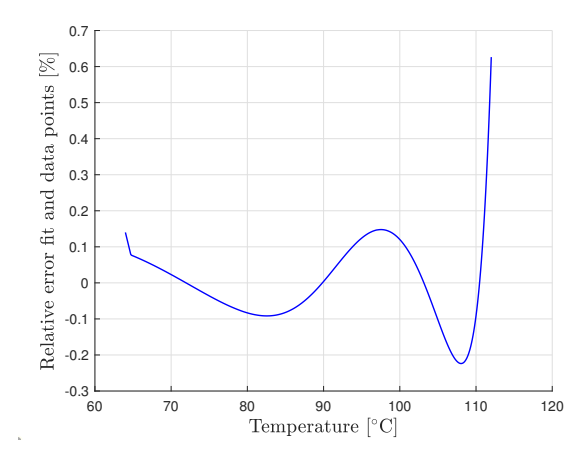
Curve fitting is the process of constructing a mathematical function that has the best fit to a set of data points. The thermodynamic model in Aspen can be used to collect property data for a fixed composition of the mixture. If the property data can be fitted to the temperature and the pressure then the properties can be described by only one function. This can be done for several desired compositions of the mixture and the thermodynamic property model is only described by a few mathematical equations. The advantage of this method is that it would be beneficial for the computational cost of the compressor model. However, it is of more importance to investigate if the property values can be fitted to the pressure and temperature with high enough accuracy.

To explore this method, a fitting curve for the enthalpy is constructed. For a fixed pressure and composition, the enthalpy is first fitted to the temperature. The pressure is fixed at 2 bar and the composition of the mixture consists of 20 wt% ammonia and 5 wt% CO₂. During the compression process, the mixture is located in the two-phase regime and, therefore, the temperature is between the dew and bubble point temperatures. For this fixed mixture composition and pressure, the two-phase regime is between a temperature of 65 °C to 112 °C. With the thermodynamic model in Aspen, the enthalpy values for this region are collected. By using the fitting tool integrated in Matlab (*cftool*) [16] different mathematical equations can be fitted to the enthalpy data and provide for the corresponding coefficients. A summation of two exponential functions showed the best results, given by the following equation:

$$h(T) = a \cdot e^{b \cdot T} + c \cdot e^{d \cdot T} \tag{2.13}$$

An example of this fit can be seen in Figure 2.3a. Figure 2.3b shows the relative error between the fit and the data points from the thermodynamic property model in Aspen. From both Figures, it can be seen that the error is very small.





(a) Fitted curve and real values of enthalpy at 2 har

(b) Error between fit and real values of enthalpy at 2 har

Figure 2.3: Enthalpy data collected from the thermodynamic model of Aspen Plus and fitted to the temperature fixed at 2 bar.

When the temperature is approaching the dew point temperature (112 °C) the fitted curve becomes less accurate. However, the relative error is still lower than the 1%.

Such a fit can be made for a finite number of pressure values for the same composition of the mixture. Between a pressure range of 1 and 15 bar, the enthalpy as function of the temperature (Eq. 2.13) shows similar results as Figure 2.3a and 2.3b.

The next step is to investigate if the coefficients can be fitted to the pressure. This would result in the following mathematical equation:

$$h(p,T) = a(p) \cdot e^{b(p) \cdot T} + c(p) \cdot e^{d(p) \cdot T}$$
(2.14)

During the fitting process of the coefficients, it was found that the coefficient 'a' and 'b' do not properly fit to the pressure. The coefficient 'c' and 'd' fitted both well to the pressure data, with again an exponential relation. Due to coefficients 'a' and 'b', the enthalpies approximated with Equation 2.14 were not accurate enough. The relative error reached values above 20 % around the dew point temperature. The only possibility left, would be to interpolate between the fitted curves of Eq. 2.13, to find the enthalpy for every desired pressure. Since interpolation is necessary anyway, the use of tables containing the properties becomes more obvious. The accuracy with the use of tables will be slightly higher, because the fitted curves contain a fitting error added to an interpolation error. The advantage of computational speed with the fitted curves still holds compared to the use of tables.

2.3.4. TABLES AND INTERPOLATION METHODS

Instead of using the fitted curves, the collected property data from Aspen can be used directly in the form of tables. The tables contain the property values for different temperatures and pressures for one specific composition of the mixture.

Interpolation between the tabulated values is needed to provide for the property values at each pressure and temperature. Different types of interpolation schemes can be considered. In case of linear interpolation two neighbouring data points in each respective

dimension are used to calculate the property value at any query point. Another, and more accurate solution would be to use a spline interpolation scheme, however, spline interpolation schemes take more computational time. Both cases are investigated.

The table refinement is of even greater importance for the accuracy. It is expected that high refined tables are needed, which means the tables can become quite large. First of all generating these tables can be computational costly. Secondly using this table interpolation method slows down the speed of the compressor model. Another disadvantage is that for each new composition of the mixture, new tables need to be made again. Therefore, a smart method of generating these tables from the thermodynamic model in Aspen must be investigated.

Another concern is that due to the use of interpolation, the properties have deviations from the real values of Aspen and can lead to thermodynamic inconsistent formulations. As mentioned before the energy and mass equations are discretized and calculated in small steps throughout the compressor. The energy and mass balance need to be conserved and when small deviations occur in different property values it can cause numerical problems. To ensure this method succeeds the tables must be sufficiently refined such that the deviations due to interpolation are minimal.

2.3.5. CONCLUSION

After evaluating the different methods a conclusion is made on which method is most suitable for the implementation of the thermodynamic properties in the compressor model. The first two methods are already rejected.

The fitting method showed that the properties can be fitted very well to the temperature. However, this method fails due to the fact that not all the coefficients could be fitted to the pressure. The only possibility is to use the fitted curves to the temperature (Equation 2.13), for some fixed pressures and interpolate for the pressure values in between the fitted curves. Since interpolation is needed anyway, it makes more sense to use the property data in the form of tables.

In conclusion, the method of using property tables will be applied into the compressor model. It is expected that the tables need to be highly refined. A method for generating the tables is developed. The interpolation functions that are integrated in Matlab are known to be quite slow. Separate spline interpolation functions are developed. In the next Chapter, the implementation of the table interpolation method into the compressor model is explained to a greater extent.

THEORETICAL MODEL OF WET COMPRESSION

In the previous chapter a review of wet compression models has been discussed. For this study a new compressor prototype, specifically designed for wet compression conditions, is being built. With the compressor model the compression process for this prototype can be numerically investigated.

To shortly recall from the previous chapter, two compressor models have been developed for the purpose of theoretically investigating the behavior of this new compressor prototype operating with ammonia water. The first model was developed by Gudjonsdottir et al. [8] and was based on an earlier developed compressor model by Zaystev [30]. However, the model developed by Zaystev requires detailed information about the geometry of the compressor, which makes his model quite complex. There are a couple of differences between the prototype used by Zaytsev and the new considered prototype. The model of Gudjonsdottir et al. [8] was developed with the new prototype in mind and the model of Zaytsev was therefore adapted. In the previous chapter, it was already mentioned that for the new prototype no liquid is injected but a two phase working fluid is compressed directly. However for this new prototype compressor not all detailed geometry is available yet and due to the complexity of this compressor model, the computational time became very long as well.

Therefore, the second model developed for the new compressor prototype, developed by Guðmundsdóttir [10], was aiming to improve the computational time. This has been done by developing a simpler model, where the geometry is described in a more general way. Finally this model developed by Guðmundsdóttir is able to predict the behavior of the new prototype compressor operating witch ammonia water with a satisfying computational time and less dependency on the geometry.

The compressor model developed by Guðmundsdóttir [10] will be used to predict the behavior of the compressor operating with NH_3 - H_2O - CO_2 . First, the compressor model by Guðmundsdóttir is discussed in more detail. The section after is discussing the modifications that are made to the compressor model.

3.1. THE COMPRESSOR MODEL

The compressor model, by Guðmundsdóttir [10], is developed for the new compressor prototype, which is a twin screw compressor. A twin screw compressor is a positive displacement compressor with two helical rotors, a male and female rotor. During the rotation of the rotors the volume of the working cavity increases from zero to its maximum value and then decreases again to zero. It is performing suction, compression and discharge processes continuously. Two types of twin screw compressors are commonly used: oil-free and oil-injected. In the case of an oil-free screw compressor, no oil is presented in the compression space and one rotor drives the other through timing gears without physical contact between the lobes. In the case of an oil-injected screw compressor, oil is injected in the compression space and no timing gears are necessary. The male rotor is driving the female rotor through an oil film between the intermeshing profiles. The oil provides for lubrication, sealing and cooling [30]. The new compressor prototype considered in this study is an oil-free screw compressor because separating the oil from a two phase working fluid can be quite tedious. Due to wet compression conditions, the liquid part of the working fluid provides for the required sealing and cooling in the compressor. Figure 3.1 shows an image of such a twin screw compressor.

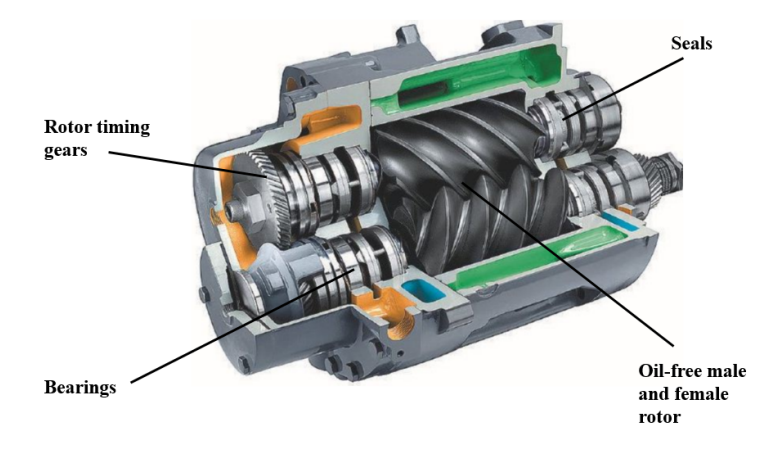


Figure 3.1: An oil-free twin screw compressor. Photo: Atlas Copco.

A detailed description of the compressor model can be found in the thesis research of Guðmundsdóttir [10]. However, the important parameters and equations of the geometry model and thermodynamic model are shortly discussed. The geometry characteristics are required as input parameters for the thermodynamic calculations, including the compressor cavity volume, the suction area, the discharge area and the leakage flows. The thermodynamic model is a homogeneous model based on mass and energy conservation.

3.1.1. GEOMETRY MODEL

The geometry model is based on a combination of previous proposed compression models as discussed in Chapter 2. Tang [21] has developed graphs for the volume cavity, port areas and leakages paths in the compressor at all rotational degrees. Zaytsev [30] developed very

similar shapes of these type of graphs for the geometry of his compressor. The main difference between the two considered compressors used by Tang and Zaytsev, is the size of the compressors. The compressor used by Zaytsev was rather small compared to the compressor described by Tang. Since the shapes of the graphs were comparable, the two models are used to scale the size of the new compressor prototype. The graphs of Tang [21] are used as a format to get the value at the specific position for the calculations in the model. When using this format, it is possible to scale the compressor size, and change the start or stop angles for different compressors [10].

The thermodynamic part is built on conservation laws applied to a control volume of the twin screw compressor. The chosen control volume is the volume of one cavity, which is the space enclosed by the mesh of the male rotor and the female rotor surfaces and the compressor housing. The volume curve of the cavity is the relation between the cavity volume V and the male rotation angle ϕ . An example of the cavity volume curve, determined by the compressor model, is presented in Figure 3.2. The function $V(\phi)$ and the change in the cavity volume $dV/d\phi$ form two important input parameters to the thermodynamic calculations of the model.

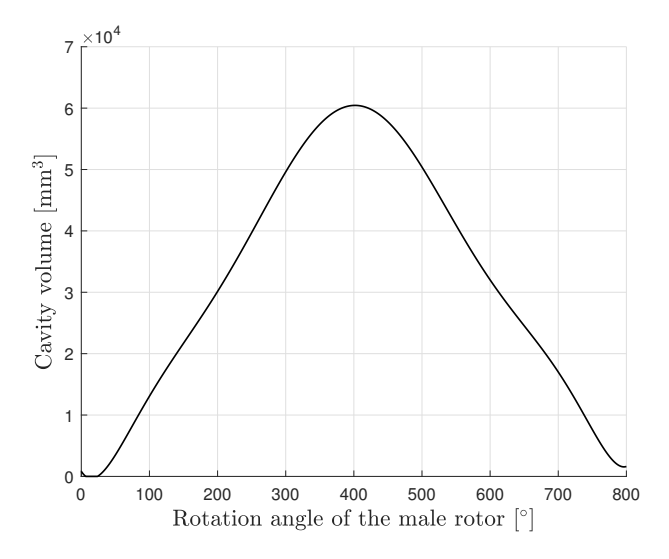


Figure 3.2: Example of the volume curve of one cavity of the compressor [30].

Between the compressor housing and the grooves of the two helical rotors there is always a little space left. These clearances exist to compensate for force deflection, machining tolerance and thermal expansion [3]. Through these spaces it is possible for some of the working fluid to leak out, effecting strongly the efficiency of the compressor. Therefore, the model takes into account the main leakage paths in screw compressors [21]:

- 1. Leakage through the contact line between the rotors. At the contact line the working fluid leaks from the compression cavity to the suction cavity.
- 2. Leakage through the sealing line between tip of the rotors and the housing. The cavity is bounded by four sealing screw lines between the rotor tips and the housing. The flow leaks from the considered cavity to the trailing cavity of the two rotors and from the leading cavity of the rotors to the considered cavity.

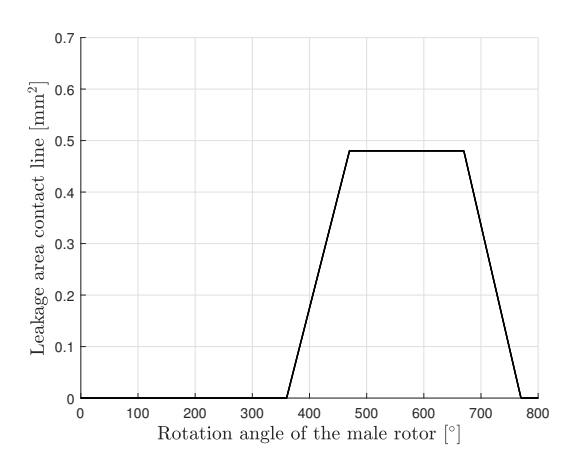
- 3. Leakage through the cusp blowholes at the compression side. The blow cusp holes refer to the opening between neighbouring cavities due to the fact that the contact line of the rotors do not reach the housing cusps.
- 4. Leakage through the compression-start blowholes at the suction side. This leakage path only exist at the beginning of the compression process.
- 5. Leakage through the discharge end clearance. There exist two kinds of this type of leakages. One is the leakage flow from the leading to trailing cavity. The second flow is coming from the discharge cavity directly to the suction cavity.

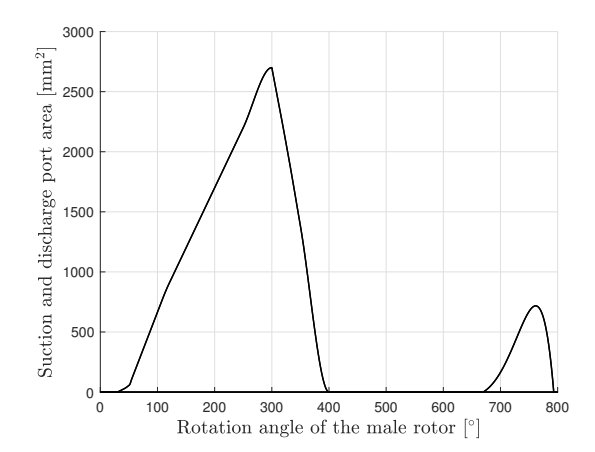
To calculate the leakage flows, the cross sectional areas of the leakage paths are determined by the geometry model. The cross sectional area is calculated with the sealing line l and the clearance height δ :

$$A = l\delta \tag{3.1}$$

The blow hole areas, leakage path 3 and 4, are calculated differently with a more complex formulation, described by Tang [21]. An example of the leakage area of the contact line determined by the model can be seen in Figure 3.3a. The leakage areas form again input parameters for the thermodynamic model, i.e. the energy and mass conservation equations that include the leakage mass flows.

The suction port is where the working fluid enters the compressor and the discharge port is where it leaves the compressor. The shape of the ports and their position determine the suction and discharge phase of the working process and influence the flow rate of the working fluid going in and out. For an efficient operation the suction port is connected to the cavity as early as possible and disconnected when the volume is at the maximum. The discharge port is disconnected as late as possible. As mentioned earlier, Tang [21] found the theoretical shapes of the suction and discharge ports that are used for the geometry part of the model. The suction and discharge port area curves can be seen in Figure 3.3b and form the last geometric input parameters to the thermodynamic calculations.





(a) Leakage area: contact line length times the clearance height.

(b) Suction port area (left), discharge port area (right).

Figure 3.3: Leakage area and suction and discharge port areas from the geometrical model.

3.1.2. THERMODYNAMIC MODEL

In the thermodynamic model the mass and energy conservation equations are solved. The conservation equations 3.2 and 3.3, derived by Zaytsev, are used. These equations are slightly modified because no liquid injection occurs during the compression. The ammonia concentration, x, is therefore not changing and kept constant during the compression process.

The solving strategy of Chamoun et al.[3], where the compression zone is divided into small finite control volumes, is used to solve the conservation equations in each of these control volumes. In order to solve Equations 3.2 and 3.3 the following quantities are needed:

(1) The enthalpy and specific volume are needed as a function of the pressure, temperature and ammonia concentration. These values are obtained by the thermodynamic property model. (2) The mass flow rate as a function of the rotation angle, $dm/d\phi$, through the suction port, discharge port and due to the leakages. The mass flow rate going in and out of the cavity volume is calculated by the continuity Equation 3.4. When the suction phase is considered, the suction port area can be used to calculate the mass going into the compressor. (3) The compressor cavity volume as a function of the male rotation angle, $V(\phi)$, and the change in cavity volume, $dV/d\phi$, determined by the geometry model.

$$\frac{dp}{d\phi} = \frac{1}{\left(\frac{\partial v}{\partial p}\right)_{T,x}} \left[\frac{v}{m} \left(\sum_{k=1}^{n} \left(\frac{dm_{out}}{d\phi} \right)_{k} - \sum_{k=1}^{n} \left(\frac{dm_{in}}{d\phi} \right)_{k} \right) + \frac{1}{m} \frac{dV}{d\phi} - \left(\frac{\partial v}{\partial T} \right)_{P,x} \frac{dT}{d\phi} \right]$$
(3.2)

$$\frac{dT}{d\phi} = \frac{T\left(\frac{\partial v}{\partial T}\right)_{P,x}\left[\frac{v}{m}\left(\sum_{k=1}^{n}\left(\frac{dm_{out}}{d\phi}\right)_{k} - \sum_{k=1}^{n}\left(\frac{dm_{in}}{d\phi}\right)_{k}\right) + \frac{1}{m}\frac{dV}{d\phi}\right]}{\left(\frac{\partial v}{\partial P}\right)_{T,x}\left(\frac{\partial h}{\partial T}\right)_{P,x} + T\left(\frac{\partial v}{\partial T}\right)_{P,x}^{2}} + \frac{\frac{\partial Q}{\partial \phi} + \sum_{k=1}^{l}(h_{in,k} - h)\left(\frac{dm_{in}}{d\phi}\right)_{k}}{m\left(\frac{\partial h}{\partial T}\right) + \frac{mT}{\frac{\partial V}{\partial P}}\left(\frac{\partial v}{\partial T}\right)_{P,x}^{2}} \tag{3.3}$$

$$\frac{dm}{d\phi} = \frac{\zeta \rho A u}{\omega} \tag{3.4}$$

In Eq. 3.4, ζ is an empirical flow coefficient and ω is the angular speed of the male rotor. The area A can be either the leakages areas or the suction and discharge port areas, depending on which part of the compression process is considered. The flow velocity u is determined as follows:

$$u = \sqrt{2 \int_{P_{down}}^{P_{up}} v dp} \tag{3.5}$$

The results of solving the conservation equation are the pressure and temperature curves as a function of the male rotor rotation angle.

When the mass and energy conservation equations are solved, the isentropic efficiency of the compressor can be determined by Eq. 3.6. The isentropic efficiency is the work of the compressor without any entropy production, calculated with the isentropic enthalpy at the discharge ($h_{is,dis}$) and the enthalpy at the suction h_{suc} , divided by the real work of the compressor \dot{W} . The isentropic enthalpy at the discharge, is the enthalpy value with the same entropy as the suction enthalpy at the final discharge pressure. The real work is computed

by Equation 3.7, where z_1 is the number of lobes of the male rotor and n are the rotations per minute.

$$\eta_{is} = \frac{\dot{m}(h_{is,dis} - h_{suc})}{\dot{W}_{ind}} \tag{3.6}$$

$$\dot{W}_{ind} = z_1 \frac{n}{60} \int p \, dV \tag{3.7}$$

The total isentropic efficiency η_{tot} is including the mechanical efficiency, η_{mech} . The main contributions to the mechanical losses are the gears, seals and bearings.

$$\eta_{tot} = \eta_{mech} \cdot \eta_{is} \tag{3.8}$$

The volumetric efficiency is determined by the ratio between the real and theoretical volumetric displacement, Eq. 3.9. The real volume is calculated by multiplying the specific volume at the suction with the mass leaving the compressor, given by Equation 3.10. The theoretical volume is the ideal maximum cavity volume obtained from the volume curve.

$$\eta_{vol} = \frac{V_{real}}{V_{th}} \tag{3.9}$$

$$V_{real} = v_{suc} \int \frac{dm}{d\phi} d\phi \tag{3.10}$$

3.1.3. STRUCTURE AND IMPLEMENTATION OF THE COMPRESSOR MODEL

Figure 3.4 is schematic diagram that represents the structure of the compressor model. The orange dashed area indicates the geometry part of the compressor model and the green dashed area contains the thermodynamic calculations of the compressor model. The blue dashed area contains the outputs of the model, consisting of the pressure and temperature as functions of the rotation angle of the male rotor, the isentropic efficiency and the indicated power of the compressor. The entropy is indicated with a dashed line because it is not an output of the conservation laws as a function of the rotation angle but used together with the other output parameters to calculate the isentropic efficiency. The indicated power is obtained by integrating over the pressure, see Eq. 3.7.

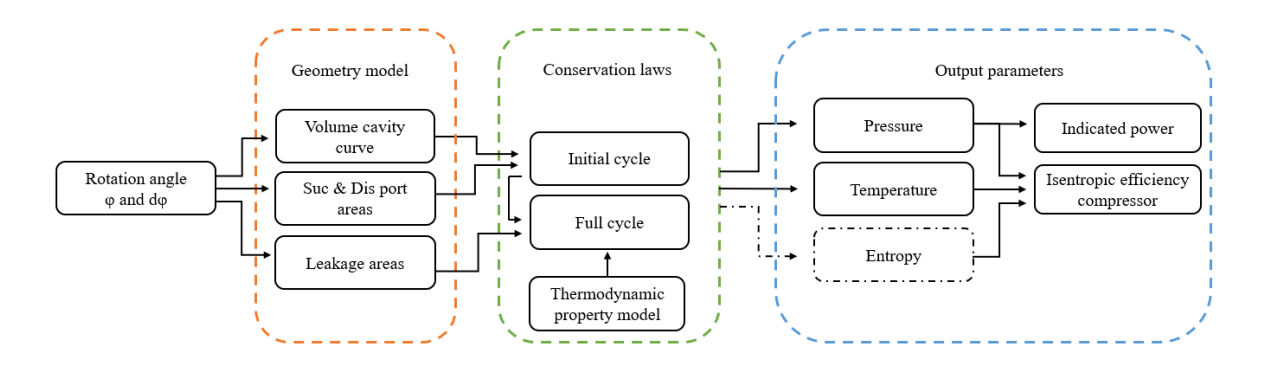


Figure 3.4: Schematic structure of the compressor model.

The model starts by discretizing the rotation angle of the male rotor. The rotation angle ϕ is considered from 0 ° to 800 ° because this represents the suction, compression and discharge process following one cavity of the compressor. The default discretization step $(d\phi)$

is 1°/50, which means that the compression process is divided into 40001 angle segments. In the previous section, the geometrical part was discussed already in quite some detail. The volume curve of the cavity, the suction port and discharge port areas and leakage areas are determined for the given discretization steps.

For the thermodynamic part, Eq. 3.2 and 3.3 are solved by using a finite volume method. The change of pressure and temperature are computed for all 40001 angle segments throughout the complete compression process. For the left side of the equations, a simple Euler method is used. The pressure change as a function of the rotation angle is then described as follows:

$$\frac{dp}{d\phi} = \frac{p(\phi + d\phi) - p(\phi)}{d\phi} \tag{3.11}$$

The temperature as a function of the rotation angle is described in the same way. In the conservation Equations 3.2 and 3.3, the thermodynamic properties are described as partial derivatives. These can be interpreted as follows:

 $\left(\frac{\partial v}{\partial p}\right)_{T,x}$: The specific volume as a function of the pressure with fixed temperature and fixed ammonia concentration.

 $\left(\frac{\partial v}{\partial T}\right)_{P,x}$: The specific volume as a function of the temperature with fixed pressure and fixed ammonia concentration.

 $\left(\frac{\partial h}{\partial T}\right)_{P,x}$: The enthalpy as a function of the temperature with fixed pressure and fixed ammonia concentration.

In order to calculate them another integration scheme is used, namely the five-point method. The first partial derivative of the thermodynamic property, the specific volume for a fixed temperature and mixture composition, is given by Equation 3.12:

$$\left(\frac{\partial v}{\partial p}\right)_{T,x} = \frac{v(p(\phi+d\phi)-2dp)-8v(p(\phi+d\phi)-dp)+8v(p(\phi+d\phi)+dp)-v(p(\phi+d\phi)+2dp)}{12dp} \quad (3.12)$$

For the other two partial derivatives, the step size is dp is replaced with step size dT. In the next section, the choices of the step sizes $d\phi$, dp, dT are discussed into more detail. When the compressor is operating with ammonia water, Rattner & Garimella is the thermodynamic property model that is used to calculate these properties.

Going back to Figure 3.4, it can be seen that the conservation laws in the thermodynamic part consist of two types of calculations in order to reach the outputs of the model: the initial cycle calculation and the full cycle calculation.

In the *Initial cycle* calculations, the mass and energy conservation equations (Eq. 3.2, 3.3) are solved without taking the leakage paths of the compressor into account. Besides the geometrical input parameters, the initial conditions of the working fluid are input parameters as well. These are the ammonia concentration, the temperature and pressure at the suction of the compressor. Then, the initial cycle calculation determines the first iteration throughout the compression process without any leakages, i.e. Eq. 3.2 and 3.3 are solved

once with the described finite volume method. The outputs of this part of the calculation are the pressure, the temperature, the specific volume and the enthalpy as functions of the rotation angle of the compression process without the leakage paths. This must not be confused with the final outputs of the model.

The output of the first iteration from the initial cycle calculation is the input for the *Full-Cycle* calculation. In this function again the mass and energy conservation equations are solved by the same procedure, but the calculations include the leakage paths. The conservation equations are solved iteratively until the solution converges. This happens when the pressure change between two iteration steps is less than 0.01 Pa. In this part of the calculation, the desired discharge pressure is an input parameter and the model forces the final pressure to be the same as the desired discharge pressure.

When the *FullCycle* calculation is converged the pressure and temperatures at each angle segment throughout the compression process are known. This part of the calculation takes up most of the computational time because the conservation laws need to be solved multiple times before converging.

At last the isentropic efficiency and indicated power of the compressor can be calculated. The suction enthalpy (h_{suc}) is determined with the suction pressure and temperature. The isentropic discharge enthalpy ($h_{is,dis}$) can be determined by using the entropy at the suction. The indicated power is determined by Equation 3.7, which is an integral over the pressure. At last the isentropic efficiency is calculated by Equation 3.6.

The calculations in the green and blue dashed areas of Figure 3.4 are currently using the Rattner and Garimella Matlab routine or REFPROP, to obtain the properties of the ammonia water mixture. When this model is used for predicting the performance of the compressor operating with NH_3 - H_2O - CO_2 , these parts of the model need to be modified. Since the same compressor prototype is considered, the functions in the orange dashed area (the geometry model) of Figure 3.4 do not need any modifications. The properties of the mixtures do not influence the geometry of the compressor.

3.1.4. SENSITIVITY ANALYSIS OF THE COMPRESSOR MODEL

While working with the model, difficulties were noticed for some input conditions to the model. These were not reported by Guðmundsdóttir [10]. Before extending the compressor model to operate with NH_3 - H_2O - CO_2 , a sensitivity analysis was done for some important parameters in order to clarify these problems.

Especially when the vapor quality of the mixture became quite high ($q \sim 0.70$), the model had problems to converge. At some point the discretization step $d\phi$ was decreased from 1°/50 to 1°/200 or even to 1°/500 in order to make it converge. This had a significant influence on the computational time of the model. Instead of a computational time in the order of minutes it became hours. In some cases even with decreasing the step size $d\phi$, the model was not able to converge. In order to continue with this model these problems needed to be solved first. During this analysis, some modeling errors were discovered and solved.

THE INFLUENCE OF STEP SIZES $d\phi$, dp, dT

As mentioned in the previous sections, the mass and energy conservation equations are calculated as functions of the step size $d\phi$. In the model it is possible to adjust the value of $d\phi$ at the start of the calculations. The step size $d\phi$ was made variable along the compression process. Such that during some critical parts, e.g. the suction phase, the step size can be decreased more and during the rest of the compression process the step size can be kept the same. This was done to keep the computational time manageable. The default case became $d\phi$ is 1°/150 during the suction part of the compression process and during the rest of the compression process $d\phi$ is 1°/50. But as mentioned, for some input values the model was not able to converge, even if the step size had to be decreased to 1°/500. This was always the case if the vapor qualities of the mixture at the suction were around 0.7 or higher. At lower vapor qualities these problems are not observed and the model converges for the default values of $d\phi$. It seems that it had something to do with the thermodynamic properties: $(\frac{\partial v}{\partial p})_{T,x}$, $(\frac{\partial h}{\partial T})_{P,x}$ and $(\frac{\partial v}{\partial T})_{P,x}$. These are solved with the integration scheme given by Eq. 3.12. The values of dp and dT in the model were 0.01 Pa and 0.000001 K respectively but not given as input values on the start of the calculations. Therefore, the choice of the steps sizes dp and dT are easily overlooked. When the thermodynamic properties were plotted to the rotation angle for a high vapor quality case, it became clear that the partial derivatives were very unstable, see in Figure 3.5.

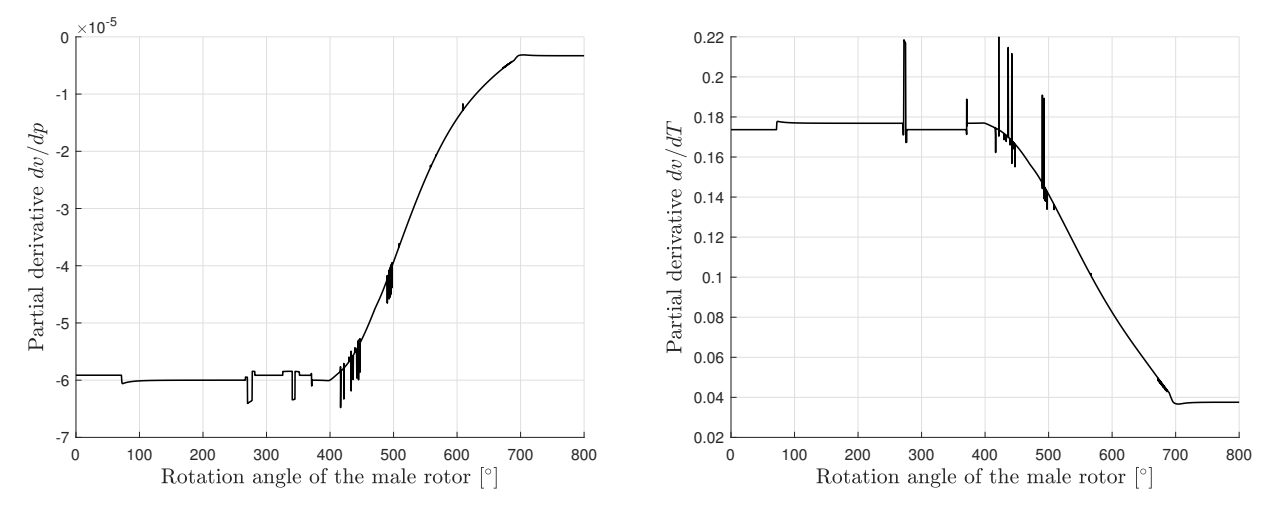


Figure 3.5: Example of the instability of the partial derivatives $\left(\frac{\partial v}{\partial p}\right)_{T,x}$ an $\left(\frac{\partial v}{\partial T}\right)_{P,x}$.

For vapor qualities of 0.7 and higher the instabilities become noticeable. The step sizes dp and dT need to be increased to 1 Pa and 0.01 K in order to get rid of the instabilities and for the model to converge. However, changing the step sizes of the properties has drastic influence on the computational time of the model. Therefore, at the start of the model a quick vapor quality check is done. If the vapor quality is lower than 0.7, the old step sizes can be used and for a vapor quality above 0.7 the new given values need to be used to make the model able to converge properly.

It was noticed already before, that at higher vapor qualities, the gradient in the thermodynamic properties became bigger, see Figure 2.3a in Chapter 2. When reaching the dew point temperature the accuracy of the enthalpy fit became less. This is probably related to the instabilities that are found during this analysis. Normally, when using such integration schemes, smaller steps lead to more accurate results but a longer computational time. When choosing the step size it is a compromise between the accuracy and computational time. For this case, Equation 3.12 is solved with the thermodynamic property model of Rattner and Garimella. In these Matlab routines the determined properties are generated in Tables as well. Due to this table method, very small step sizes lead to the instabilities when gradients in the properties are very high.

With the new step sizes dp and dT the convergence problems for higher vapor qualities are solved and for the step size $d\phi$, the value 1°/50 is sufficiently small, as well for the suction phase of the compression.

When the influence of $d\phi$ to the isentropic efficiency of the compressor is analyzed some new problems were discovered. The model did converge for a $d\phi$ of 1°/50, i.e. the pressure difference between two iteration steps was less than 0.01 Pa. However, for the same input conditions and only changing $d\phi$ to 1°/100, 1°/200 or 1°/500, the isentropic efficiency kept on increasing. For each chosen $d\phi$ the pressure was converging, however the isentropic efficiency must also converge for the same inlet conditions and not be increased by only $d\phi$. Finally the cause of this problem was found:

- 1. In the continuity Equation 3.4, the mass flow rate is given as a function of the rotation angle $d\phi$, which is given in [°]. However, the angular speed was given in [rad/s]. Using two different units in the same equation was causing problems.
- 2. As mentioned the geometrical shapes of the port areas and leakage areas are scaled to the size of the new compressor prototype. Some leakage areas were not scaled properly and as well some adjustments in the calculations of the leakage mass flows were made, which improved the model.

After solving these problems, the isentropic efficiency converges when changing the step size $d\phi$. Figure 3.6 shows the isentropic efficiency for fixed inlet conditions as a function of different step sizes $d\phi$. It can be seen that the isentropic efficiency is stabilizing already from a step size of 1°/10. The step size of 1°/150 during the suction phase is unnecessary and is only disadvantageous for the computational time of the model. A step size of 1/50° seems to be sufficient for all cases, as long as dp and dT are well chosen, and convergence is reached within 10 iteration steps.

The step sizes dp or dT need to be changed only for higher vapor qualities. In the case of a low vapor quality, changing dp or dT between the new and old values does not influence the isentropic efficiency. Table 3.1 is summarizing the values for the step sizes.

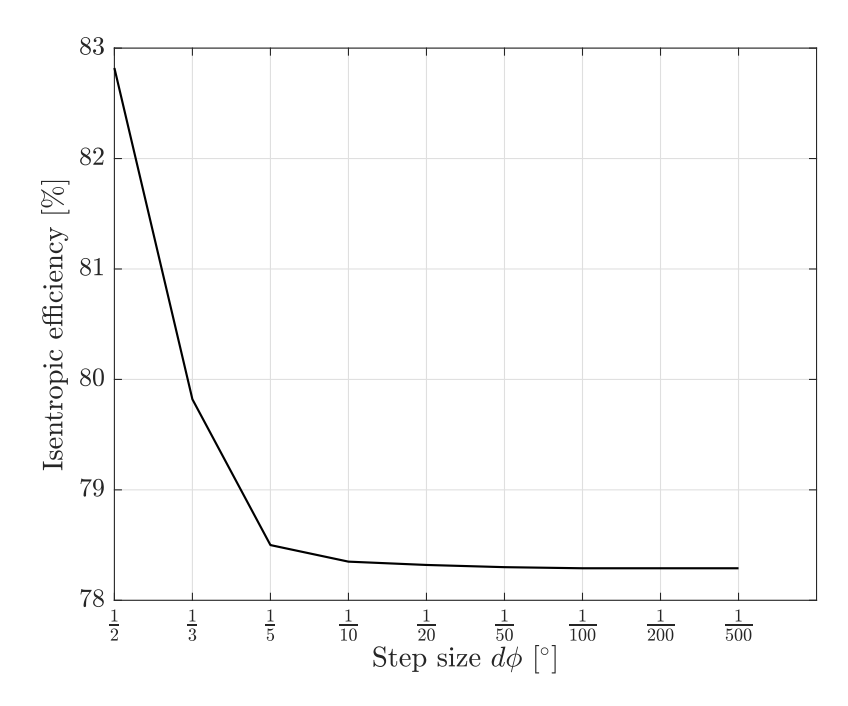


Figure 3.6: Isentropic efficiency versus different step sizes.

Table 3.1: Settings of the step sizes coming from the discretized conservation equations and the partial derivatives of the thermodynamic properties.

Discretization of the male rotation angle $d\phi$,°	1/50
Vapor quality < 0.7 step size dp , Pa	0.01
Vapor quality < 0.7 step size dT , K	0.000001
Vapor quality > 0.7 step size dp , Pa	1.0
Vapor quality > 0.7 step size dT , K	0.01

CONVERGENCE CRITERION

When the step sizes $d\phi$, dp and dT are set to the proper values, the model is solving the mass and energy conservation equations until the pressure in the compressor stabilizes. The convergence criterion is, as mentioned earlier, that the pressure difference between two iterations is smaller than 0.01 Pa. However, the value that is of interest, is the isentropic efficiency of the compressor. In the current model, the isentropic efficiency is calculated only at the end, with the final values from the solved conservation equations.

For complex models it can be dangerous to just handle only one convergence criterion. Before the described problems were solved and the isentropic efficiency was determined after each iteration, it was observed that for some cases the isentropic efficiency was still fluctuating while the pressure difference reached a value below 0.01 Pa. This could happen if, for example, the step sizes dp and dT were not chosen properly. To avoid these mistakes the isentropic efficiency is calculated for each iteration, as a back-up convergence criterion. The isentropic efficiency must become stable in order to conclude that the model has converged.

Figure 3.7 shows an example of the isentropic efficiency versus the number of iterations. After nine iterations the pressure difference between two iteration steps has reached 0.01 Pa and the model has converged. It can be seen that after four iterations the efficiency is already completely stable, which happens with a pressure difference of 1.0 Pa. The last five iterations give the same isentropic efficiency and the tolerance criteria of 0.01 Pa can be increased to 1.0 Pa to save computational time.

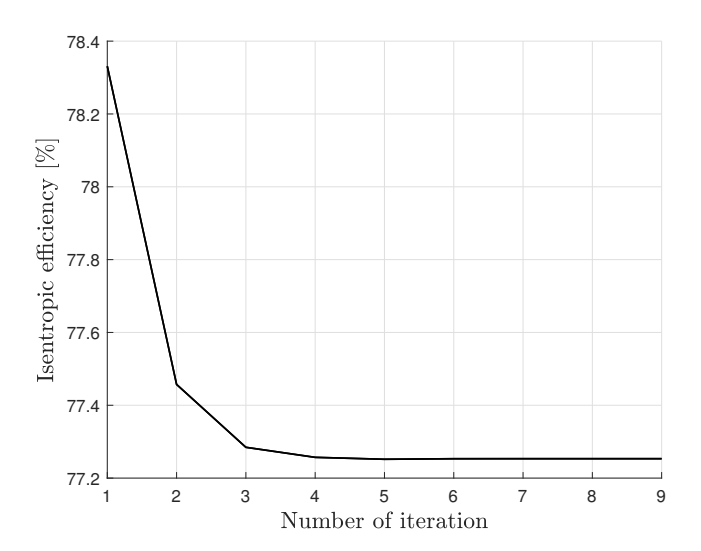


Figure 3.7: Isentropic efficiency versus the number of iteration steps.

After the sensitivity analysis, it can be concluded that the model is more reliable and stable. The model has no longer problems to converge for higher vapor qualities and the computational time has been improved by proper choices of the discretization step sizes.

3.2. The compressor model operating with NH_3 - H_2O - CO_2

In Chapter 2, several implementation methods of the thermodynamic properties of NH_3 - H_2O - CO_2 for the compressor model are discussed. It was concluded that the most suitable approach is to generate tables containing the properties from the thermodynamic model of NH_3 - H_2O - CO_2 in Aspen Plus and to use an interpolation scheme to obtain the property values in between the tabulated values.

As seen before, the two fundamental equations of the compressor model (Eq. 3.2, 3.3), contain the following partial derivatives of the thermodynamic properties: $(\frac{\partial v}{\partial p})_{T,x}$, $(\frac{\partial h}{\partial T})_{P,x}$ and $(\frac{\partial v}{\partial T})_{P,x}$. In order to obtain these partial derivatives, two tables are needed. One table containing the enthalpies for different values of pressure and temperature and a fixed composition of the mixture components. The other table containing the specific volume for different values of pressure and temperature and fixed composition of the mixture components.

Besides the thermodynamic properties in the conservation equations, the property entropy is needed in order to calculate the isentropic efficiency of the compressor. A table with the entropy for the same range of pressures and temperatures and fixed composition of the mixture is needed.

The property vapor quality is not required for solving the conservation equations in the compressor model or used in the efficiency calculation. However, as earlier mentioned, the vapor quality is a critical factor because for both, too high or too low values, the compressor can be damaged. Especially when experiments are done in the future, it can become of interest to analyze the vapor quality throughout the whole compression process. The vapor quality is a function of pressure, temperature and mixture composition as well. Thus, with the full cycle calculation done, the vapor quality can be determined for each pressure and temperature during the compression process. A table containing the vapor qualities for the particular pressure and temperature range is necessary. For now, the vapor quality as a function of the rotation angle is not a priority. When the suction and discharge pressure and temperature are known the vapor quality can be determined for these conditions and an average vapor quality during the compression is calculated.

3.2.1. TABLE LAYOUT AND REFINEMENT

The focus lies on generating the tables for the enthalpy, specific volume and entropy as functions of pressure and temperature. The refinement of the tables is a crucial aspect in order to make this method work properly. It is expected that a high refinement is necessary to ensure a high accuracy for the interpolated values of the properties. If the interpolated values are not accurate enough, the model is not able to converge or even crashes during the calculations. The step size of the pressure is the most critical. There are two factors that influence the necessary pressure refinement the most: the vapor quality and the pressure range of the table. Figure 3.8 shows a schematic layout of the property tables and the rules of thumb for the pressure refinement (dp) and temperature refinement (dT) to ensure that the model converges properly.

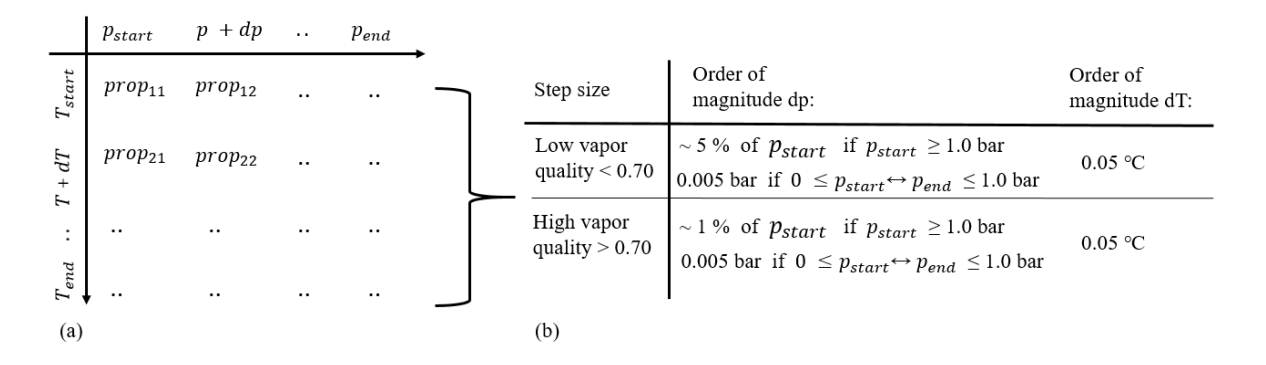
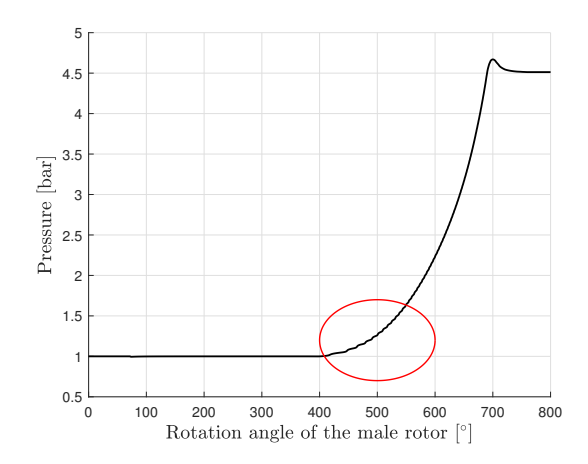


Figure 3.8: Representation of (a) the property table layout and (b) the necessary refinement of tables for the compressor model with $NH_3-H_2O-CO_2$.

For the compressor model with ammonia water, it was observed that different step sizes are needed for higher vapor qualities. At high vapor qualities, the properties are changing very rapidly for small pressure and temperature changes. The tables need to be more refined for higher vapor qualities. If the pressure range of the table is for example from 1.0 bar to 8.0 bar, for lower vapor qualities a step size 0.05 bar is sufficient. However, for vapor qualities above 0.70 a step size of 0.01 bar is necessary. Otherwise, the pressure and temperature curves show instabilities. Figure 3.9 shows an example of a compression process from 1.0 to 4.5 bar, where NH₃-H₂O-CO₂ has a suction vapor quality of 0.85. The step size dp of the used table was 0.05 bar, although the model was able to converge the curves show some instabilities in the red circles. With a step size dp of 0.01 bar, the curves are smooth.



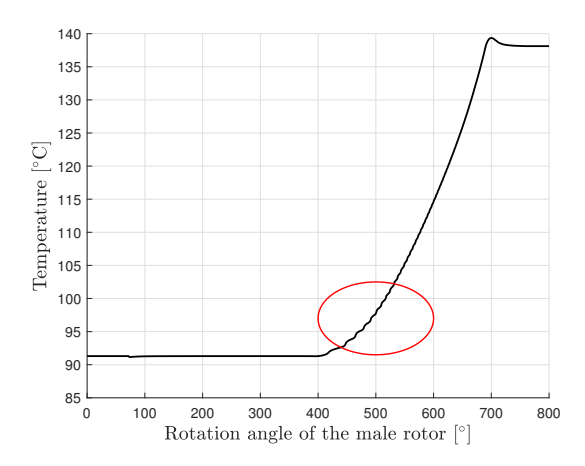


Figure 3.9: Example of the instabilities in the pressure and temperature distribution with insufficient refinement of the tables.

Obviously when the same pressure step is used at a lower pressure range, for example a table from 0.1 bar to 1.0 bar, the relative step becomes bigger because the order of magnitude of the pressure range is different. Again instabilities and convergence problems occur. Therefore, the pressure step for tables that contain pressure ranges beneath 1.0 bar need to be more refined. In this case, for any vapor quality, a pressure step of 0.005 bar is sufficient for proper convergence. The temperature step is always taken as 0.05°C.

3.2.2. TABLE GENERATOR

It has become clear that the tables need to be highly refined in order to obtain proper results with the model. The thermodynamic property model for NH_3 - H_2O - CO_2 is implemented in the software Aspen plus. The mixture composition, pressure and temperature can be declared and the desired property is determined by the thermodynamic property model. However, the temperature or the pressure need to be declared as one fixed value and the other one can be given as a range of values. For a pressure fixed at 1.0 bar, the temperature can be determined between a range of 0 °C and 200 °C in steps of 0.05 °C all at once. This calculation takes already quite some computation time in Aspen. The problem is that this calculation has to be repeated for a range of pressures as well. If the pressure range is from 0.1 to 1.0 bar in steps of 0.005 bar, this calculation has to be done 181 times. Generating the tables becomes, therefore, a very time consuming process especially when this has to be done manually.

For every mixture composition, different property tables need to be generated and a solution that can obtain the property tables automatically is found.

In chapter 2, the option of linking Matlab to Aspen was investigated. It turned out that an intermediate software program, e.g. Excel, is needed to make this connection possible. With the programming language VBA from Excel a function is made that generates the tables automatically. Figure 3.10 is a schematic representation of how the tables are generated. Matlab is able to communicate with the VBA code and is providing the input parameters for the table. The input parameters are the composition of the mixture, the desired temperature and pressure range and the step sizes dp and dT. The VBA code is able to communicate with Aspen plus. The VBA code consists of a double for loop, going through the pressure range and temperature range for the given step sizes dp and dT. First, for one fixed pressure step the VBA code calls the properties for each temperature step from Aspen. Aspen Plus determines the properties for all temperatures and the VBA code collects these properties. Finally, for one fixed pressure step three columns are collected for the three properties for the complete temperature range. Then the next pressure step is determined. For each pressure step, the three columns containing the properties are send back to Matlab and each column is placed in the corresponding table. When all the pressure steps are done, the output of the Matlab file are three property tables.

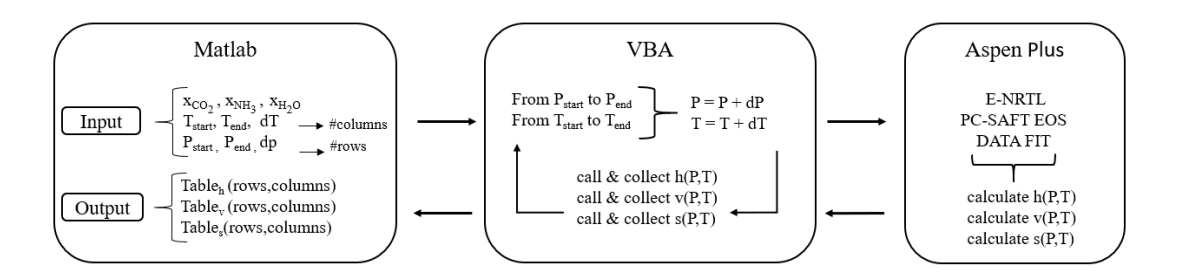


Figure 3.10: Schematic representation of the table generator.

3.2.3. Spline interpolation method

Different types of interpolation schemes were already mentioned in the previous chapter (2.3.5.). First a linear interpolation scheme was tested to see if the desired accuracy could be reached. Finally a spline interpolation scheme was necessary for the interpolation calculations.

A spline is a piecewise polynomial that is connected smoothly in the nodes (data points) [28]. The interpolation interval is divided into subintervals and an interpolation polynomial is constructed on each interval. In the case of cubic spline interpolation, the interpolation polynomials are of the third degree and thus at least four data points are used in order to construct these polynomials. A cubic spline interpolation must satisfy that the first and second derivatives are continuous as for linear interpolation only the curves itself are continuous. Matlab features for one and two dimensional spline interpolation functions. However these codes are written in such a general way that it contains many calculations that are not needed for the specific calculations in this study. To improve the computational speed, a spline interpolation algorithm is developed.

If the desired pressure and the temperature are equal to the tabulated values, no interpolation is needed and the values from the table can be used directly. If the pressure is a tabulated value and the temperature is in between tabulated values, the spline interpolation algorithm takes six property data points from the table for the six temperatures closest to the desired value. Between the data points, five cubic splines $S_n(P,T)$ are determined. When interpolating between the temperatures, the pressure in the spline function is fixed, see Figure 3.11(a). When the desired temperature is between T_3 and T_4 , the spline function $S_3(P,T_3,T_4)$ is used to obtain the thermodynamic property. Vice versa, if the temperature is a tabulated value and the pressure is in between tabulated values, the spline interpolation algorithm takes six property data points from the table for the six pressures closest to the desired value, see Figure 3.11(b).

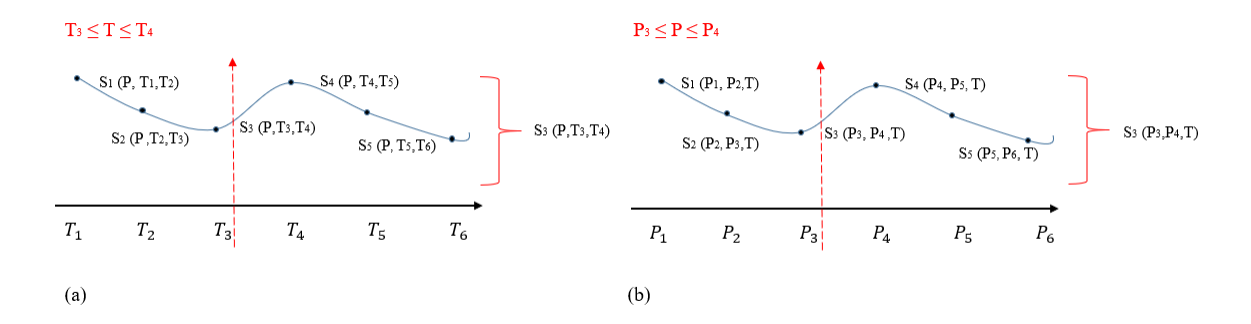


Figure 3.11: Schematic representation of the one dimensional spline interpolation, (a) interpolation for the temperature (b) interpolation for the pressure.

At last when both, the pressure and temperature are in between tabulated values, a two dimensional spline interpolation is used. The spline interpolation algorithm takes six by six property data points from the table for the six temperatures and pressures closest to the desired values. When again, the desired temperature is between T_3 and T_4 , the spline function $S_3(P, T_3, T_4)$ is determined 6 times for the six pressure values. If the desired pressure is as well between P_3 P_4 , the spline function $S_3(P_3, P_4, T_3, T_4)$ is used to determine the thermodynamic property, see Figure 3.12

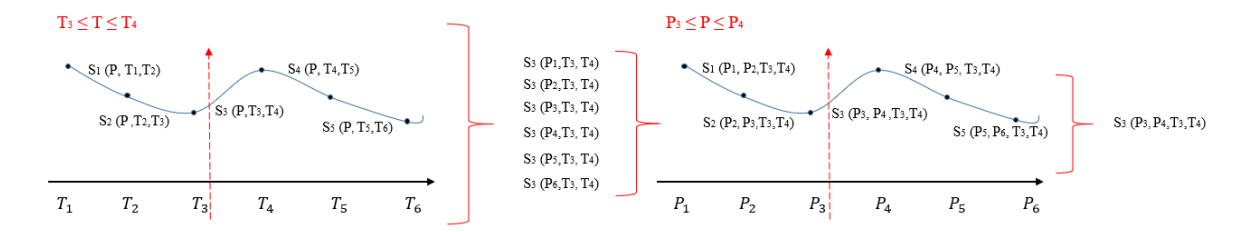


Figure 3.12: Schematic representation of two dimensional spline interpolation.

When the spline interpolation algorithms were implemented instead of the interpolation functions integrated in Matlab, the computational speed was twice as fast.

3.2.4. The implementation of the property function for NH_3 - H_2O - CO_2 .

The function XNH_3CO_2 is developed to provide for the property values of the new proposed mixture. This function serves as an intermediate between the property tables and the interpolation algorithm and is directing which thermodynamic property is desired for which pressure and temperature. Each property call that is done in the current model with the Rattner and Garimella Matlab routine or REFPROP is replaced by this function.

Going back to Figure 3.4, the green and blue dashed areas contain the thermodynamic calculations. These parts can be seen again in Figure 3.13 together with the extension in order to make the model operate with NH_3 - H_2O - CO_2 , indicated by yellow and red dashed areas. The orange dashed area from Figure 3.4 is omitted in this figure because it is containing the geometric calculations for the compressor and no modifications have been done to that part. This applies as well for the discretization of the rotation angle of the male rotor and the analogy of solving the conservation laws.

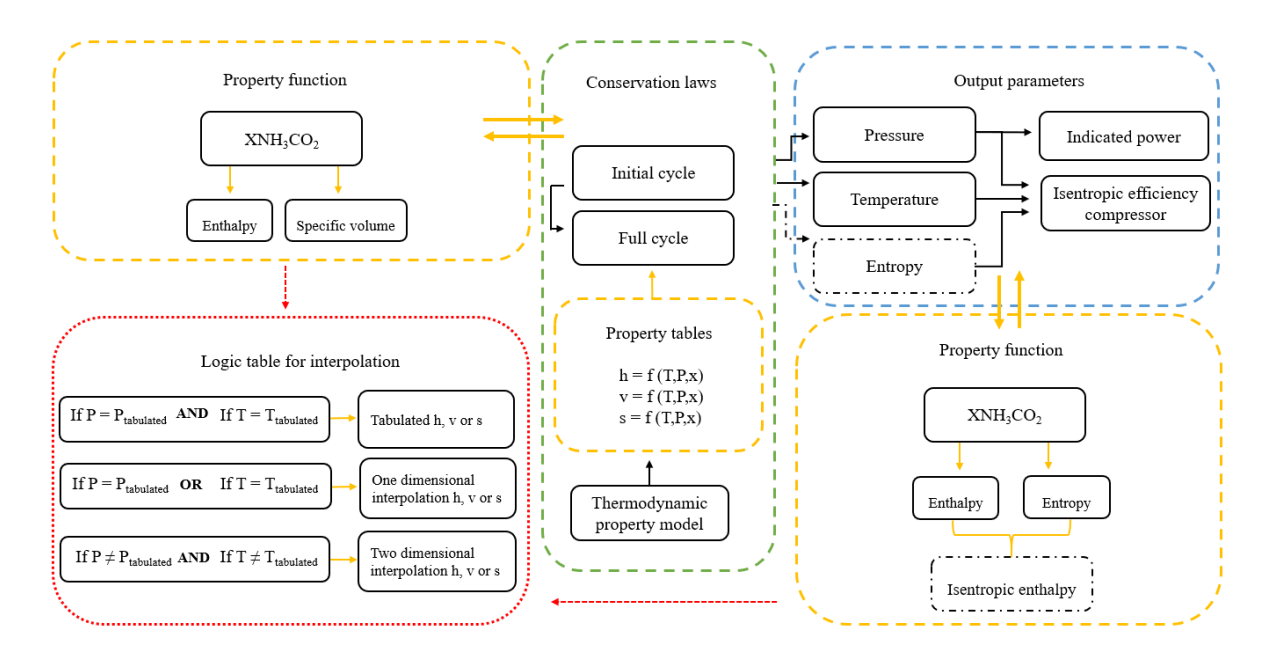


Figure 3.13: Schematic structure of the compressor model operating with NH_3 - H_2O - CO_2 . The green and blue dashed areas are taken from Figure 3.4 and the modifications of these parts are presented by the yellow and red dashed areas. The orange dashed area from Figure 3.4 is left out because no modifications are done to that part of the model.

It is clear that the thermodynamic properties are determined by the thermodynamic property model in Aspen plus and are collected in property tables. The enthalpy, specific volume and entropy tables are uploaded at the start of the Matlab model, see the green dashed area of Figure 3.13. The tables are saved as global variables in order to call the table values in the different functions that are used during the calculation, e.g the property function. In this way the tables are not reloaded every time a property value is needed.

During the initial and full cycle calculations, the property function XNH_3CO_2 is called each time a thermodynamic property is needed. For solving the conservation equation, enthalpy and specific volume are needed, see the left yellow dashed area of Figure 3.13. The input values for the XNH3CO2 function are explained by the use of the following example. The desired property is the enthalpy, h, as a function of the pressure, P, at 10^5 Pa and the temperature, T, at 353 K. The function converts the pressure to bar and the temperature to degrees Celsius because these are the tabulated units. In the compressor model, all the thermodynamic values are in SI units,



Figure 3.14: Example of using the function XNH₃CO₂.

flag: This is the desired property of the mixture that needs to be determined for the cycle calculations, i.e. the enthalpy, specific volume or entropy. Each property is indicated by a real number. For this example, the desired property that needs to be determined is the enthalpy and this property is indicated with a 1. Table 3.2 shows the other options for *Flag*.

Table 3.2: Options for the function XNH_3CO_2 .

	flag:
1	Enthalpy
2	Entropy
3	Specific volume

P: In order to find the desired property (for this example the enthalpy), two other thermodynamic properties must be known and in case of a mixture the concentration of the components must be known as well. The pressure is one of these two thermodynamic properties that is always given in order to determine the desired property. Therefore the value of the pressure (in this example 10^5 Pa), can be a direct input.

 $input_2$ and choice: The second thermodynamic property in order to calculate the enthalpy (flag), can be different. In this case the enthalpy is determined by the pressure and the temperature, however, the enthalpy can be determined as well with the pressure and any other thermodynamic property. choice is again a real number, which indicates the second thermodynamic property that is used. If the temperature is chosen as the second property, it is indicated with a 2. The parameter $input_2$ is the actual value of that property, which in this case is 353 K.

For this model, the thermodynamic properties are always a function of pressure and temperature. Therefore, the default of *choice* is 2. This function can be extended to the input of other thermodynamic properties and the parameter *choice* becomes useful.

x: This input is referring to the particular combination of concentrations of the mixture. Due to the use of tables, the concentration for one set of tables is fixed. If another combination of concentrations needs to be analyzed a different set of tables has to be generated. Therefore, x, is a real number assigned to a set of tables with a fixed composition. For example, when x is indicated by a 1, the mixture is composed as follows: H_2O : 75 wt%, NH_3 : 20 wt%, CO_2 : 5 wt%. When x is indicated by a 2, it refers to another composition and thus to another set of tables.

Thus, while solving the conservation equations, a thermodynamic property is needed for a certain pressure and temperature. The property function XNH_3CO_2 is directing to that desired property. If the desired property is the enthalpy, the function XNH_3CO_2 sends the pressure and temperature to the enthalpy property function, see again left yellow dashed area 3.13. The enthalpy property function is using the logic table (red dashed area) in order to decide whether (1) no interpolation, (2) one dimensional interpolation or (3) two dimensional interpolation is necessary. The enthalpy property function collects the data points from the property table, carries out one of the three options and sends the value for the enthalpy back to the cycle calculations.

When the full cycle calculation is finished the isentropic efficiency can be calculated. In order to calculate the efficiency, the isentropic discharge enthalpy is needed $h_{is,dis}$. This is the enthalpy at the discharge of the compressor with the same entropy as the suction entropy of the compressor.

$$s_{suc} = s_{dis} \tag{3.13}$$

The entropy at the suction s_{suc} of the compressor is determined with the property function XNH_3CO_2 , where the input flag is indicated by 2, see Table 3.2. The isentropic enthalpy can be found as a function of the suction entropy and the discharge pressure. However, the available enthalpy table is a function of pressure and temperature as well as the available entropy table. These tables are combined in order to find the enthalpy as a function of entropy and pressure. A different function, showed in the yellow dashed part on the right side of Figure 3.13, is developed to calculate the isentropic enthalpy $h_{is,dis}$. With the entropy table (s = f(P, T, x)) all the entropy values at the discharge pressure are calculated. This vector is subtracted from the suction entropy and the point where this vector becomes zero, Equation 3.13 holds. In this way the discharge temperature T_{dis} is found. The discharge pressure and discharge temperature are known and these two values can be used again in the enthalpy property function to determine the isentropic enthalpy.

4

THE COMPRESSOR PERFORMANCE OPERATING WITH NH₃-H₂O-CO₂

With the developed compressor model operating with NH_3 - H_2O - CO_2 , described in the previous chapter, the behavior of the mixture during the compression process can be predicted. The isentropic efficiency of the compressor is the most important result from the model as performance indicator for the NH_3 - H_2O - CO_2 mixture. The results are compared with the model operating with ammonia water.

There are many parameters that influence the isentropic efficiency of a compressor. Such parameters can be the geometrical characteristic of the compressor itself, for example the clearances of the compressor. The clearances are the spaces between the compressor housing and the tips of the rotors, or the contact line between the male and female rotors. Furthermore, it can be the operational conditions such as the the rotational speed of the compressor or the suction and discharge conditions of the working fluid. The influence of the important geometrical characteristics were investigated with the compressor model operating with ammonia water by K.Guðmundsdóttir [10]. This study showed how the isentropic efficiency depends on clearance sizes. Larger clearance sizes results in larger leakage flows which decrease the isentropic efficiency of the compressor. Furthermore, this study stated that a lower rotational speed leads to a lower isentropic efficiency of the compressor.

Both working fluids, ammonia water and NH_3 - H_2O - CO_2 , use the same geometrical model. The influence of the clearance sizes as well as the rotational speed is not showing any significant differences on the isentropic efficiency.

The influence of the pressure ratio, vapor quality and CO_2 concentration on the performance of the compressor operating with NH_3 - H_2O - CO_2 is investigated more extensively in this Chapter. Table 4.1 shows the geometrical characteristics and operation conditions of the compressor that are kept constant in the model during these calculations.

Maximum volume per cavity	$6.04 \cdot 10^{-5}$	$[m^3]$
Length of the compressor rotor	336.6	[mm]
Rotational speed	10000	[rpm]
Number of lobes on male rotor	5	[-]
Number of lobes on female rotor	6	[-]
Clearances	50	$[\mu \mathrm{m}]$
Discharge opens at	690	[°]
Stop angle	760	[°]
Mechanical efficiency	90	[%]

Table 4.1: Geometrical characteristics and operation conditions of the compressor that are kept constant during the performance analyses of the compressor.

4.1. EFFECT OF PRESSURE RATIO

In order to investigate the effect of the pressure ratio on the performance of the compressor, the discharge pressure is increased from 2.0 bar to 8.0 bar. The suction pressure is kept constant at a value of 1.0 bar. The working fluid that is considered has 5 wt% addition of CO_2 to an ammonia water mixture. In Table 4.2 the operation conditions that are used for these calculations are listed.

Table 4.2: Operation conditions used for the comparison of different pressure ratios.

CO ₂ concentration	5	[wt%]
NH ₃ concentration	20	[wt%]
Suction pressure	1.0	[bar]
Suction temperature	85	[°C]
Suction vapor quality	47	[%]

Figure 4.1 shows the pressure as function of the rotation angle of the male rotor for the different pressure ratios. During the initial calculation of the model, the mass and energy conservation equations are solved without taking the leakage flows into account. This results in a final pressure at the discharge of the compressor. For the conditions listed in Table 4.2, the initial calculation gives a final pressure around 3.5 bar.

During the full calculations, including the leakages, the final pressure is forced to the desired discharge pressure, which is an input value to the model. For the pressure ratios 2 and 3 (Figure 4.1) it can be seen that the pressure is forced to go down quickly to the desired discharge value when the discharge port opens at 690°. This is called under compression. In the case of high pressure ratios, the opposite occurs, the pressure is forced to rise quickly in order to reach the desired discharge pressure, this is known as over compression. Figure 4.2 shows the temperature distribution during the compression process for the different pressure ratios, where the same trend can be observed.

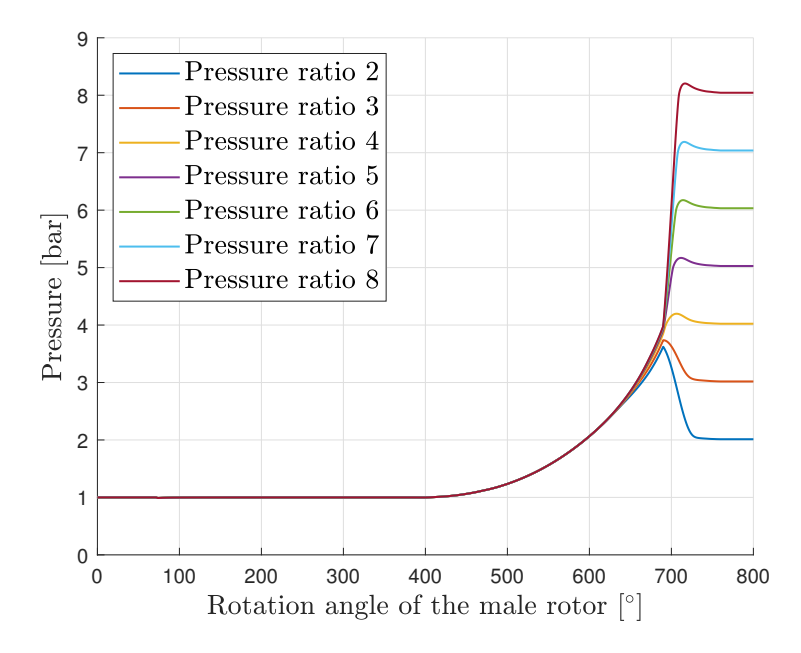


Figure 4.1: Pressure distribution during the compression process for different pressure ratios.

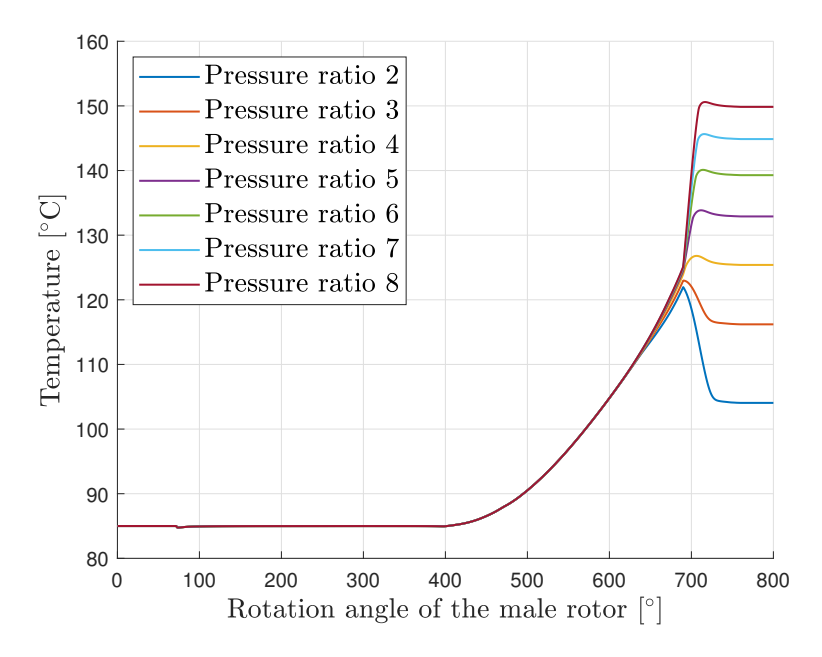


Figure 4.2: Temperature distribution during the compression process for different pressure ratios.

Table 4.3 presents the isentropic and total efficiency of the compressor operating with NH_3 - H_2O-CO_2 for the different pressure ratios. The isentropic efficiencies for the case of ammonia water are listed as well in this Table, in order to compare the results of the two mixtures. The efficiencies determined for ammonia water use the same suction pressure and ammonia concentration as in Table 4.2. To obtain the same suction vapor quality the suction temperature is slightly increased to 86.82 °C.

For both mixtures the same trend can be observed. The highest efficiency is reached at a pressure ratio of 4. The isentropic efficiencies for NH_3 - H_2O - CO_2 show an improvement up to 3.54 % at a pressure ratio of 4. It is observed that the highest efficiency is reached when the desired discharge pressure is close to the final pressure determined by the initial calculation of the model. Both, over and under compression, lower the efficiency of the compressor. Especially in the case of under compression large efficiency losses are observed.

Table 4.3: Isentropic and total efficiency for the compressor operating with different pressure ratios.

Working fluid	Pressure ratio	2	3	4	5	6	7	8
Ammonia water	η_{is} [%]	61.99	77.13	79.60	77.99	75.40	72.52	69.61
NH ₃ -H ₂ O-CO ₂	η_{is} [%]	63.57	79.34	83.14	80.48	77.87	74.96	72.07
NH ₃ -H ₂ O-CO ₂	η_{tot} [%]	57.21	71.4	74.83	72.43	70.08	67.46	64.86

4.2. EFFECT OF VAPOR QUALITY

To investigate the influence of the vapor quality on the compressor performance the suction temperature is varied. In Table 4.4 the operation conditions that are used during these calculations are listed.

Table 4.4: Operation conditions used for the comparison of different vapor qualities.

CO ₂ concentration	5	[wt%]
NH ₃ concentration	20	[wt%]
Suction pressure	1.0	[bar]
Discharge pressure	4.5	[bar]

The pressure and temperature as functions of the rotation angle of the male rotor for different suction vapor qualities are shown in Figure 4.3 and 4.4, respectively. A higher vapor quality causes the pressure to rise at an earlier stage of the compression process. Therefore, the discharge of mass from the compressor starts earlier. This can be seen in Figure 4.3, as the pressure curve shifts more to the left with higher vapor qualities. This is due to the fact that the vapor quality has influence on the leakages in the compressor. With a higher vapor quality, the mixture has a higher specific volume and therefore pushes more flow back through the leakages paths. This trend can be seen as well in Figure 4.4, however, it is less visible. In order to increase the inlet vapor quality, the suction temperature has to be increased and thus the curves do not overlap. At 690 ° the discharge port opens and in Figures 4.3 and 4.4 a change in the slopes of the curves can be observed.

In Figure 4.3 it can be seen that when going to lower vapor qualities, especially for the vapor quality of 20 %, the discharge pressure is getting slightly higher, while the discharge pressure is kept at a constant input value to the model of 4.5 bar. In the case of ammonia water this same trend is observed for lower vapor qualities. However, the overshoot is quite small and does not have much influence on the efficiency of the compressor.

It is observed that for low vapor qualities at the inlet of the compressor ($q_{inlet} < 50$ %), the vapor quality is decreasing during the compression process. For example, when the suction vapor quality is 20 %, the quality at the outlet of the compressor has decreased to 15 %. Going to even lower suction vapor qualities will result in vapor qualities of zero during the compression process and the model fails. Obviously this is not possible, since a liquid becomes incompressible. For higher vapor qualities at the inlet ($q_{inlet} > 50$ %), the vapor quality is increasing during the compression. A higher vapor quality than 85 % at the inlet, therefore, results in superheating at the outlet of the compressor, which is undesirable.

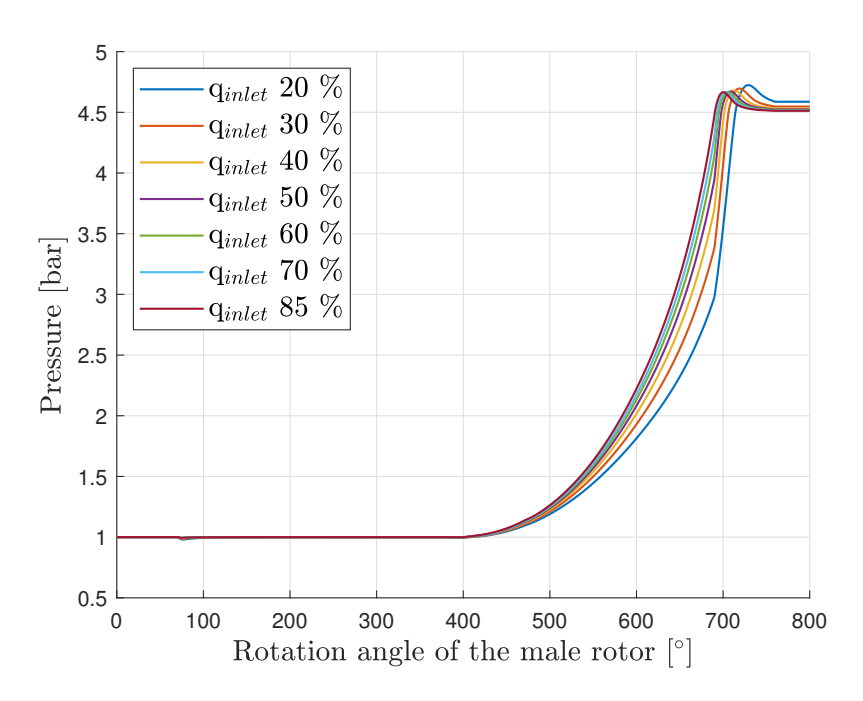


Figure 4.3: Pressure distribution during the compression process for different suction vapor qualities. At 690 ° the discharge port opens.

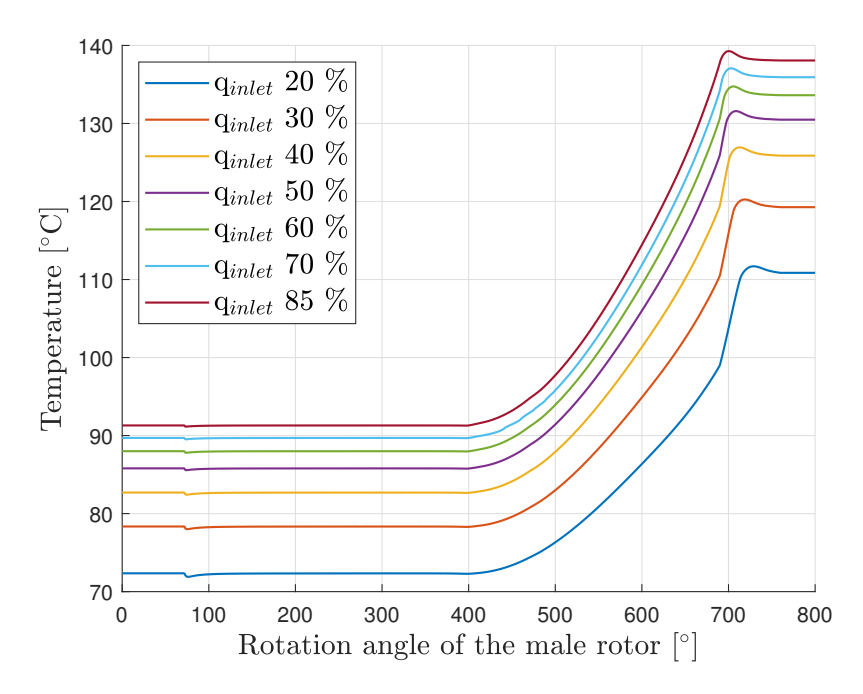


Figure 4.4: Temperature distribution during the compression process for different suction vapor qualities. At 690 ° the discharge port opens.

Table 4.5 gives an overview of the isentropic and total efficiencies of the compressor operating with NH₃-H₂O-CO₂ for the different vapor qualities. Again, the isentropic efficiencies for the case of ammonia water are presented as well in Table 4.5 for comparison.

As mentioned earlier, higher vapor qualities induce more leakages and lower the performance of the compressor. Therefore, it is expected that for lower vapor qualities the isentropic efficiencies increase. This, indeed can be seen in Table 4.5 for both mixtures. Again the NH $_3$ -H $_2$ O-CO $_2$ mixture gives higher isentropic efficiencies than in the case of ammonia water. However, the isentropic efficiency of NH $_3$ -H $_2$ O-CO $_2$ is increasing very rapidly for the lower suction vapor qualities compared to ammonia water. The trend of both mixtures is no longer the same. The addition of CO $_2$ gives for a vapor quality of 20 % an improvement in the efficiency of 14 % and results in an efficiency of 94.56 %. Such a high isentropic efficiency is very uncommon. Therefore, the output parameters of the model are investigated in further detail for both mixtures.

Table 4.5: Isentropic and total efficiency for the compressor operating with different suction vapor qualities.

Working fluid	Vapor quality [%]	20	30	40	50	60	70	85
Ammonia water	η_{is} [%]	80.55	80.14	79.46	78.80	78.21	77.68	77.05
NH ₃ -H ₂ O-CO ₂	η_{is} [%]	94.56	86.41	83.95	81.84	81.09	79.81	78.33
NH ₃ -H ₂ O-CO ₂	η_{tot} [%]	85.10	77.77	75.55	73.66	72.98	71.83	70.50

4.2.1. MODEL LIMITATIONS

Table 4.6 shows the input values to the compressor model for both mixtures in order to investigate the unexpected outcome of the model with NH_3 - H_2O - CO_2 for low suction vapor qualities.

Table 4.6: Operation conditions used for the comparison of $NH_3-H_2O-CO_2$ and ammonia water.

	NH ₃ -H ₂ O-CO ₂	Ammonia water	
CO ₂ concentration	5	-	[wt%]
NH ₃ concentration	20	20	[wt%]
Suction pressure	1.0	1.0	[bar]
Discharge pressure	4.5	4.5	[bar]
Suction temperature	72.35	73.54	[°C]
Suction vapor quality	20	20	[%]

As can be seen in Table 4.6 the suction temperature of NH_3 - H_2O - CO_2 is slightly lower such that the suction vapor quality is for both mixtures exactly 20 %. In Table 4.7 some important output parameters of the model are listed. Most of the output values of the model give similar results for both mixtures.

In Figure 4.5a and 4.5b the pressure and temperature distributions during the compression process can be seen. The pressure curves of the mixtures completely overlap and the temperature curve of $NH_3-H_2O-CO_2$ is slightly lower as mentioned, but shows the same trend as for the ammonia water case.

The indicated power of both mixtures, listed in Table 4.7, is of the same order of magnitude. This is expected since the calculation of the indicated power is based on an integral over the pressure curves.

Due to the fact that a low suction vapor quality is considered, the input values are pushing the limits of the compressor model because the mixture almost becomes an incompressible fluid. However, when looking to the density change during the compression process for both mixtures in Figure 4.6a, it shows that the densities are in the acceptable range. The same trend for both mixtures is observed and the values are of the same order of magnitude.

In Table 4.7 the mass flow is presented as well, but it does not give any information about the leakages during the compression. Therefore, in Figure 4.6b the change in mass during the compression is visualized according to equation 4.1, which includes the inflow and outflow of the leakage paths.

$$\frac{dm}{d\phi} \cdot d\phi + \frac{dm_{in}}{d\phi} \cdot d\phi - \frac{dm_{out}}{d\phi} \cdot d\phi \tag{4.1}$$

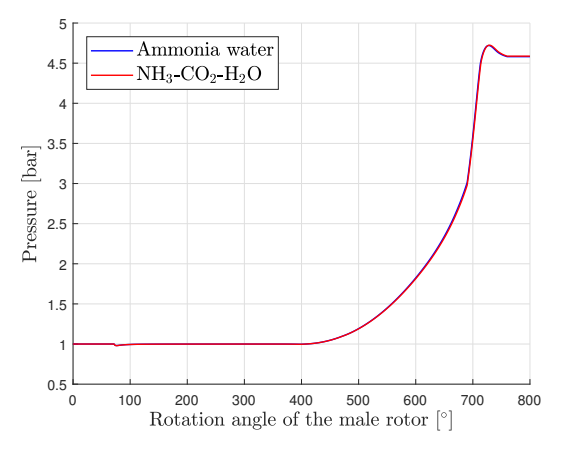
Again, the curves almost completely overlap and the compressor model seems to work satisfactory for both mixtures.

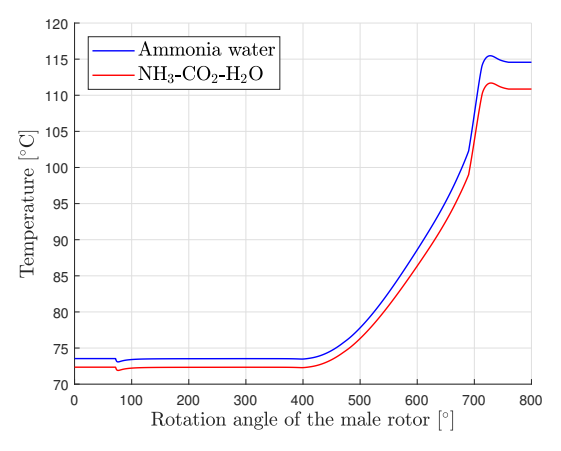
Going back to Table 4.7, it is clear that the enthalpy values of the mixtures are totally different. This is due to the difference in the thermodynamic modeling of the properties of the mixtures using a different reference state. As enthalpy is a thermodynamic potential it must be referred to a defined reference point. The change in enthalpy during the compression

is what is actually used during the calculations and it can be seen that the difference in the suction and isentropic enthalpy is a lot higher for NH₃-H₂O-CO₂ than for ammonia water.

Table 4.7: Output parameters of the model for NH₃-H₂O-CO₂ and ammonia water.

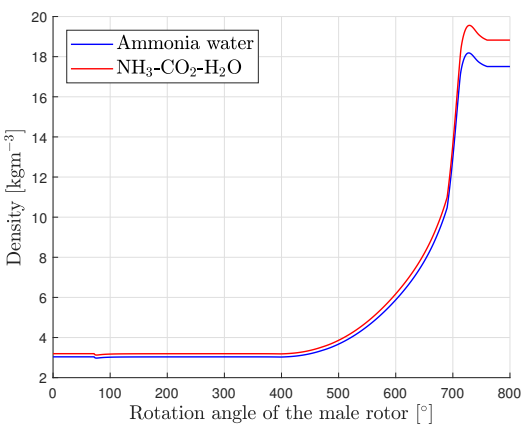
	NH_3 - H_2O - CO_2	Ammonia water	
Discharge temperature	110.86	114.57	[°C]
Mass flow	0.1397	0.1328	$[ms^{-1}]$
Specific volume at the suction	0.3130	0.3292	$[\mathrm{m}^3\mathrm{kg}^{-1}]$
Enthalpy at the suction	$-1.2779 \cdot 10^7$	$6.2889 \cdot 10^5$	$[Jkg^{-1}]$
Isentropic enthalpy	$-1.2728 \cdot 10^7$	$6.7503 \cdot 10^5$	$[Jkg^{-1}]$
$\Delta \left(h_{is}$ - $h_{suc} ight)$	$5.1218 \cdot 10^4$	$4.6139 \cdot 10^4$	$[Jkg^{-1}]$
Indicated power	7565.5	7606.5	[W]
Isentropic efficiency	94.56	80.55	[%]

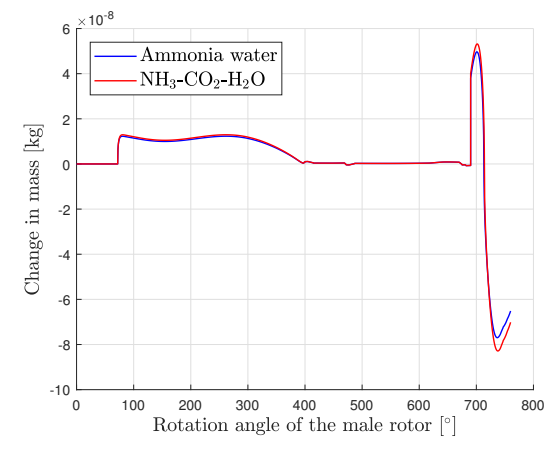




- (a) Pressure distribution during compression.
- (b) Temperature distribution during compression.

Figure 4.5: Output parameters of the compressor model compared for both mixtures.





- (a) Density distribution during compression.
- (b) Change in mass during the compression.

Figure 4.6: Output parameters of the compressor model compared for both mixtures.

As is described in the previous chapter, the model is calculating the isentropic efficiency of the compressor according to the following equation:

$$\eta_{is} = \frac{\dot{m}(h_{is} - h_{suc})}{\dot{W}_{ind}} \tag{4.2}$$

As the indicated power for both mixtures is very similar, the higher value of Δ (h_{is} - h_{suc}) for NH₃-H₂O-CO₂ explains the high isentropic efficiency. The suction enthalpy is determined with the thermodynamic property model based on the inputs pressure and temperature to the model. The pressure and temperature distributions during the complete compression process are determined by solving the mass and energy balances for a control volume of the compressor cavity. During these calculations the change in enthalpy is used at all times, again coming from the property model. The final pressure and temperature distributions are comparable for both mixture. This would indicate that the unexpected behavior is most probably in the isentropic enthalpy calculation. The isentropic enthalpy is the only parameter in the compressor model that is using the entropy of the mixture and the isentropic efficiency calculation is the only parameter that shows significant deviation compared to ammonia water.

In Figure 4.7, the isentropic lines of both mixtures are visualized for the pressure range of this case. Going from right to left over the isentropic lines, the vapor quality gets lower. On first sight the isentropic lines look very similar and especially for the low vapor qualities the lines are almost vertical. From this perspective the isentropic lines for NH₃-H₂O-CO₂ do not clarify the reason for the significant difference in Δ (h_{is} - h_{suc}) of the mixtures.

Next step is to zoom in at the suction and discharge values of the operating conditions listed in Table 4.6, see Figure 4.8 for ammonia water and Figure 4.9 for NH₃-H₂O-CO₂.

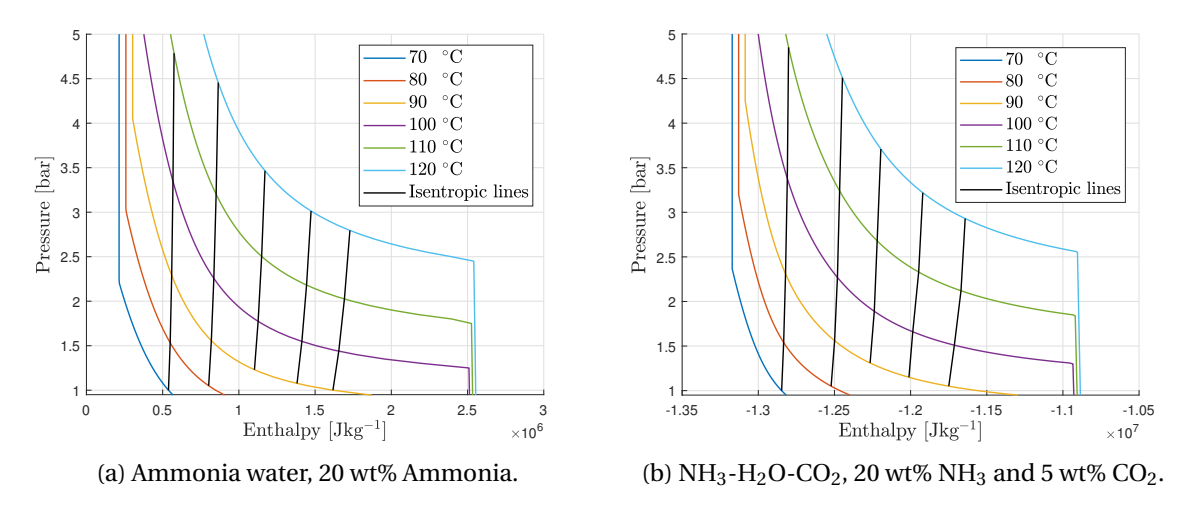


Figure 4.7: Enthalpy-pressure diagram with isentropic lines.

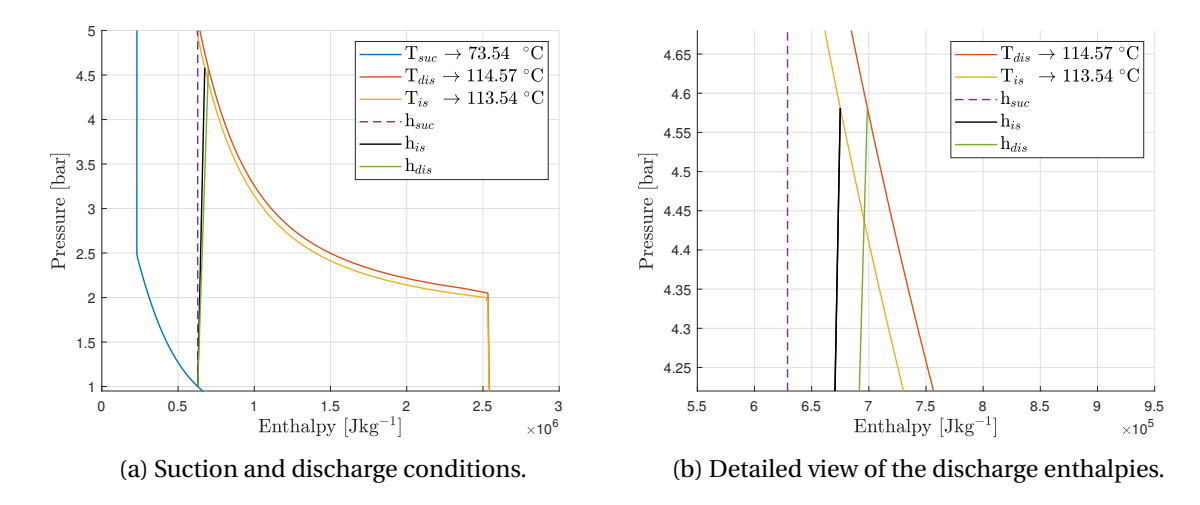


Figure 4.8: Enthalpy-pressure diagram with the suction and discharge conditions of the compression process for ammonia water.

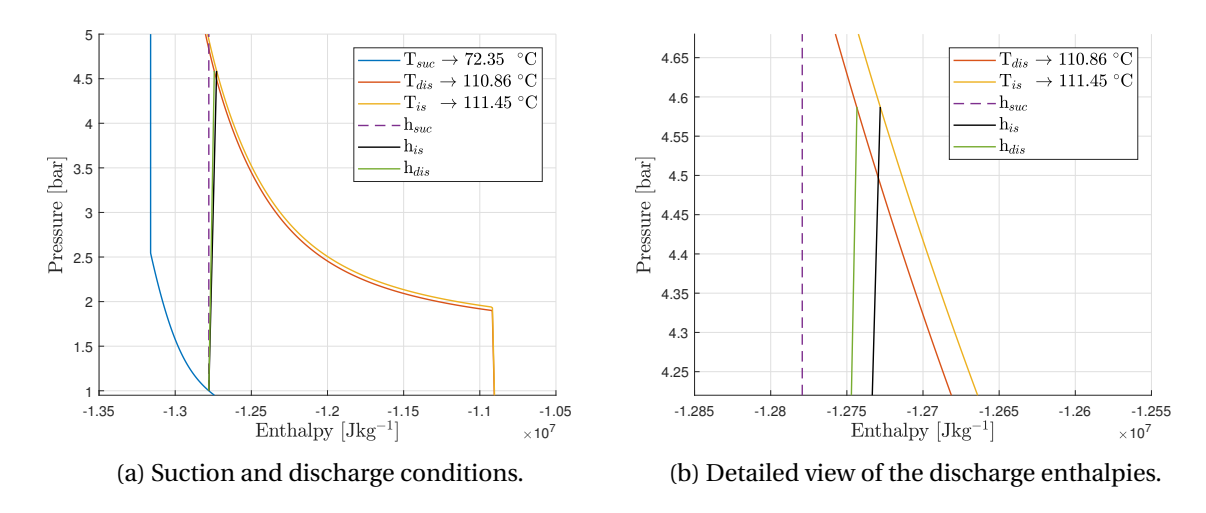


Figure 4.9: Enthalpy-pressure diagram with the suction and discharge conditions of the compression process for NH₃-H₂O-CO₂.

For the ammonia water case (Figure 4.8), it can be seen that the discharge temperature and discharge enthalpy are larger than the isentropic temperature and enthalpy. Isentropic values indicate ideal values, and for an ideal compressor less work is expected than for a compressor where losses are taken into account. The discharge enthalpy needs to be larger than the isentropic enthalpy, otherwise efficiencies larger than one will be reached which is fundamentally wrong. Looking at the case of $NH_3-H_2O-CO_2$ (Figure 4.9), it is actually observed that the isentropic values are higher.

As mentioned, the enthalpy values are determined by the thermodynamic property model. For NH_3 - H_2O - CO_2 the thermodynamic property model developed by Gudjonsdottir et al. [9] is used. This model was based on the electrolyte NRTL model developed by Que and Chen [18]. In this research experimental data on vapor liquid equilibrium, solid liquid equilibrium, heat capacity, heat of dilution and speciation have been regressed to identify the

model parameters. Additional experimental data is used to validate the model. It was concluded that the model enables reliable calculations of the thermodynamic properties with temperature up to 473 K and pressure up to 7 MPa. The model by Gudjonsdottir et al. [9] has even used additional experimental data to regress the model parameters.

The isentropic enthalpy is the only parameter in the compressor model that is determined by using the property entropy. Entropy is not a thermodynamic property that can be directly observed. The entropy has to be calculated and it can not be regressed or compared to measured experimental data. It is possible that the entropy values of the thermodynamic model are calculated incorrectly or contain more inaccuracies. This can result in inaccurate calculations of the isentropic enthalpy values. The entropy calculation in the thermodynamic model developed by Que and Chen [18] is based on the Gibbs free energy, enthalpy and the heat capacity, see Equation 4.3. The reference state Gibbs energy for ionic species i is chosen to be the Gibbs energy at aqueous phase infinite dilution.

$$S_i^{\infty,aq} = \frac{\Delta_f H_{i,298}^{\infty,aq} - \Delta G_{i,298}^{\infty,aq}}{298} + \int_{298}^T \frac{C_{p,i}^{\infty,aq}}{T} dT$$
 (4.3)

The heat capacity is assumed to be temperature independent. Que and Chen [18] do not further exclude whether this assumption is grounded or that some temperature correlation to the heat capacity can exist. This might be a reason for incorrect or inaccurate determined entropy values.

Yaşar Demirel investigated the calculation of excess entropy for binary liquid mixtures by NRTL and UNIQUAC models [6]. In this study an attempt is made to evaluate the accuracy of the excess of entropy predictions by the models with temperature dependent parameters. In a separate study of Yaşar Demirel, the temperature dependence of the energy interaction parameters of the NRTL model, to determine the excess heat capacity, is investigated for 55 binary liquid mixtures [6]. Linear and nonlinear temperature dependencies of the parameters were estimated. It was concluded that the effect of the type of temperature dependence on the performance of the NRTL model was marginal. The performance of the model with nonlinear temperature dependence was slightly better. However, this paper is describing different type of mixtures and equations and there is no guarantee that these findings are applicable for this study. More extensive research is needed on the topic of the temperature dependency of the heat capacity for the NH₃-H₂O-CO₂ mixture.

It should be mentioned that the final enthalpy value at the discharge calculated by the compressor model contains inaccuracies as well. The mass and energy conservation equations include certain assumptions, subsequently the equations are discretized and solved by using enthalpy properties which are interpolated values. If the discharge temperature was only 1 °C higher, the discharge enthalpy would have been larger than the isentropic enthalpy and Figure 4.9b would have been physically correct.

In the previous section, Table 4.5, it was observed that at higher vapor qualities the isentropic efficiencies of ammonia water and NH_3 - H_2O - CO_2 are more comparable. For these suction vapor qualities, similar curves as for Figure 4.9b have been drawn and can be find in Appendix A. At suction vapor qualities from 45% and higher, the isentropic temperature and enthalpy are lower than the discharge values. It is, therefore, expected that the results for higher suction vapor qualities (q > 45%) of the model with NH_3 - H_2O - CO_2 are more reliable than for the lower vapor qualities. For the lower vapor qualities the results present a

non physical solution and the high isentropic efficiencies should not be expected in practice.

Going back to the first section, where different pressure ratios are investigated with the model, the suction vapor quality was 47 %. This vapor quality is sufficiently high and both mixtures showed comparable isentropic efficiencies during this comparison. These calculations are therefore not revisited. Still, it is important to keep in mind these limitations of the model and look to other performance indicators then only the isentropic efficiency, especially for lower suction vapor qualities. The indicated power can be a performance indicator for the compressor as well. The indicated power is not only influenced by the pressure ratio or the vapor quality of the working fluid. The mass flow of the working fluid has a large influence on the indicated power. In order to compare the indicated powers, these operation conditions for both mixtures must be comparable. Then, if a lower indicated power for NH_3 - H_2O - CO_2 is determined it can indicate that the performance of the compressor is higher.

Tables 4.8 and 4.9 present the indicated powers for the previous investigations, i.e. different pressure ratios and different vapor qualities. When increasing the pressure ratio the indicated power increases. This is expected since the indicated power is calculated by the integral over the pressure curve. To reach the same pressure ratio, $NH_3-H_2O-CO_2$ gives slightly lower indicated powers than for ammonia water. However, it should be kept in mind that the mass flow in the case of $NH_3-H_2O-CO_2$ is slightly higher than for ammonia water. A higher mass flow results in a higher indicated power. Even then, $NH_3-H_2O-CO_2$ still shows slightly lower indicated powers, however, the differences are less than 1%.

When the suction vapor quality increases, it follows that the indicated powers are higher since the pressure curve shifts to the left, see Figure 4.3. The indicated powers for NH $_3$ -H $_2$ O-CO $_2$ are slightly lower than for ammonia water. However, the mass flows for NH $_3$ -H $_2$ O-CO $_2$ are again slightly higher than for ammonia water.

Table 4.8: Indicated power for the compressor operating with different pressure ratios.

Working fluid	Pressure ratio	2	3	4	5	6	7	8
Ammonia water	\dot{W}_{ind} [kW]	4.92	6.32	7.77	9.25	10.69	12.11	13.51
NH ₃ -H ₂ O-CO ₂	\dot{W}_{ind} [kW]	4.91	6.30	7.75	9.23	10.67	12.09	13.49

Table 4.9: Indicated power for the compressor operating with different vapor qualities.

Working fluid	Vapor quality [%]	20	30	40	50	60	70	85
Ammonia water	\dot{W}_{ind} [kW]	7.61	8.07	8.36	8.57	8.73	8.86	9.01
NH ₃ -H ₂ O-CO ₂	\dot{W}_{ind} [kW]	7.57	8.02	8.33	8.55	8.72	8.85	9.00

4.3. EFFECT OF CO₂ CONCENTRATION

At last the effect of CO₂ addition to ammonia water is investigated. Due to the previous findings, the suction vapor quality is chosen above 45 %. As is observed in the previous results, the vapor quality and pressure ratio have large influences on the isentropic efficiency of the compressor. In order to compare the influence of only the addition of CO₂ on the performance of the compressor, these parameters must be excluded in the comparison. For all four cases the pressure ratio is kept constant at 5. The ammonia concentration is for all cases equal to a value of 20 wt%. During the calculation, the specific volume at the inlet is kept constant as well. This is done because the specific volume has influence on the mass flow displaced by the compressor. By keeping the specific volumes the same, the mass flows of the working fluids are equal as well. Then the indicated power of the compressor can be compared for both working fluids. Furthermore, when the specific volume is larger the compressor needs to be larger to displace the same mass flow, and the capital cost becomes higher. In that case, the addition of CO₂ can still be disadvantageous and thus the size of the compressor is kept constant as well. In order to keep the specific volume and the vapor quality at the suction constant, the suction pressure and temperature are slightly varied for each case. Four cases are investigated, with 0, 2.5, 5 and 10 wt% CO₂ addition. Table 4.10 gives an overview of the operation conditions for the following calculations.

Table 4.10: Operation conditions used for the comparison of 0, 2.5, 5 and 10 wt% CO_2 addition to the ammonia water working fluid.

CO ₂ concentration	0	2.5	5	10	[wt%]
NH ₃ concentration	20	20	20	20	[wt%]
H ₂ O concentration	80	77.5	75	70	[wt%]
Specific volume at the suction	1.064	1.068	1.068	1.067	$[\mathrm{m}^3\mathrm{kg}^{-1}]$
Pressure ratio	5	5	5	5	[-]
Suction pressure	1.0	0.965	0.952	0.917	[bar]
Discharge pressure	5.0	4.825	4.76	4.585	[bar]
Suction temperature	90.0	88.3	87.3	84.8	[°C]
Quality at the suction	63.2	63.1	63.4	63.4	[%]

The pressure as a function of the rotation angle of the male rotor for the different concentrations of CO_2 is presented in Figure 4.10. In order to keep the specific volume and vapor quality at the suction the same, the suction pressure slightly decreases when the addition of CO_2 increases. It follows automatically that the discharge pressures are lower to keep the pressure ratio the same.

The temperature as a function of rotation angle of the male rotor for the different concentrations is presented in Figure 4.11. The same trend as for the pressure can be seen in the temperature distribution. When the amount of CO_2 increases the temperature is slightly lower to keep the same specific volume and vapor quality.

Finally Table 4.11 gives the isentropic efficiency of the compressor for the different concentrations of CO_2 . In the case of 2.5 wt% and 5 wt% CO_2 addition, the isentropic efficiency increases with 2.7 % and 3.5 % respectively, compared to the working fluid with only am-

monia water. The difference between the 5 wt% and 10 wt% CO_2 addition is very small. For the 10 wt% CO_2 the performance of the compressor is predicted to decrease slightly compared to 5 wt% CO_2 . The indicated power for the different concentrations of CO_2 is tabulated as well. In this comparison, the mass flows are the same for all working fluids and the indicated power with CO_2 addition decreases. With the mass flows being the same, the difference in indicated power of NH_3 - H_2O - CO_2 and ammonia water can be much better observed than in Tables 4.8 and 4.9 and gives a better indication about the performance the compressor.

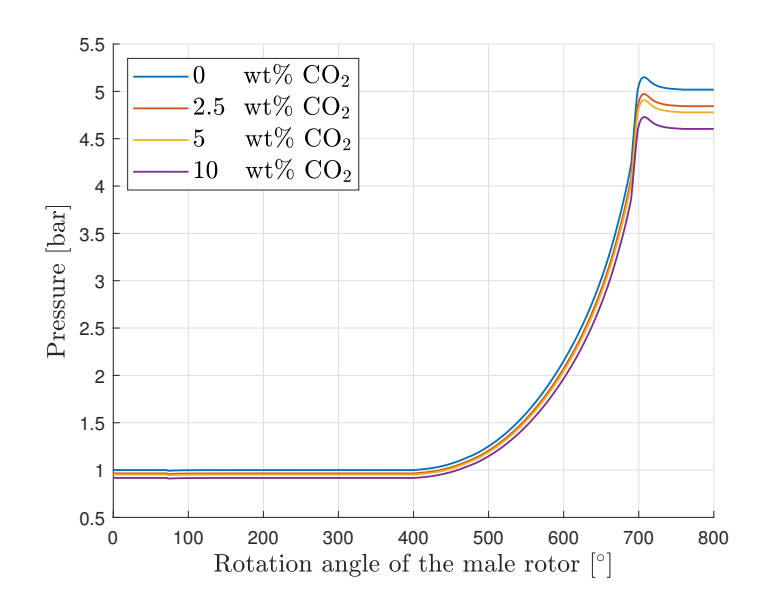


Figure 4.10: Pressure during the compression process for 0, 2.5, 5 and 10 wt% $\rm CO_2$ addition, where the pressure ratio is kept constant at 5.

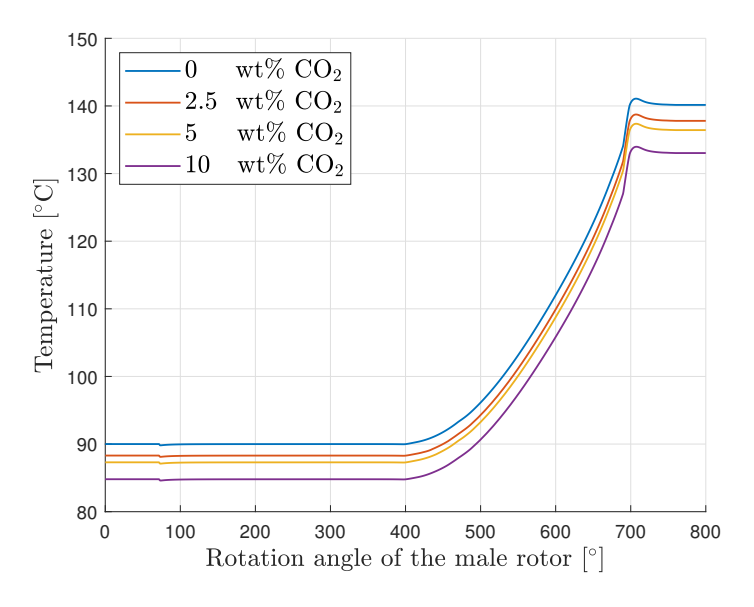


Figure 4.11: Temperature during the compression process for 0, 2.5, 5 and 10 wt% CO₂ addition.

4.4. CONCLUSION 55

Table 4.11: Isentropic and total efficiency of the compressor for different concentrations of CO_2 addition to ammonia water.

CO ₂ addition [wt%]	0	2.5	5	10
η_{is} [%]	77.25	79.95	80.77	80.33
η_{tot} [%]	69.53	71.96	72.69	72.30
\dot{W}_{ind} [kW]	9.53	9.19	9.06	8.72

4.4. CONCLUSION

The effect of pressure ratio, vapor quality and CO_2 concentration are studied with the compressor model operating with NH_3 - H_2O - CO_2 . It can be concluded that the addition of CO_2 has a beneficial effect on the performance of the compressor. The isentropic efficiencies of the compressor with NH_3 - H_2O - CO_2 are higher compared to ammonia water for all investigated cases.

However, for low suction vapor qualities, the efficiency for $\mathrm{NH_3\text{-}H_2O\text{-}CO_2}$ is increasing very rapidly and reaches unexpectedly high values of even 94%. It was found that for low vapor qualities (q < 0.45) the isentropic values at the discharge are higher than the actual discharge values, which is physically incorrect. The problem is probably caused by inaccuracies of the thermodynamic property model implemented in Aspen. Extended research is needed. The indicated power should be used as a performance indicator instead. This parameter can be used to compare the different working fluids only if the operation conditions, such as pressure ratio, vapor quality and mass flow, are the same.

For higher vapor qualities (q > 0.45), the isentropic efficiencies of NH₃-H₂O-CO₂ and ammonia water are more comparable and improvements of the efficiency for NH₃-H₂O-CO₂ are up to 3.5%. These results are considered more reliable.

The analysis of the efficiency of the compressor can be continued in the calculations of the performances of CRHP cycles. Preliminary research investigated that the addition of CO_2 can lead to higher performances of CRHP cycles for certain applications. However during these calculations the isentropic efficiency was assumed to be the same for the different working fluids. When the results of the compressor model are combined with the cycle calculations, the advantage of CO_2 addition in the cycle can become even greater. Therefore, the next step is to combine the results of the compressor model with the performance calculations of a CRHP cycle.

THE HEAT PUMP CYCLE PERFORMANCE

The performance of ammonia water and NH₃-H₂O-CO₂ operating in a CRHP cycle has been calculated previously [9]. In these heat pump cycle calculations, the isentropic efficiency of the compressor was always taken as a constant value. Even though, different working fluids were considered in the cycles, which lead as well to different operating conditions during the compression process, e.g. suction and discharge pressure. These parameters influence the compression process and should result in different performances of the compressor. The isentropic efficiency of the compressor has a great influence on the COP of the heat pump and it was not investigated if the addition of CO₂ and the difference in operation conditions affected the performance of the compressor. Indeed, when the efficiency is taken as a constant value, the addition of CO₂ can lead to higher COP values in certain applications, as reported by Gudjonsdottir [9]. However, when the compressor model indicates lower isentropic efficiencies for NH₃-H₂O-CO₂, the benefits of CO₂ addition may disappear and vice versa, the benefits can become even greater. With the availability of this compressor model the isentropic efficiency can be investigated for ammonia-water and for NH₃-H₂O-CO₂ and take the difference in operating conditions of the heat pump cycle into account as well. In conclusion, the COP values that follow in this report include a more detailed calculation of the compression process, which may prove if the addition of CO₂ indeed can accomplish higher COP values compared to the ammonia water case.

One of the final goals of this research is to improve the performances of CRHPs. The more conventional VCHPs use the well-known dry compression process and for these compressors isentropic efficiencies of 75 % are plausible. The performance of a wet compression resorption cycle is still largely dependent on the isentropic efficiency of the compressor. In Chapter 4, the compressor model was used to compare the efficiencies of the compressor with ammonia water and NH_3 - H_2O - CO_2 . The compressor model showed promising results for the efficiency of both mixtures. When the operation conditions were kept constant, the addition of CO_2 resulted in even higher efficiencies. This way CRHPs can actually compete with the more conventional VCHPs.

5.1. PERFORMANCES OF THE COMPRESSION-RESORPTION HEAT PUMP CYCLE

Zühlsdorf et al. [33] analyze approaches for the selection of working fluids for the design of heat pump cycles based on numerical modeling. In their research, Zühlsorf et al. develop a general method for evaluating and comparing different pure and binary working fluids for a heat pump cycle. The focus lies on comparing the performance of different working fluids rather than different cycle layouts. The considered cycle layout during their research is a VCHP cycle. For comparing the performances of the different working fluids economic and thermodynamic performance indicators are introduced. The thermodynamic performance indicator is the COP of the heat pump. The analysis of the performance for the different working fluids is on the basis of specific applications. It is mentioned that when the comparison of the working fluids is based on only internal cycle temperatures, the COP constitutes an insufficient indicator for comparison. The solutions are able to operate between different boundary conditions in terms of source and sink temperatures and the same COP corresponds to different second law efficiencies. Therefore, Zühlsdorf et al. introduce two case studies that provide for the boundary conditions in which the heat pump needs to operate. The case studies consist of the inlet and outlet temperatures of the heat source and sink, e.g. the heating and cooling requirements. Additionally, one parameter was defined for defining the load of the cycle. This could be either duty of the sink or source. One of these case studies, presented in Table 5.1, is used to compare the performances of ammonia water and NH₃-H₂O-CO₂ in the CRHP cycle and with the best performing fluids in a VCHP cycle reported by Zühlsdorf et al. The case study focuses on the integration of a heat pump to utilize the excess heat from data centers for supplying district heating.

Table 5.1: Thermodynamic boundary conditions and modelling assumptions for the heat pump design of the case study.

Thermodynamic boundary conditions:		
Heat source, $T_{source,in} \rightarrow T_{source,out}$	$50 \rightarrow 25$	[°C]
Heat sink, $T_{sink,in} \rightarrow T_{sink,out}$	$50 \rightarrow 75$	[°C]
Supplied cooling source, \dot{Q}_{source}	500	[kW]
Heat pump modelling assumptions:		
Analyzed cycle	CRHP	
Analyzed cycle Isentropic compressor efficiency	CRHP 75	[%]
	01111	[%] [%]

Outlet resorber Working fluid phase

For the given modelling assumptions of Figure 5.1, an extra constraint is added since a CRHP is considered instead of a VCHP. The working fluid has to be in the two-phase regime during the complete cycle. For a VCHP the working fluid is superheated during the compression process and the outlet of the resorber is subcooled.

Saturated liquid

Two-phase regime

The best performing working fluids in the VCHP for this application, based on the highest COP values, reported by Zühlsorf et al. are listed in Table 5.2. The economic performance indicators are not included in these COP values since it is outside the scope of this research. During their analysis a theoretical ideal cycle is described, where the term ideal refers to the abstraction of the fluids to show a linear temperature behavior in the heat exchangers. This would yield to an ideal performance as the temperature glides of the source and sink perfectly match the temperature glide of the working fluid, as shown in Figure 5.1.

Table 5.2: Best performing working fluids in VCHP for the case study of Table 5.1 reported by Zühlsorf et al. [33].

Composition working fluid	COP
50 wt% DME / 50 wt% Isopentane	6.4
30 wt% DME / 70 wt% Isopentane	6.7
40 wt% Hexane/ 60 wt% R-1234ze(Z)	6.7
30 wt% Propylene/ 70 wt% R-1234ze(Z)	6.2

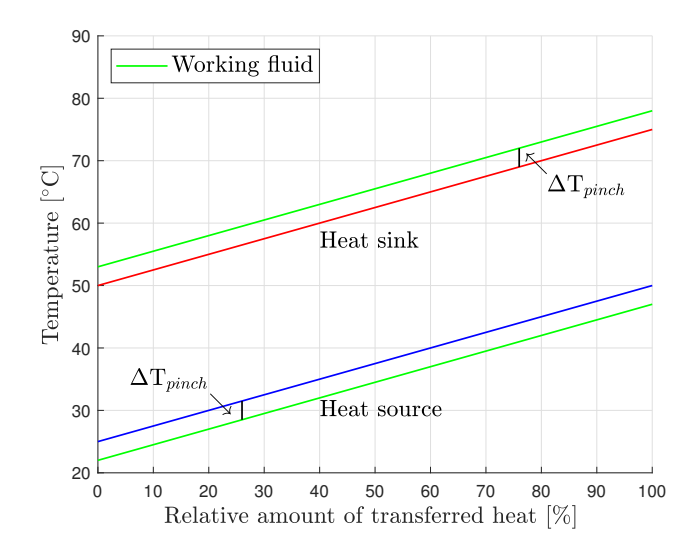


Figure 5.1: Heat transfer diagram for the case study of Table 5.1. The working fluid shows an ideal temperature glide.

The performances of a CRHP operating with ammonia water and NH_3 - H_2O - CO_2 are first investigated with an assumed theoretical ideal cycle, as shown in Figure 5.1. Then the real temperature glides of the working fluids along the HEXs are investigated. Additionally, the compressor model is used to investigate the performance of the wet compression process for ammonia water and NH_3 - H_2O - CO_2 for this application.

PERFORMANCES OF THE CRHP WITH A THEORETICAL IDEAL CYCLE

The equations used to model CRHP cycle are listed in Figure 5.2. The cycle calculations are carried out in Matlab. During the cycle calculation it is assumed that the expansion valve behaves adiabatically and therefore the enthalpy of the working fluid over the expansion

valve is constant. There are no pressure losses taken into account in the resorber and desorber, which means that $p_1 = p_4$ and $p_2 = p_3$. The pressure level in desorber is referred as the lower pressure level in the heat pump (p_1, p_4) and the pressure level in resorber is referred as the higher pressure level (p_2, p_3) . For the thermodynamic properties of ammonia water REFPROP [14] is used and to obtain the thermodynamic properties of NH₃-H₂O-CO₂ the thermodynamic property model in Aspen plus is used, namely the new fit developed by Gudjonsdottir et al. [9]. As mentioned in Chapter 2, the new fit is based on the e-NRTL model developed by Que and Chen [18]. It is reported that the limit of the model by QUE and Chen is to be at 30 wt % ammonia. The new fit by Gudjonsdottir et al. is fitted to additional experimental data, as well, at higher ammonia concentrations and it should give a better indication for ammonia concentrations above 30 wt %. However, the amount of experimental data at high ammonia concentrations is limited and the model still becomes inaccurate when the ammonia concentrations are too high. The comparison between the two mixtures is, therefore, limited to lower ammonia concentrations. To analyze the CRHP cycle with NH₃-H₂O-CO₂, a connection between Matlab and Aspen plus is made via VBA functions in Excel. The method to connect the software is explained in Chapter 3. For the cycle calculations, there is no need to use the property tables since only a few state points need to be calculated. The property values of NH₃-H₂O-CO₂ can be called from Aspen into Matlab via the VBA functions and the performance of the cycle can be analyzed.

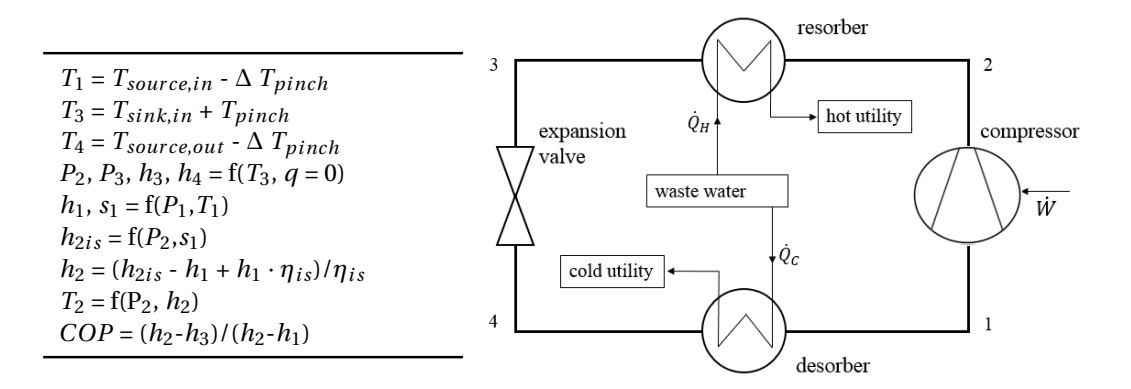


Figure 5.2: Equations used to model a CRHP

When the temperature behavior of the working fluid is assumed to behave linearly, as in Figure 5.1, the cycle calculation comes down to four state points, e.g at the inlet and outlet of the resorber and desorber.

For ammonia water, the results of the maximum COP values can be seen in Figure 5.3. Two maxima can be observed. One at a low ammonia concentration of 16.5 wt% and one at a high ammonia concentration of 82.5 wt%, with COP values of 6.47 and 6.93 respectively. It is observed that for low ammonia concentrations the pressure levels are quite low, see Tables 5.3 and 5.4. The final COP values in Table 5.4 include the motor efficiency. For the ammonia water case with 16.5 wt% ammonia, the lower pressure level is only 0.16 bar, which can be difficult to achieve in practice. When the lower pressure level is restricted to 0.30 bar the ammonia concentration has to increase to 23.5 wt% and the COP is decreasing to 6.40. For the ammonia concentration of 82.5 wt%, the lower and higher pressure levels are 7.2 bar and 17.8 bar respectively, which are acceptable values.

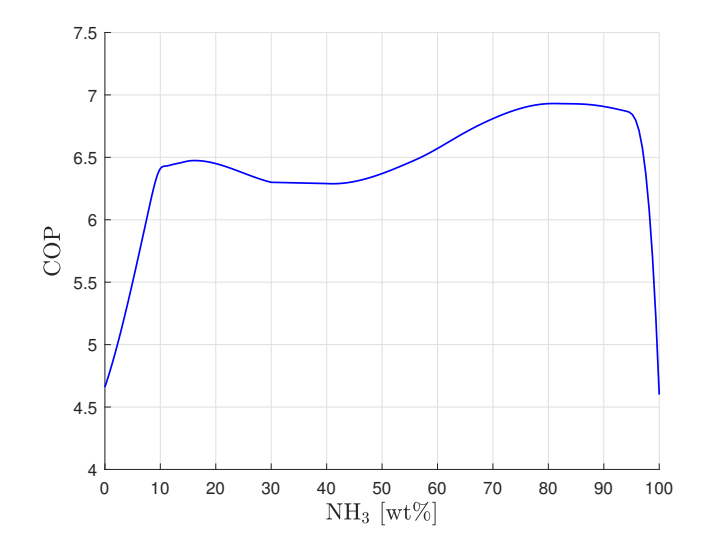


Figure 5.3: Optimum COP of a CRHP with an ammonia water working fluid for the heating and cooling requirements presented in Table 5.1.

For the ammonia water case, the highest COP is reached at an ammonia concentration of 82.5 wt%. However, the thermodynamic property model for NH_3 - H_2O - CO_2 is limited to low ammonia concentrations. Ammonia concentrations up to 50 wt% have been included in the analysis, however, this is pushing to the limits of the thermodynamic property model. Figure 5.4 shows the optimum COPs as a function of the addition of CO_2 , compared to the lower maximum of the ammonia water case (16.5 wt% ammonia). In general, when the addition of CO_2 increases, the ammonia concentration has to be increased as well to reach the optimal cycle performance, see Tables 5.3 and 5.4.

Figure 5.4 shows that no significant improvements are reached witch the addition of CO_2 . Around 10 wt% of CO_2 addition the COP reaches the highest value, which is still slightly lower compared to the ammonia water case. When increasing the addition of CO_2 more than 10 wt% the COP is decreasing again. For 30 wt% CO_2 , the COP has decreased to 5.43, see Tables 5.3 and 5.4.

For the NH_3 - H_2O - CO_2 case the same argument counts that due to the low ammonia concentrations the lower pressure levels are hard to achieve in practice. For the case of 10 wt% CO_2 the lower pressure level is 0.18 bar. When this has to be increased to 0.3 bar, the ammonia concentration is increased from 18.5 to 22.8 wt%, however, the COP decreases from 6.46 to 5.74, see Tables 5.3 and 5.4.

From these results, ammonia water seems to be more suitable for the considered application since the addition of CO_2 shows no improvements. However the real behavior of the mixtures in the resorber and desorber should be taken into account to see the actual applicability of the mixtures in the CRHP for this application.

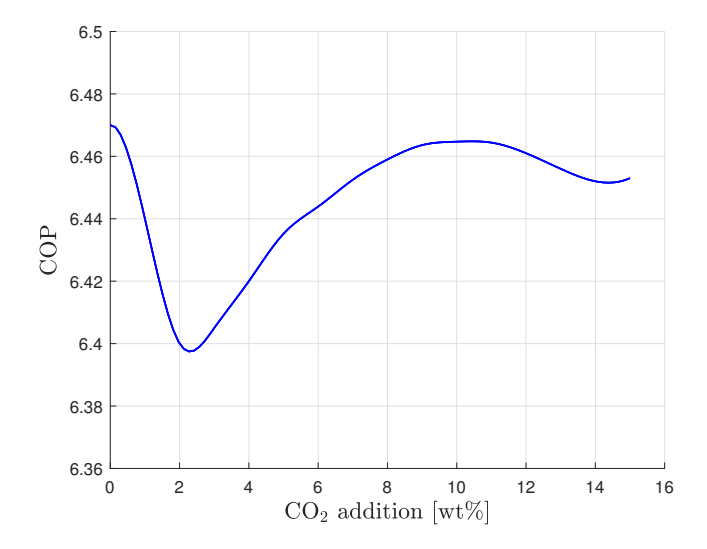


Figure 5.4: Optimum COP of a CRHP with CO_2 wt% addition to an ammonia water working fluid for the heating and cooling requirements presented in Table 5.1. The reference case, no CO_2 addition, is the ammonia water case with 16.5 wt% ammonia.

Table 5.3: Mixture composition, average vapor quality compressor, temperature and pressure for the CRHP cycle for the heating and cooling requirements of the case study presented in Table 5.1. Based on linear temperature profiles of the working fluids.

Model	wt %			q_{avg} (-)	T_1 (°C)	T_2 (°C)	T_3 (°C)	T_4 (°C)	P_{low} (bar)	P_{high} (bar)
	NH ₃	H_2O	CO_2	-						
REFPROP	16.5	83.5	0	0.47	47	87.96	53	22	0.158	0.937
REFPROP	23.5	77.5	0	0.27	47	85.60	53	22	0.3	1.61
REFPROP	82.5	17.5	0	0.65	47	83.33	53	22	7.20	17.8
Aspen Plus, new fit	16	79	5	0.56	47	88.77	53	22	0.156	0.957
Aspen Plus, new fit	18.5	71.5	10	0.57	47	88.92	53	22	0.177	1.08
Aspen Plus, new fit	22.8	67.2	10	0.28	47	83.63	53	22	0.3	1.59
Aspen Plus, new fit	28.5	41.5	30	0.68	47	100.38	53	22	0.3	2.86

Table 5.4: Mixture composition, enthalpy and COP for the CRHP cycle for the heating and cooling requirements of the case study presented in Table 5.1. Based on linear temperature profiles of the working fluids.

Model	wt %		h ₁ (kJ/kg)	h ₂ (kJ/kg)	h ₃ (kJ/kg)	h ₄ (kJ/kg)	COP	
	NH ₃	H ₂ O	CO_2					
REFPROP	16.5	83.5	0	1146.7	1318.4	148.4	148.4	6.47
REFPROP	23.5	77.5	0	675.4	770.0	132.5	132.5	6.40
REFPROP	82.5	17.5	0	1142.3	1259.2	405.9	405.9	6.93
Aspen Plus, new fit	16	79	5	-12534.3	-12332.9	-13696.9	-13696.9	6.44
Aspen Plus, new fit	18.5	71.5	10	-12007.7	-11809.1	-13160.4	-13160.4	6.46
Aspen Plus, new fit	22.8	71.5	10	-12139.1	-12034.2	-12668.3	-12668.3	5.74
Aspen Plus, new fit	28.5	41.5	30	-9795.6	-9533.1	-11033.1	-11033.1	5.43

REAL BEHAVIOR OF THE WORKING FLUIDS ALONG THE HEXS

Instead of just calculating the four state points through the CRHP, the resorber and desorber are discretized to see the actual behavior of the working fluid in the heat exchangers. Figure 5.5 shows the real temperature glides of ammonia water in the resorber and desorber for the ammonia concentrations that gave the highest COPs in the previous analysis. It can be seen that the behavior of ammonia water is far from ideal for these concentrations of ammonia.

At low ammonia concentrations there is a temperature crossover in the desorber. To avoid the temperature crossover in the desorber the temperatures at the inlet and outlet of the desorber need to be decreased. The temperature glide of ammonia water is, therefore, not optimally fitted to the heat source, as in the ideal case, and the COPs for the CRHP cycle decrease. In the case of 16.5 wt%, the temperature outlet of the desorber is decreased from 47 °C to 39.95 °C in order to reach the required pinch of 3 K. The COP decreases to 6.24, see Tables 5.5 and 5.6. Again the motor efficiency is included in the final COP values listed in Table 5.6. At high ammonia concentrations there is a temperature crossover in the resorber. For this case it is not possible to optimally fit the temperature glide of ammonia water to the heat sink. To prevent the temperature crossover in the resorber, the temperature at the outlet of the resorber must be increased and the COP decreases. In the case of 82.5 wt%, the temperature outlet of the resorber is increased from 53 °C to 58.8 °C which lowers the COP to 5.86, see Tables 5.5 and 5.6.

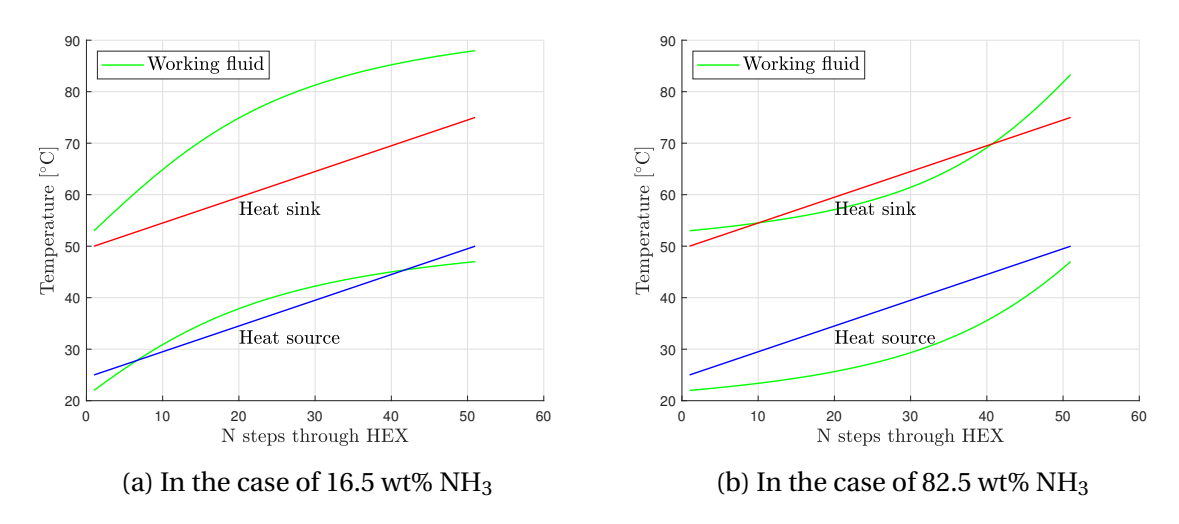


Figure 5.5: Real behavior of the working fluid ammonia water along the HEXs.

Figure 5.6 shows how the COP changes by investigating the actual behavior of ammonia water in the resorber and desorber. For ammonia concentrations between 38 wt% and 48 wt% the two curves overlap. This indicates that ammonia water behaves approximately ideal in the resorber and desorber for this region. Finally, the highest COP of the CRHP with ammonia water is reached in this region, at an ammonia concentration 47.4 wt% and a COP of 6.31. At this ammonia concentration the temperature glides match almost optimal with the heat source and sink, as can be seen in Figure 5.7. The pressure levels at this ammonia concentration are more practical as well, see Tables 5.5 and 5.6.

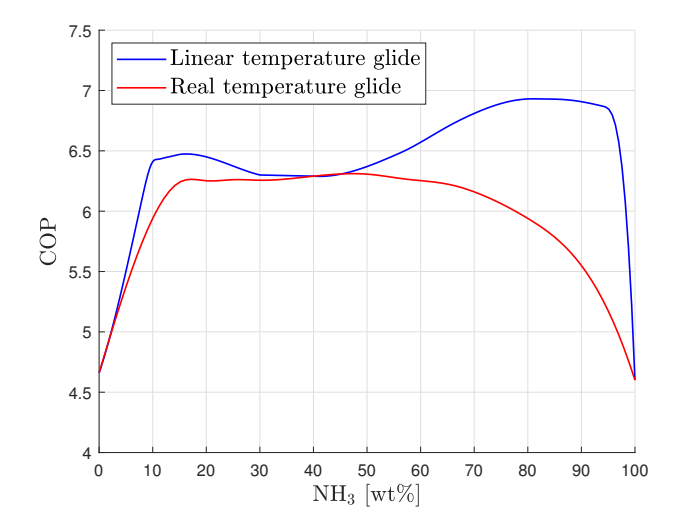


Figure 5.6: Optimum COP of CRHP over the composition of an ammonia water working fluid for the heating and cooling requirements presented in Table 5.1, in the case of a linear temperature glide and the actual behavior of the working fluid along the HEX.

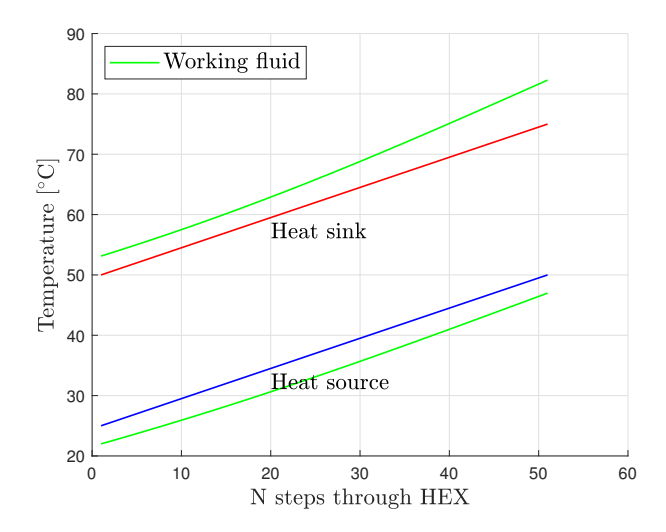


Figure 5.7: Real behavior of the working fluid ammonia water along the HEXs. In the case of 47.4 wt% ammonia, the highest COP of the CRHP cycle is reached for the application presented in Table 5.1.

When the behavior of NH_3 - H_2O - CO_2 is investigated in the resorber and desorber, an even more non ideal behavior is observed compared the ammonia water mixture. Figure 5.8 shows the temperature glide in the desorber of ammonia water and of NH_3 - H_2O - CO_2 with 10 wt% CO_2 addition, where the ammonia concentration is kept constant. It can be seen that the temperature glide of ammonia water fits better to the temperature glide of the heat source than as for the NH_3 - H_2O - CO_2 mixture. To reach the required temperature pinch of 3 K, the inlet and outlet temperature of NH_3 - H_2O - CO_2 at the desorber must be decreased even more, which lowers the performance of the cycle. While increasing the addition of CO_2 , the deviation between the temperature glides of NH_3 - H_2O - CO_2 and the heat source becomes even greater and the performance of the CRHP cycle is declining, see Figure 5.9.

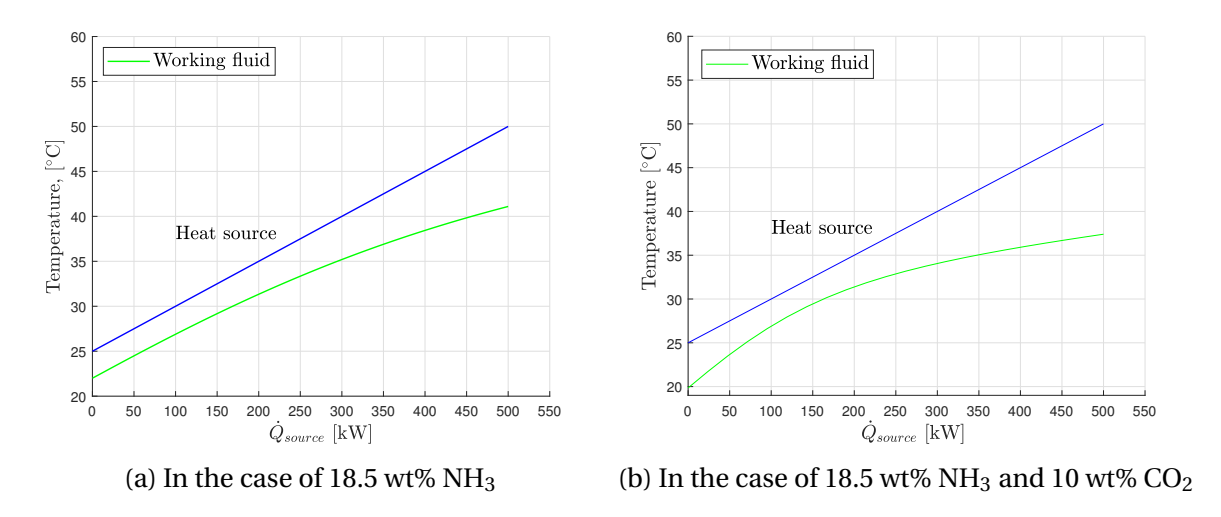


Figure 5.8: Real behavior of the working fluid ammonia water along the HEXs.

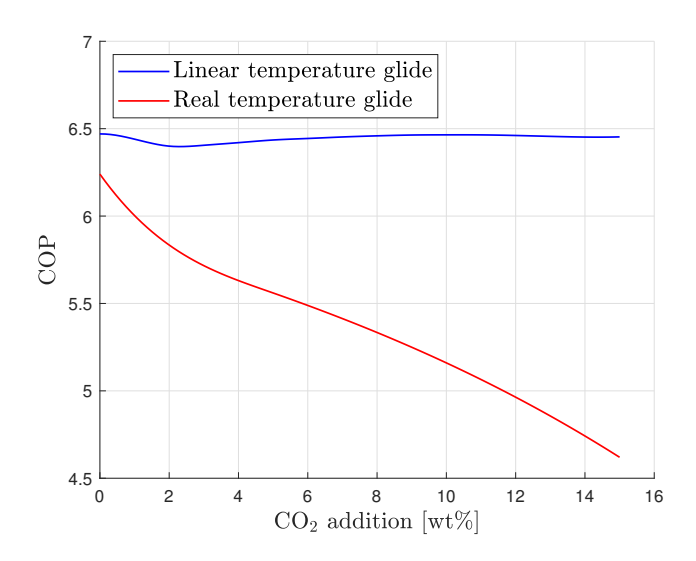


Figure 5.9: Maximum COP of a CRHP with CO_2 wt% addition to an ammonia water working fluid for the heating and cooling requirements presented in Table 5.1, in the case of a linear temperature glide and the actual behavior of the working fluid along the HEX.

In the case of 5 wt% CO_2 addition, the maximum COP was found with an ammonia concentration of 16 wt%. When considering the actual behavior of NH_3 - H_2O - CO_2 in the HEXs, the COP decreases from 6.44 to 5.56, see Figure 5.9 and Tables 5.5 and 5.6

For NH_3 - H_2O - CO_2 the same trend can be observed that as the ammonia concentration increases to values around 40 wt% / 50 wt% the mixture is behaving more ideal. Therefore, slightly higher COPs are found at higher ammonia concentrations. When the ammonia concentration is increased to 50 wt%, for 5 wt% CO_2 , the COP increases to 5.73, see Tables 5.5 and 5.6. It should be mentioned that this ammonia concentration is pushing the limits of the thermodynamic model of NH_3 - H_2O - CO_2 . Therefore, the result can be less accurate but it can still gives an indication of the performance of the cycle.

In this analysis, it becomes clear that the addition of CO_2 for this application is not beneficial. When more CO_2 is added to the ammonia water mixture, the COP of the CRHP decreases even more. The low performances of the CRHP operating with NH_3 - H_2O - CO_2 compared to ammonia water is due to the fact that the temperature glide of NH_3 - H_2O - CO_2 is not fitted well to the heat source. More addition of CO_2 to ammonia water is making this problem only larger.

Previous heat exchanger experiments have confirmed that the heat transfer rate increases with the addition of CO_2 [15]. It follows that, when there is only a heating requirement advantages with the addition of CO_2 can be reached. If an application is considered with only heat requirements, the maximum cycle performance can be found by fitting the temperature glide of the working fluids only to the heat sink. Considering a heating application, the temperature glide in the desorber becomes irrelevant and benefits of the addition of CO_2 become noticeable. Therefore, in section 5.2 two heating applications with a CRHP are considered for NH_3 - H_2O - CO_2 and ammonia water.

Table 5.5: Mixture composition, average vapor quality compressor, temperature and pressure for the CRHP cycle for the heating and cooling requirements of the case study presented in Table 5.1. Based on real temperature profiles of the working fluids.

Model	wt %		q_{avg} (-)	T_1 (°C)	T_2 (°C)	T_3 (°C)	<i>T</i> ₄ (°C)	P_{low} (bar)	P_{high} (bar)	
	NH_3	H_2O	CO_2							
REFPROP	16.5	83.5	0	0.23	39.95	78	53	22	0.158	0.937
REFPROP	47.4	52.6	0	0.27	47	82.3	53.13	22	1.84	6.87
REFPROP	82.5	17.5	0	0.65	47	90	58.8	22	7.14	20.56
Aspen Plus, new fit	16	79	5	0.24	38.72	78	53	21.1	0.147	0.957
Aspen Plus, new fit	50	45	5	0.28	47	83.90	53	22	2.25	8.08
Aspen Plus, new fit	18.5	71.5	10	0.27	37.4	78	53	19.85	0.152	1.08
Aspen Plus, new fit	50	40	10	0.28	47	84.43	53	22	2.40	8.39

Table 5.6: Mixture composition, enthalpy and COP for the CRHP cycle for the heating and cooling requirements of the case study presented in Table 5.1. Based on real temperature profiles of the working fluids.

Model	wt %		h_1 (kJ/kg)	h ₂ (kJ/kg)	h ₃ (kJ/kg)	h ₄ (kJ/kg)	COP	
	NH ₃	H ₂ O	CO_2					
REFPROP	16.5	83.5	0	611.4	694.5	148.4	148.4	6.24
REFPROP	47.4	52.6	0	567.4	640.9	153.0	153.0	6.31
REFPROP	82.5	17.5	0	1144.8	1282.2	434.9	434.9	5.86
Aspen Plus, new fit	16	79	5	-13237.1	-13142.3	-13697.0	-13697.0	5.56
Aspen Plus, new fit	50	45	5	-9329.1	-9245.7	-9748.7	-9748.7	5.73
Aspen Plus, new fit	18.5	71.5	10	-12660.1	-12547.1	-13160.4	-13160.4	5.16
Aspen Plus, new fit	50	71.5	10	-9089.6	-8999.6	-9489.8	-9489.8	5.18

COMPARISON OF THE PERFORMANCES OF THE CRHP AND THE VCHP

It is clear that the working fluid NH_3 - H_2O - CO_2 in the CRHP is not beneficial for this type of applications. The performances of the CRHP operating with ammonia water for the given application shows promising results. The highest COP is 6.31 with an ammonia concentration 47.4 wt%. The performances of ammonia water in a CRHP is comparable with the best performing working fluids in a VCHP reported by Zühlsorf et al. [33] for the same application. However, Table 5.2 shows that a few working fluids in a VCHP perform better than ammonia water in a CRHP. The working fluids DME isopentane with 30 wt% DME and hexane R-1234Ze(Z) with 40 wt% hexane result in the highest COP values of 6.7.

Zühlsorf et al. based their analysis on the assumptions of a theoretical ideal cycle, where the working fluids show a linear temperature behavior along the HEXs, see Figure 5.1. For ammonia water and NH_3 - H_2O - CO_2 it was observed that for lower and higher ammonia concentrations significant temperature crossovers occurred in the HEXs. The addition of CO_2 only made it worse, see Figure 5.8. The temperatures at the inlet and outlet of the desorber and at the outlet of the resorber needed to be adjusted to avoid the temperature crossovers.

Zühlsorf et al. used REFPROP to obtain the thermodynamic properties of the working fluids. Since this software is accessible, REFPROP can be used to investigate the temperature glides along the HEXs for the best performing working fluids in a VCHP of Table 5.2. Figure 5.10 shows the temperature glides along the HEXs of DME isopentane for two different mixture compositions. The temperature glides of DME isopentane with 30 wt% DME, Figure 5.10a, shows a very linear behavior. The black dashed lines indicate the required temperature pinch. It can be seen that no temperature crossovers occur and the temperatures at the inlet and outlet of the desorber and at the outlet of the resorber do not need to be adjusted. Other mixture compositions of DME isopentane are investigated, since for ammonia water the non ideal behavior was especially observed for the lower and higher ammonia concentrations. When for the mixture DME Isopentane, the concentration for DME is increased and decreased it is indeed observed the behavior becomes less ideal, see Figure 5.10b. The COP decreases for this composition to 5.84. For DME isopentane the same shape as the red curve of ammonia water shown in Figure 5.6 can be observed. The highest COPs are reached when the concentrations of the components of the mixture lie closer to each other, in this region the temperature glide is almost linear. The COP decreases when the concentration of the components lie further apart from each other. The other working fluids presented in Table 5.2 are investigated as well and the same observations are found. Not all the working fluids reported by Zühlsorf et al. behave this way. Some working fluids that are reported, do show the highest COPs at the lower and higher concentrations of one of the two components, e.g. propane isopentane.

However, the values reported by Zühlsorf et al. should be considered with care, since temperature crossovers have been neglected by these authors.

In conclusion, the performance of ammonia water in the CRHP is quite comparable with the best performing working fluids in the VCHP. A few working fluids in a VCHP reported by Zühlsorf et al. perform slightly better. It is provided that the compressor has an isentropic efficiency around 75%. The isentropic efficiency is taken as a constant value during this analyses. Therefore, the wet compression process is investigated making use of the compressor model.

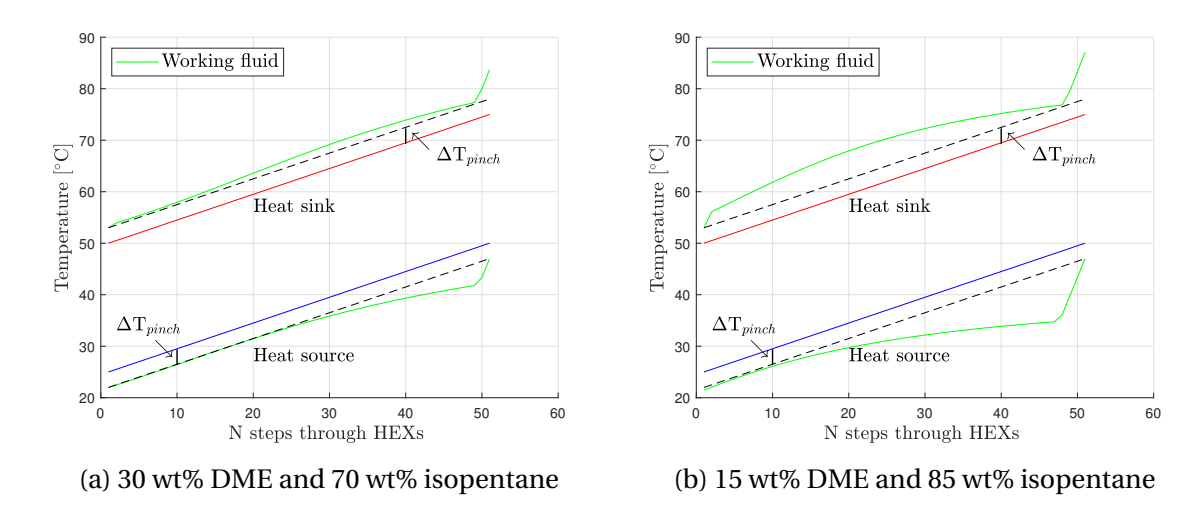


Figure 5.10: Temperature glides along the HEXs of DME isopentane in a VCHP reported by Zühlsorf et al. (Table 5.2) for the application presented in Table 5.1

COMPRESSOR MODEL

In Chapter 4, it was indicated that the addition of CO_2 has positive effects on the isentropic efficiency of the compressor. In the comparison of the mixtures many factors that can influence the isentropic efficiency besides the addition of CO_2 were kept constant, i.e. the pressure ratio, vapor quality and the mass flow. In this analysis, the two mixtures are compared as working fluids in a CRHP for a specific application. It is not possible to exclude all these factors from the comparison and still satisfy the requirements of the application due to the differences in the properties of the mixtures. The results from the compressor model for ammonia water and NH_3 - H_2O - CO_2 should, therefore, not be compared on its own. The focus lies on the final results of the determined efficiencies by the compressor model included in the calculations of the COP for the CRHP for this specific application.

The results from the heat pump cycle calculation provide the input values to the compressor model i.e. the suction pressure and temperature, discharge pressure and mixture composition. The application, presented in Table 5.1, include the duty of the heat source. From this requirement, the mass flow through the heat pump cycle is determined according to:

$$\dot{m} = \frac{\dot{Q}_{source}}{(h_1 - h_4)} \tag{5.1}$$

However the mass flow in the compressor model is restricted by the geometry of the compressor. The determined mass flows in the compressor model do not match with the mass flows determined in the heat pump cycle with Equation 5.1. To match the mass flows, the

compressor sizes must be scaled up. In this study, the compressor model is used as an indication of the isentropic efficiency of the compressor and only this value is included in the performance calculation of the heat pump cycle. In the COP calculation the mass flows is cancelled out.

Figure 5.11 presents the isentropic efficiency of the compressor for the different compositions of ammonia water in the CRHP for this specific application. It is emphasized that the operation conditions are different for the different compositions, thus this graph is not presenting a direct relation between isentropic efficiency and ammonia concentration.

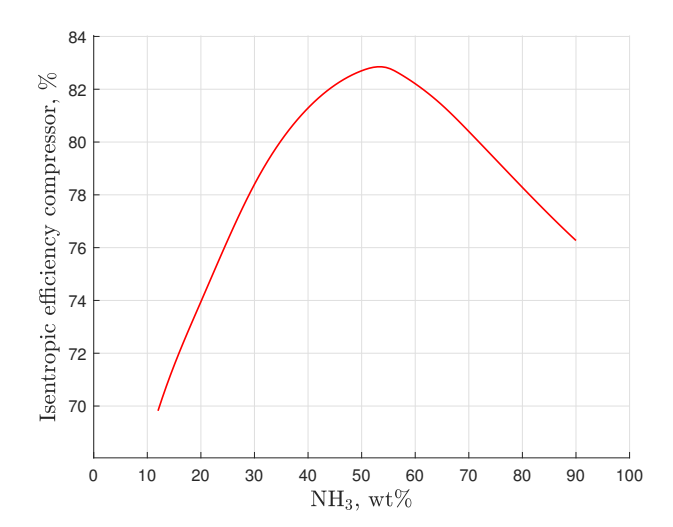


Figure 5.11: Isentropic efficiency vs ammonia wt% predicted by the compressor model. Different compositions of the mixture lead to different operating conditions

The highest isentropic efficiency of the compressor determined by the model is 82.8 % at an ammonia concentration of 55 wt%. For ammonia concentrations above 25 wt%, higher isentropic efficiencies than 75 % for the compressor are predicted by the model and for these cases the COP values are increasing. Table 5.7 presents the mass flow, indicated power and isentropic efficiency predicted by the compressor model for several mixture compositions. It can be seen that the indicated power increases with higher mass flows. Table 5.7 shows how the COP is changing by the results of the compressor model. It shows that the isentropic efficiency has significant influence on the performance of the cycle. The highest COP that was found for the CRHP with ammonia water at the ammonia concentration of 47.4 wt% is increased from 6.31 to 6.83 due to the higher predicted isentropic efficiency of the compressor. The COP values in Table 5.7 include the motor efficiency of 95%.

The isentropic efficiency of the compressor operating with NH_3 - H_2O - CO_2 is determined for the cases of 2.5, 5, 10 wt% CO_2 . However, Tables 5.5 and 5.6 show that the average vapor quality in the compressor is quite low. The low vapor qualities are the result from the thermodynamic boundary conditions of the application. In the previous chapter, section 4.2, it was observed that for low vapor qualities the compressor model with NH_3 - H_2O - CO_2 determined very high isentropic efficiencies, which are not expected to be reached in practice.

Table 5.7: Results of the compressor model for different compositions of ammonia water as working fluid. The COP with the assumed isentropic efficiency of 75% and the new COP with the isentropic efficiency predicted by the compressor model. The COP values include the motor efficiency of 95%.

NH ₃ [wt%]	$ q_{avg} $	\dot{m} [kgs ⁻¹]	\dot{W}_{ind} [kW]	$\eta_{is}[\%]$	$\eta_{tot} [\%]$	$COP_{75\%}$	COP_{new}
16.5	0.23	0.018	1.59	72.28	68.67	6.24	6.05
20	0.21	0.028	2.09	73.95	70.23	6.19	6.11
47.4	0.27	0.186	12.53	82.39	78.27	6.31	6.83
55	0.31	0.256	18.01	82.80	78.66	6.29	6.82
82.5	0.65	0.332	44.22	77.76	73.87	5.86	6.04

Table 5.8 presents the isentropic efficiencies for NH_3 - H_2O - CO_2 predicted by the model. Again the isentropic efficiencies determined by the compressor model are very high. Especially for the mixture compositions of 5 wt% CO_2 with 30 wt% and 50 wt% ammonia, indicated by red in Table 5.8. The new determined COP values become 6.86 and 6.97 respectively. For the case of 2.5 wt% CO_2 and 14.8 wt% ammonia the efficiency is 80.57 %, which is not immediately noticed as an uncommon value. However, for the ammonia water mixture with 14.8 wt% ammonia the efficiency is 71 %, see Figure 5.11. This is a difference of 9.5 %. Again it is emphasized that for lower vapor qualities the isentropic efficiencies from the model with NH_3 - H_2O - CO_2 are not to be trusted.

The mass flow and indicated power, listed in Table 5.8, are predicted by the compressor model. These values are very comparable to ammonia water. For the ammonia water mixture with 16.5 wt% ammonia and the NH $_3$ -H $_2$ O-CO $_2$ mixture with 16 wt% ammonia and 5 wt% CO $_2$ the indicated powers are 1.59 kW and 1.58 kW respectively. This indicates that the isentropic efficiencies with NH $_3$ -H $_2$ O-CO $_2$ will probably be more closely to the presented isentropic efficiencies of ammonia water in Table 5.7 than to the efficiencies in Table 5.8. However, it is not possible to compare the performances of only the compression process between both mixtures since the operating conditions of the mixtures are different. The final results of the mixtures performing in the heat pump cycle is what matters.

Table 5.8: Results of the compressor model for different compositions of NH_3 - H_2O - CO_2 as working fluid. The COP with the assumed isentropic efficiency of 75% and the new COP with the isentropic efficiency predicted by the compressor model. The COP values include the motor efficiency of 95%.

NH ₃ [wt%]	CO ₂ [wt%]	$ q_{avg} $	\dot{m} [kgs ⁻¹]	\dot{W}_{ind} [kW]	$\eta_{is}[\%]$	$\eta_{tot} [\%]$	$COP_{75\%}$	COP_{new}
14.8	2.5	0.22	0.019	1.52	80.57	76.54	5.77	6.14
16.0	5	0.24	0.019	1.58	84.47	80.25	5.56	6.15
18.5	10	0.27	0.018	1.76	88.55	84.12	5.16	5.90
30	5	0.21	0.076	4.74	96.05	91.25	5.56	6.86
50	5	0.28	0.224	14.9	95.03	90.28	5.73	6.97

In conclusion, when the cycle calculations are combined with the compressor model the CRHP with ammonia water is performing slightly better than the reported working fluids by Zühlsorf et al.[33]. The compressor model determines higher isentropic efficiencies than 75% for ammonia concentrations above 25 wt%. The COP of the best performing cycle with an ammonia concentration of 47.4 wt% increased to 6.83 due to the increased isentropic efficiency to 82.39%. The compressor model is not able to predict the isentropic efficiency with NH₃-H₂O-CO₂ correctly, due to the low vapor qualities in the compressor. This is caused by the thermodynamic boundary conditions of the application. The indicated powers of both mixtures are very comparable, thus the isentropic efficiencies of NH₃-H₂O-CO₂ are expected to be more in the range of the efficiencies of ammonia water, as in Table 5.7. However, it was already concluded that NH₃-H₂O-CO₂ is not a beneficial working fluid in a CRHP for this application anyway. To investigate the advantage of NH₃-H₂O-CO₂ compared to ammonia water, two heating applications are considered. In the following analysis the thermodynamic conditions are chosen such that the vapor qualities are much higher and the isentropic efficiencies computed by the compressor model with NH₃-H₂O-CO₂ show more reliable results.

5.2. HEATING APPLICATIONS: UPGRADING WASTE WATER STREAMS WITH A CRHP

In the introduction of this report it was mentioned that the application of the CRHP is focused on applications of upgrading waste streams of separation processes. In the previous section, the performances of ammonia water and NH_3 - H_2O - CO_2 in a CRHP were compared for a application with a heating and a cooling requirement. These results were as well compared to several working fluids in a VCHP reported by Zühlsorf et al.[33]. Ammonia water was performing better than NH_3 - H_2O - CO_2 for this application. However, a few of the working fluids in a VCHP performed better than ammonia water in a CRHP, if the isentropic efficiencies were assumed to be equal. In literature it has been reported that CRHPs achieve more advantages especially for large temperature glide applications ([25], [26]). The previous application was selected by Zühlsorf et al. to analyze the performance of a VCHP. In this section larger temperature glides of the heat sink are considered to analyze the performance of a CRHP.

The performance of ammonia water and NH_3 - H_2O - CO_2 in a CRHP are investigated into more detail for two heating cases. The first application is a waste stream of 60 °C upgraded to a temperature of 105 °C by passing the working fluid through the resorber. The waste stream is used as well in the desorber of the cycle to heat up the mixture before it enters the compressor. During this analysis the focus lies on the heating demand of the cycle. This heat application has been investigated by Gudjonsdottir et al. [9] except that the isentropic efficiency of the compressor was an assumed value and not simulated by a theoretical model of the compressor. With the compressor model the isentropic efficiency is determined and the cycle calculations are repeated with these new values.

The second heat application is a higher temperature application, where the waste stream of 95 °C is upgraded to a temperature of 140 °C. This high temperature application is cho-

sen because large application potentials have been recognized for high temperature heat pumps in waste heat recovery processes [1]. First the method of the analysis is shortly discussed, followed by the results for both applications.

METHODOLOGY

The performance of the CRHP cycle is compared for three different working fluids with 0 wt%, 5 wt% and 10 wt% addition of CO_2 to an ammonia water mixture. The approach is similar as the previous analysis. An application is chosen to set the thermodynamic boundary conditions for the cycle, e.g. the temperature glide of the heat sink. During this analysis the vapor quality at the outlet of the compressor is given as a constraint as well. This is done for two reasons. First of all the vapor quality has influence on the COP of the cycle. When the vapor quality of the mixture at the outlet of the compressor is higher, the mixture enters the resorber with an higher vapor quality as well and this results automatically in a higher value for the COP. Theoretically, the highest COP is reached for a quality of 1 at the outlet of the compressor [27]. However, the superheated region must be avoided thus the vapor quality is kept lower than 1. Secondly, the vapor quality has influence on the isentropic efficiency of the compressor. Keeping the vapor quality equal, the isentropic efficiencies can be better compared to each other as well. The vapor qualities are fixed above 0.45 to obtain reliable results from the compressor model with NH $_3$ -H $_2$ O-CO $_2$.

In Figure 5.12 and Table 5.1 the requirements given by the thermodynamic boundary conditions of the applications and the modeling assumptions are summarized. As can be seen in the Figure, the inlet and outlet temperature of the working fluid at the resorber are fixed. This way, all the considered working fluids have the same temperature glide over the resorber. The inlet temperature of the working fluid at the compressor is fixed as well, and thus the temperature lift over the compressor is the same for all cases. The quality at the outlet of the resorber must be 0 such that the mixture is in a saturated liquid state when leaving the resorber.

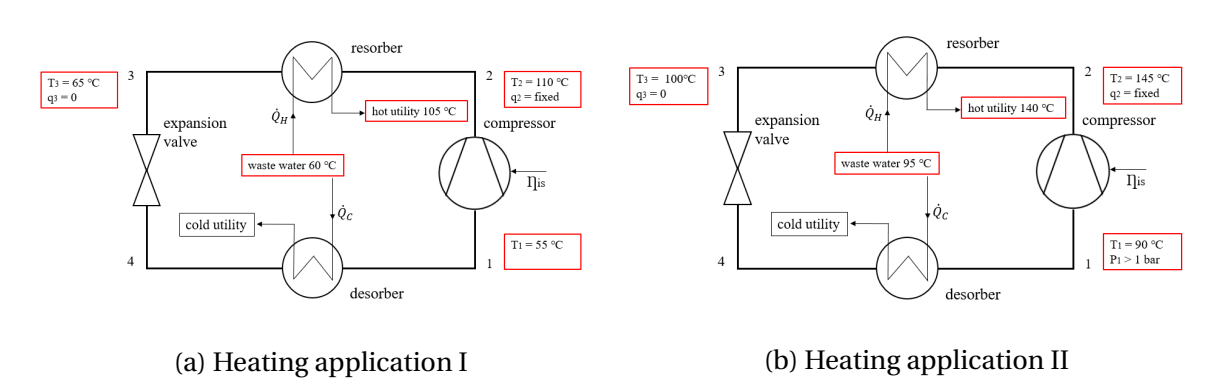


Figure 5.12: Constraints for the heating applications of upgrading waste streams with CRHP cycles operating with working fluids ammonia water and NH₃-H₂O-CO₂.

For the second application, an extra constraint is added to the inlet conditions of the compressor, namely an inlet pressure higher than 1 bar. The prototype compressor, which will be tested in the lab, does not operate well at pressures below 1 bar. The operation conditions of this application can be tested in the lab and the values coming from the compressor model can be validated.

Table 5.9: Thermodynamic boundary conditions and modelling assumptions for the CRHP design of the two heating applications.

Thermodynamic boundary conditions:		
Heat sink application I, $T_{sink,in} \rightarrow T_{sink,out}$	$60 \rightarrow 105$	[°C]
Heat sink application II, $T_{sink,in} \rightarrow T_{sink,out}$	$95 \rightarrow 140$	[°C]
Heat pump modelling assumptions:		
Analyzed cycle	CRHP	
Isentropic compressor efficiency	Compressor model	
Mechanical efficiency	90	[%]
ΔT_{pinch}	5	[K]
Outlet resorber	Saturated liquid	
Working fluid phase	Two-phase regime	
Vapor quality outlet compressor	Fixed	

The CRHP cycle is modelled with the same set of equations listed in Figure 5.2, discussed in the previous section. A simple iteration process is done between the compressor model and the heat pump cycle calculations. First a value for the isentropic efficiency is assumed, for example 70 % is chosen. With the isentropic efficiency and the prescribed conditions of Figure 5.12 and Table 5.9, there are only three parameters left that can be varied. The inlet and outlet pressure of the compressor and the ammonia concentration of the mixture. When for example the inlet pressure is chosen, there is just one combination left for the outlet pressure and ammonia concentration that satisfy the requirements. A Matlab script is used to find the pressure values and the mixture composition leading to the highest COP value for this application.

The inlet pressure, outlet pressure and the composition of the mixture are the input parameters to the compressor model. The compressor model determines the actual expected value for the isentropic efficiency of the compressor. With the new isentropic efficiency from the model, the heat pump cycle calculation is repeated again. The pressure values and the composition of the mixture need to be slightly adjusted to reach again the highest possible COP of the cycle. This calculation is done a couple of times until the isentropic efficiency from the compressor model stabilizes. Figure 5.13 shows this iterative process schematically.

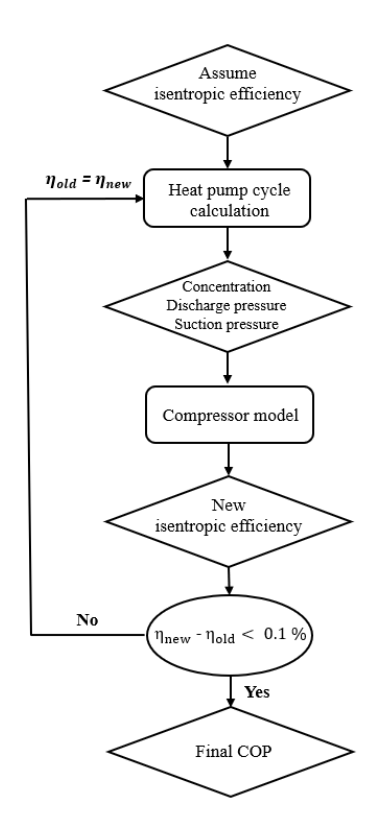


Figure 5.13: Schematic representation of the iteration process between the heat pump cycle calculations and the compressor model.

RESULTS HEATING CASE I

For the ammonia water case, a concentration of 19.1 wt% ammonia results in the highest COP value for this application, investigated by Gudjonsdottir et al. [9]. The isentropic efficiency was assumed to be 70 % and a COP of 5.18 was determined. The iteration procedure of Figure 5.13 is carried out and the isentropic efficiency stabilizes after a few iterations to 67.35 %, which results in a COP value of 4.52. The optimum ammonia concentration is still 19.1 wt%. The final values of the heat pump cycle are presented in Tables 5.11 and 5.12. The COP values in Table 5.12 include the mechanical efficiency of the compressor of 90%.

For the 5 wt% and 10 wt% CO_2 cases, the first assumed isentropic efficiency to determine the heat pump cycle is the efficiency of the ammonia water case of 67.35 %. The optimum mixture compositions that give the highest COP for this application are found. At this point, the efficiency is still equal for all three working fluids and a small increment in the COP is observed. For the case of 5 wt% CO_2 , compared to zero addition, the increment is just around 1% and for the 10 wt% CO_2 it is around 3 %. Then in the iterations that follow, the compressor model is used to determine the isentropic efficiencies of the 5 wt% and 10 wt% CO_2 cases. The isentropic efficiency becomes higher for the cases with added CO_2 . Table 5.10 gives the final isentropic efficiencies for the different working fluids that are used in the final cycle calculations. The final results of the heat pump cycle are presented in the Tables 5.11 and 5.12. From Table 5.11 and 5.12 it can be clearly seen that with the addition of CO_2 the COP is increasing. Due to the better performance of the compressor, the COP values for the addition of CO_2 become higher than expected. In the case of an addition of 5

wt% CO_2 the COP is increasing with 4.4 % to a COP of 4.72, compared to no CO_2 addition. When the CO_2 addition is 10 wt% the COP is increasing with 6.6 % to a COP of 4.82. Both COPs include the mechanical efficiency of the compressor.

Table 5.10: Mass flow, indicated power, isentropic and total efficiency of the compressor operating with a 0, 5, 10 wt % CO_2 addition.

CO ₂ addition [wt%]	0	5	10
\dot{m} [kg ⁻¹]	0.0067	0.0075	0.0083
\dot{W}_{ind} [kw]	3.06	3.13	3.36
$\eta_{is}\left[\% ight]$	67.35	70.33	70.81
η_{tot} [%]	60.62	63.30	63.73

Table 5.11: Mixture composition, temperature and pressure for the CRHP cycle for heating a waste stream from 60 °C to 105 °C, combined with the isentropic efficiency coming from the compressor model, presented in Table 5.10

Model	wt %			q ₂ (-)	<i>T</i> ₁ (°C)	T ₂ (°C)	<i>T</i> ₃ (°C)	T ₄ (°C)	P _{low} (bar)	Phigh (bar)
	NH ₃	H ₂ O	CO_2							
REFPROP										
& Compressor model	19.1	80.9	0	0.973	55	109.94	65.04	24.93	0.202	1.76
Aspen Plus new fit & Compressor model	18.5	76.5	5	0.973	55	110.11	65.60	25.70	0.21	1.82
Aspen Plus new fit & Compressor model	20.4	66.7	10	0.972	55	110.10	65.22	25.72	0.226	1.95

Table 5.12: Mixture composition, enthalpy, mass flow through the compressor, heat delivered by resorber and the COP for the CRHP cycle for heating a waste stream from 60 °C to 105 °C, combined with the isentropic efficiency coming from the compressor model, presented in Table 5.10.

Model	wt %		h_1 (kJ/kg)	h_2 (kJ/kg)	h_3 (kJ/kg)	h_4 (kJ/kg)	Q (kW)	COP	
	NH ₃	H ₂ O	CO ₂	•					
REFPROP									
& Compressor model	19.1	80.9	0	2033.0	2490.1	194.3	194.3	15.4	4.52
Aspen Plus new fit & Compressor model	18.5	74.1	5	-11564.0	-11140.4	-13360.9	-13360.9	16.7	4.72
Aspen Plus new fit & Compressor model	20.4	66.7	10	-11122.0	-10714.5	-12896.5	-12896.5	18.1	4.82

The mass flow in the compressor for each case is listed in Table 5.10. With the addition of CO_2 the mass flow increases. The operation conditions and mixture compositions are different for each case, therefore, the specific volumes are different as well. Due to the fact that the volume of the cavities is the same, the mass flows differ. At last the produced heat in the resorber is determined with the mass flow from the compressor model:

$$\dot{Q}_H = \dot{m}(h_2 - h_3) \tag{5.2}$$

With the addition of CO_2 the produced heat in the resorber is significantly increasing, which contributes to the higher COP values for this heat application, see Table 5.12. For the 5 wt% CO_2 case the produced heat is increased with 8.4%. For the 10 wt% CO_2 case the produced heat is even improved by 17.5 %.

The indicated power, listed in Table 5.10, is slightly higher for the cases with addition of CO_2 . This is expected since the mass flows are higher. The pressure ratio of the compressor is getting slightly lower by the addition of CO_2 .

Figures 5.14 and 5.15 show the pressure and temperature distributions respectively for the different working fluids in the compressor. The temperature curves overlap due to the fact that the same temperature lift over the compressor is considered. At the rotation angle of 690° the slope of the curves are changing. At this angle the discharge port starts to open and the temperature and pressure rise to the final discharge values. To satisfy the boundary conditions of the application the suction and discharge pressure shift upwards with the addition of CO₂, see Figure 5.14.

Gudjonsdottir et al. [9] determined that an improvement of 5 % in the COP can be reached with 18 wt% CO_2 addition to an ammonia water working fluid. During these calculations the isentropic efficiency of the compressor was the same assumed value for the different working fluids. When using the compressor model during the cycle calculations, even less than 10 wt% of CO_2 addition is needed to reach the same improvement of 5 % in the COP. This is a very favorable result because high additions of CO_2 comes together with some risks. The extended UNIQUAC model predicts salt formations (ammonium bicarbonate) above the 18 wt% CO_2 , which is unwanted in the heat pump since it causes blockages. With the compressor model it is indicated that lower concentration of CO_2 results in significant improvements in the COP for this type of applications.

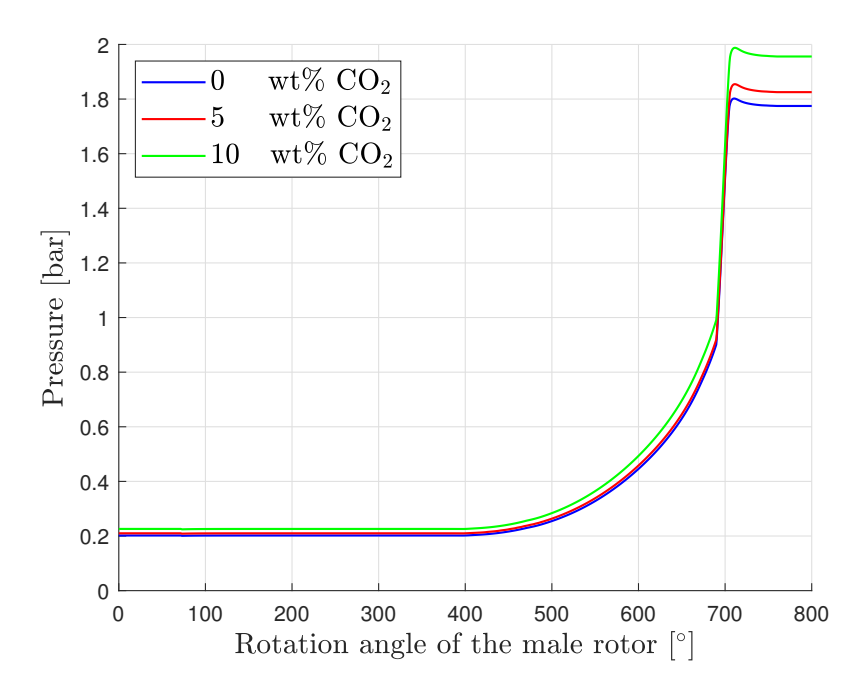


Figure 5.14: Pressure during the compression process for 0, 5 and 10 w% $\rm CO_2$ addition for the same application of heating waste water from 60 °C tot 105 °C. At 690° the discharge port opens.

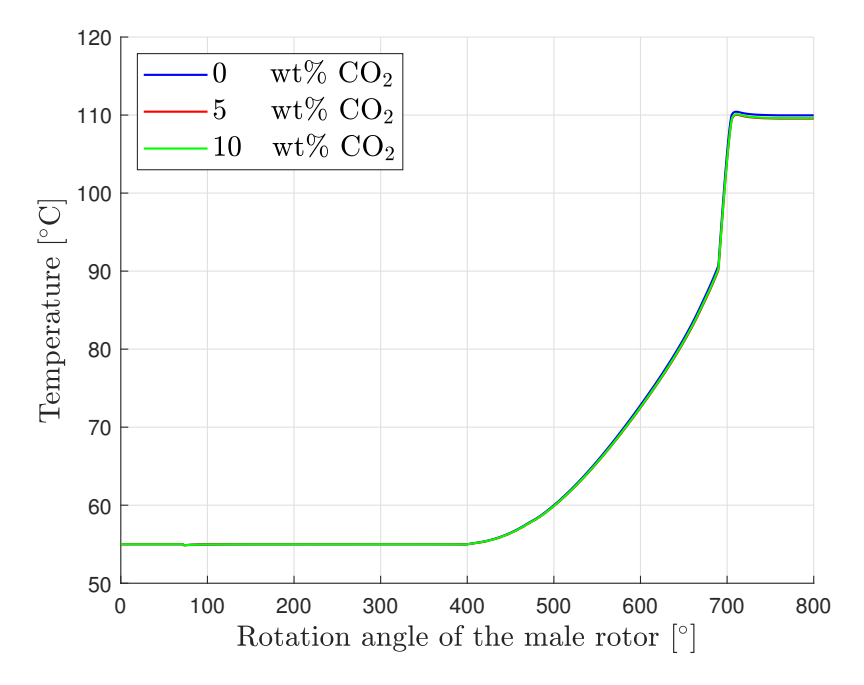


Figure 5.15: Temperature during the compression process for 0, 5 and 10 w% $\rm CO_2$ addition for the same application of heating waste water from 60 °C tot 105 °C. At 690° the discharge port opens.

RESULTS HEATING CASE II

The same analysis is done for the second application, which is a higher temperature application. To start again with the ammonia water case. The inlet and outlet pressure of the compressor and the composition of the mixture are varied until it satisfies the requirements of the cycle. After the iteration process it is found that a concentration of 21.1 wt% ammonia is leading to the highest COP value of 5.33. The isentropic efficiency of the compressor determined by the model is 75.74 % and the mechanical efficiency of 90% is included. The results of the heat pump cycle are presented in the Tables 5.14 and 5.15.

For the 5 wt% and 10 wt% CO_2 , the cycle is first determined with the same isentropic efficiency of the ammonia case (75.74 %). The COP of the cycle for the 5 wt% and 10 wt% CO_2 cases shows again a small improvement with relatively the same percentages $\sim 1\%$ and $\sim 3\%$ respectively. When the iteration process is continued with the compressor model, the isentropic efficiency is again increasing with the addition of CO_2 , see Table 5.13.

Due to the higher isentropic efficiencies, the COPs increase even more. Tables 5.14 and 5.15 present the final results for the heat pump cycle including the isentropic efficiencies determined by the model. The COP has improved with 3.9% for the 5% CO₂ addition and 5.4% for the 10% CO₂ addition, compared to no CO₂ in an ammonia water working fluid. The mechanical efficiency of the compressor is included in the COP values.

Table 5.13: Mass flow, indicated power, isentropic and total efficiency of the compressor operating with a 0, 5, 10 wt % CO_2 addition.

CO ₂ addition [wt%]	0	5	10
<i>m</i> [kg ⁻¹]	0.0386	0.0438	0.0508
\dot{W}_{ind} [%]	10.61	11.17	12.43
η_{is} [%]	75.74	78.49	78.18
η_{tot} [%]	68.17	70.64	70.36

Again with the addition of CO_2 the pressure ratio of the compressor is slightly decreasing. The mass flow increases for the cases with CO_2 addition, and therefore the indicated power increases as well. The heat from the resorber is again determined with the mass flow from the compressor model, listed in Table 5.13, and Equation 5.2. The produced heat increases significantly by the addition of CO_2 . For the 5 wt% CO_2 case the produced heat is increased by almost 10 %. and for the 10 wt% CO_2 case the produced heat is even improved by 25 %, see Table 5.15. The isentropic efficiencies for this application are higher than for the previous application. In the previous application there was a larger over compression that lowered the efficiency.

Table 5.14: Mixture composition, temperature and pressure for the CRHP cycle for heating a waste stream from 95 °C to 140 °C, calculated with the isentropic efficiency coming from the compressor model, presented in Table 5.13

Model	wt %			q ₂ (-)	<i>T</i> ₁ (°C)	<i>T</i> ₂ (°C)	<i>T</i> ₃ (°C)	T ₄ (°C)	P _{low} (bar)	P _{high} (bar)
	NH ₃	H ₂ O	CO_2	•						
REFPROP & Compressor model	21.1	78.9	0	0.719	90	144.95	99.93	59.20	1.0	5.7
Aspen Plus new fit & Compressor model	20.9	74.1	5	0.714	90	144.98	100.82	60.27	1.06	6.01
Aspen Plus new fit & Compressor model	23.3	66.7	10	0.712	90	144.97	100.90	60.24	1.19	6.69

Table 5.15: Mixture composition, enthalpy, mass flow through the compressor, heat delivered by resorber and the COP for the CRHP cycle for heating a waste stream from 95 $^{\circ}$ C to 140 $^{\circ}$ C, calculated with the isentropic efficiency coming from the compressor model, presented in Table 5.13

Model	wt %		h ₁ (kJ/kg)	h ₂ (kJ/kg)	h ₃ (kJ/kg)	h ₄ (kJ/kg)	Q (kW)	COP	
	NH ₃	H ₂ O	CO_2	-					
REFPROP									
& Compressor model	21.1	78.9	0	1697.1	1971.5	346.3	346.3	62.7	5.33
Aspen Plus new fit & Compressor model	20.9	74.1	5	-11618.5	-11363.1	-12935.3	-12935.3	68.9	5.54
Aspen Plus new fit & Compressor model	23.3	66.7	10	-11120.9	-10873.8	-12417.1	-12417.1	78.4	5.62

In Figure 5.16 and 5.17 the pressure and temperature can be seen as functions of the rotation angle of the male rotor, respectively. The results are very similar as for the other application and no significant differences can be observed between the results of both applications.

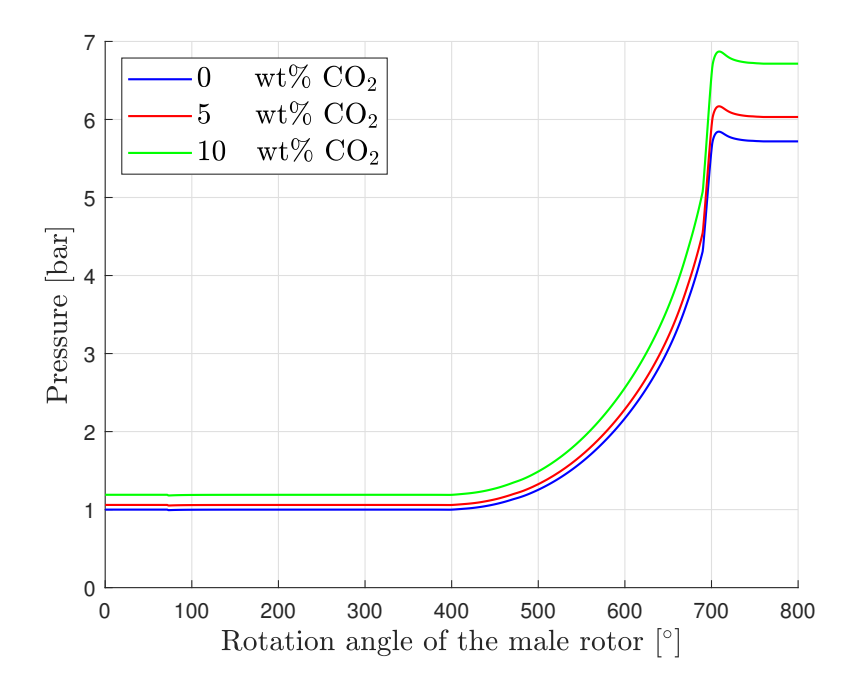


Figure 5.16: Pressure during the compression process for 0, 5 and 10 w% $\rm CO_2$ addition for the same application of heating waste water from 95 °C tot 140 °C. At 690° the discharge port opens.

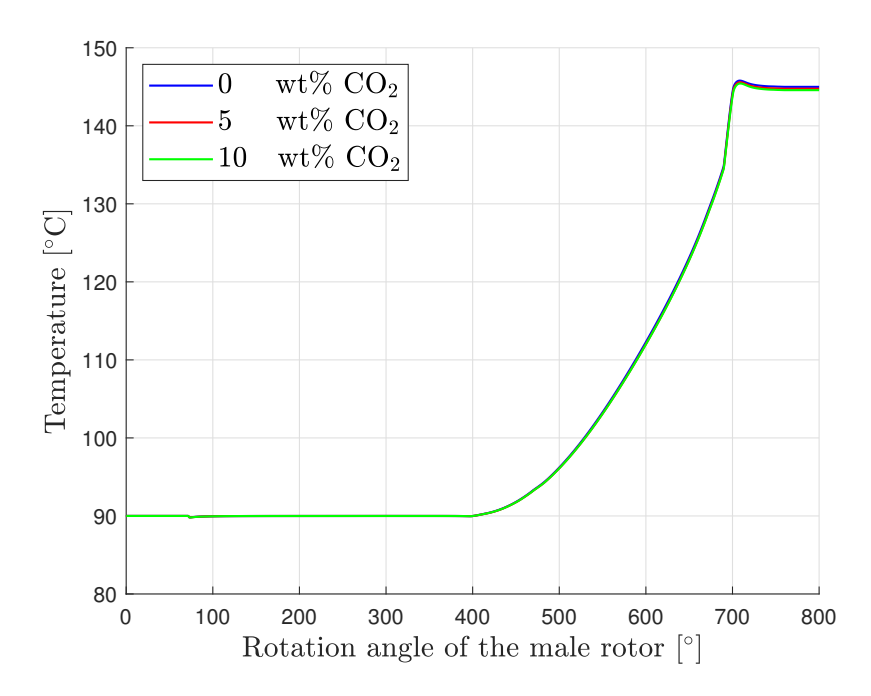


Figure 5.17: Temperature during the compression process for 0, 5 and 10 w% CO_2 addition for the same application of heating waste water from 95 °C tot 140 °C. At 690° the discharge port opens.

Summarized, for these two heating applications 2 conclusions can be made:

- 1. The performance of the heat pump increases with the addition of CO_2 to an ammonia water working fluid when the isentropic efficiency is kept constant for the different working fluids. The main reason is that with the addition of CO_2 the produced heat in the resorber significantly increases.
- 2. More importantly, when the cycle calculations are combined with the compressor model, it shows that the addition of CO_2 has beneficial effects on the compressor itself as well. The model operating with NH_3 - H_2O - CO_2 predicts an improvement of the isentropic efficiency of the compressor. This means that even higher COP values for the heat pump cycle with the addition of CO_2 can be reached than was determined earlier. Less than 10 wt% CO_2 added to an ammonia water working fluid results already in a 5 % improvement in the COP.

Both of these results can be accomplished without any significant changes in the application, the heat pump system or in the compressor itself. Only adding a small amount of CO_2 to an ammonia water working fluid causes an improvement of the COP.

EXPERIMENTAL SETUP AND PREPARATIONS

In this Chapter the experimental setup and the preparations for the experiments are described. The experimental setup serves to test the performance of the compressor and to validate the presented model of the compressor. This setup is used to validate the model operating with ammonia water and with $NH_3-H_2O-CO_2$. Since there are some technical problems with the compressor, it was not possible to start the experiments during the cause of this thesis.

6.1. EXPERIMENTAL SETUP

A schematic diagram of the experimental setup is presented in Figure 6.1. The main test section of the setup is the compressor. The new compressor prototype is designed in such a way that it is able to compress a two-phase mixture. Around the compressor there are many other components in order to measure and control all the important parameters around and in the compressor.

To start with the separator. The working fluid is fed into to bottom. The separator is dividing the working fluid in a liquid stream and a vapour stream. On the bottom of the separator a heating element is used to induce a two-phase mixture during the start up of the experiments. After the start up, a two-phase flow enters the seperator and the heating element is no longer necessary. The vapour stream is leaving the separator at the top and the liquid stream is leaving the separator at the bottom. The separator is added to the setup for two important reasons. The first reason is that the mass flow of the working fluid needs to be measured. The available two-phase flow meters are not suitable for the requirements of the experimental setup. The desired flow velocities of the working fluid in the setup are higher than the measuring range of these flow meters. Furthermore, these flow meters require that the liquid and vapor streams are separated in the pipe, while the aim is to have a mixed two-phase flow. This leads to the second reason for the necessity of the separator. The separated liquid can be sprayed into the vapour line with a spray nozzle to ensure that the two-phase flow is entering the compressor completely mixed. Thus, two flow meters are installed in the setup, one flow meter in the liquid line and one flow meter in the vapour line. The complete mass flow of the working fluid, is the summed value of both flow meters.

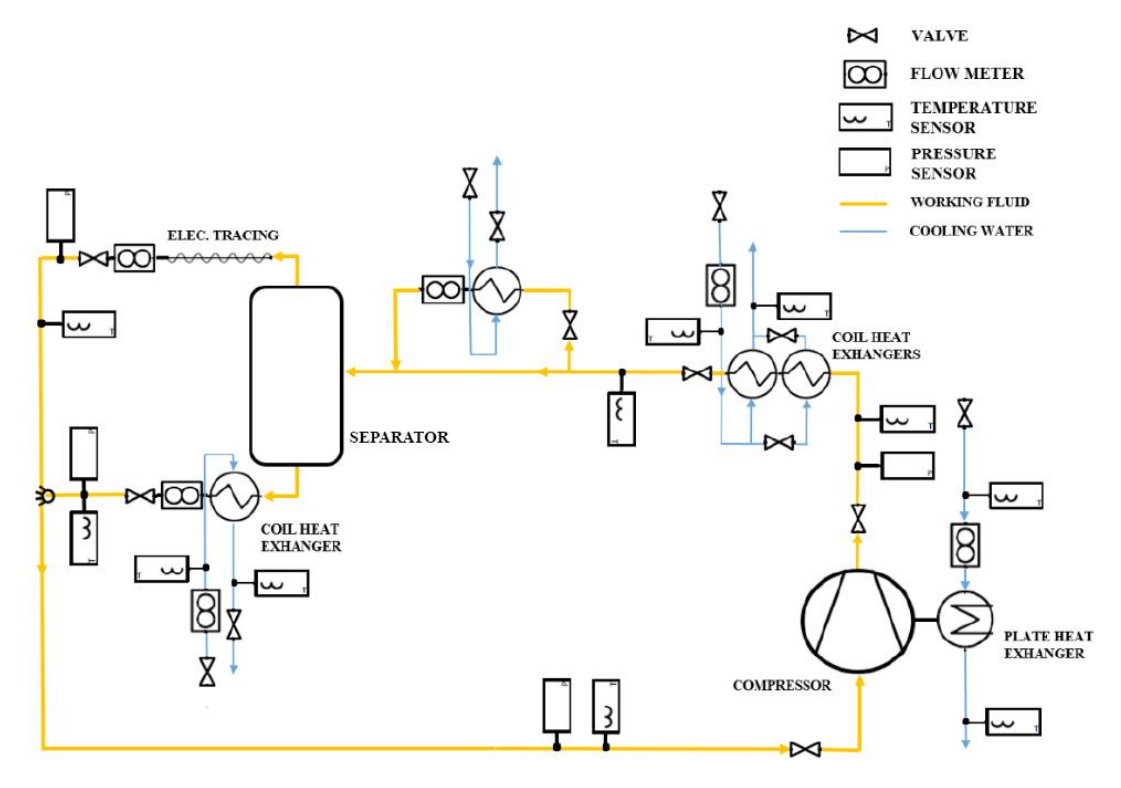


Figure 6.1: Schematic drawing of the experimental setup.

In the vapour line, the flow goes through an electric tracing coil to superheat the flow before it goes into the vapor flow meter. This is done to ensure that the flow does not contain any liquid. In the liquid line, the flow is first subcooled before it enters the liquid flow meter. In the vapour and liquid lines temperature and pressure sensors are installed. With these values the other properties in the vapor and liquid lines can be obtained.

Before the separator, a parallel flow with a heat exchanger and a flow meter can be observed. A part of the working fluid is going through this line and the flow meter is used to measure the density of the flow. With the density, the measured temperature and pressure, the concentration of ammonia in the working fluid can be determined. With the known temperature, pressure and concentrations the quality of the mixture at the inlet of the separator can be calculated.

The mixed two-phase flow enters the compressor and the pressure and temperature are measured before and after the compressor. An extra heat exchanger at the compressor is installed to cool down the compressor lubricant. The compressor is oil-free on the process side, however lubrication is needed for the bearings, gears and seals.

After the compressor, the flow is cooled by two heat exchangers to reach the desired conditions at the inlet of the separator. After the heat exchangers another temperature sensor can measure the temperature of the working fluid at the inlet of the separator.

Several valves are placed throughout the setup to close off sections. The placed valves in the vapor and liquid lines are able to control the mass flows of the vapor and liquid streams. In the cooling water lines, flow meters and temperature sensors are placed to determine the heat removed from the working fluid.

6.2. EXPERIMENTAL PREPARATIONS

The experimental set up is in preparation. Unfortunately, there were many technical problems with the compressor and the compressor had to be removed from the setup. The major problem is that the compressor is not completely leak tight. Since the working fluid contains ammonia, which is toxic and corrosive in small amounts, the compressor must be 100 % leak tight. Furthermore, these small leakages will cause difficulties in reaching steady state in the system. This is a prerequisite to obtain useful experimental data. The setup is considered to be leak proof when the pressure drop is less than 0.01 bar per hour. It was observed when the compressor was installed in the set up the pressure drop exceeded this criterion.

Once the compressor is considered to be leak tight, it can be reinstalled. Again a leakage test over the complete setup must be done. By putting nitrogen to the system the pressure can be built up. The pressure in this setup can be built up to around 14/15 bar. If over night the average pressure drop is lower than 0.01 bar per hour, the experiments can start.

All the other components and sensors have been tested and calibrated. Most temperature sensors have been calibrated by the production company. A few temperature sensors still needed to be calibrated. The sensor specifications and the performed calibrations can be found in Appendix B.

The sensors that are shown in Figure 6.1 are connected to a remote computer. The readings of the sensors and transmitters are displayed real time in LabView. LabView is a graphical programming approach that can visualize the measurement data of the setup. With LabView it is possible to log the data during experiments, in order to analyze it afterwards.

The rotational speed of the compressor controls the mass flow through the complete set up. In LabView the setpoints of the valves in the liquid line and the vapor line can be automatically changed. The values can be set from 0 to 100, where at 100 the valves are open at the maximum. The valves let the smallest flow through at a setpoint of 14, lower than 14 no flow can be detected. By changing the setpoints of the valves in the vapor line or liquid line, the liquid and vapor streams can be controlled separately.

The other values in the setup are opened or closed manually and have the purpose of closing of sections instead of controlling the conditions of the flow.

A Matlab script for ammonia water is developed by Guðmundsdóttir [10] to predict the conditions of the working fluid at several state points throughout the setup . With this Matlab script the inlet conditions to the compressor can be predicted, since the compressor has certain vapor quality limits.

The inlet conditions of the separator are varied to examine the effect on the vapor quality after the vapor and liquid streams have been mixed, i.e the inlet vapor quality to the compressor. REFPROP or Rattner and Garimella is used to obtain the thermodynamic properties of ammonia water.

The ammonia concentration and the temperature at the inlet of the separator are varied. When the ammonia concentration increases, the vapor quality after mixing slightly decreases. However, the maximum difference is less than 0.5 % [10]. Higher inlet temperatures at the separator lead to higher inlet vapor qualities at the separator and thus higher vapor qualities after the separation process. However, the vapor quality before and after the separation process is not significantly changed.

The amount of superheating in the vapour line or the amount of subcooling in the liquid line can be manually varied and can influence the inlet conditions of the flow to the compressor as well. The effect is investigated with the Matlab script. The amount of subcooling has a greater effect on the mixed vapor quality than the amount of superheating.

For NH_3 - H_2O - CO_2 this same analysis can be done. The thermodynamic property model in Aspen is needed again to obtain the properties of NH_3 - H_2O - CO_2 . To predict the conditions in the setup, Aspen Plus can be used directly to simulate the processes of the setup. This is shortly discussed in Appendix C.

6.2.1. UNCERTAINTY ANALYSIS

In the setup many different sensors are installed to measure the pressure, temperature and mass flow throughout the complete setup. Each of these instruments has an amount of uncertainty in its measurements. Experimental data without an uncertainty analysis is meaningless and therefore a statistical analysis is applied to estimate the uncertainties of the measurements. The sensor specifications are listed in Appendix B. The sensor specifications include the uncertainties for directly measured parameters by the sensors. To determine the uncertainties for indirectly measured parameters, the following error propagation estimation must be done. It should be clear that it uses absolute quantities that should follow from the experiments. The methodology of the error propagation follows.

ERROR PROPAGATION

With the accuracy of the sensors known, the error in the indirect measured parameters can be obtained. One of the most important parameters to obtain with the setup is the isentropic efficiency of the compressor.

The general way to calculate the error propagation of an indirectly measured parameter is as follows. When the indirect measured parameter, f, is a function of the direct measured parameter, x, ..., z, with known uncertainties, $U_x, ..., U_z$, then the uncertainty in this parameter is:

$$U_f = \sqrt{\frac{\partial f}{\partial x}U_x + \dots + \frac{\partial f}{\partial z}U_z}$$
 (6.1)

The uncertainties U_f and U_x , ..., U_z are absolute errors.

However, it is not always the case that the direct and indirect measured parameters are expressed in an explicit functional relationship. If the relationship of parameter, q, is unknown the method that can be applied is as follows:

$$U_q = \sqrt{(q(x+U_x,...,z) - q(x,...,z))^2 + ... + (q(x,...,z+U_z) - q(x,...,z))^2}$$
(6.2)

Uncertainty of the isentropic power \dot{W}_{is}

Isentropic power is calculated by the following equation:

$$\dot{W}_{is} = \dot{m} \cdot (h_{is} - h_{suc}) \tag{6.3}$$

In order to calculate the uncertainty in the isentropic power, equation 6.1 is used as follows:

$$U_{\dot{W}_{is}} = \sqrt{\left(\frac{\partial \dot{W}_{is}}{\partial \dot{m}} U_{\dot{m}}\right)^2 + \left(\frac{\partial \dot{W}_{is}}{\partial h_{suc}} U_{h_{suc}}\right)^2 + \left(\frac{\partial \dot{W}_{is}}{\partial h_{is}} U_{h_{is}}\right)^2}$$
(6.4)

The uncertainty of the mass flow and the enthalpies need to be determined. The mass flow is a directly measured parameter. As earlier mentioned, the mass flow is measured in the liquid line and in the vapor line. Before the working fluid enters the compressor, these lines are combined and the total mass flow is simply a summation of the liquid and vapour mass flows. For the uncertainties the same reasoning applies:

$$U_{\dot{m}} = U_{\dot{m}_L} + U_{\dot{m}_V} \tag{6.5}$$

The enthalpy is an indirectly measured value and is a function of pressure, temperature and concentration.

$$h = h(P, T, x) \tag{6.6}$$

For the uncertainty in the suction enthalpy, the pressure and temperature values at the suction of the compressor need to be used and Equation 6.2 becomes as follows:

$$U_h = \sqrt{(h(P+U_p, T, x) - h(P, T, x))^2 + (h(P, T+U_T, x) - h(P, T, x))^2 + h(P, T, x+U_x) - h(P, T, x))^2}$$
 (6.7)

In the case experiments are done with the working fluid ammonia water, x is the ammonia concentration with the uncertainty in the determined ammonia concentration U_{NH_3} . When the experiments are done with NH₃-H₂O-CO₂, the CO₂ concentration with the uncertainty U_{CO_2} is added.

The uncertainties of the pressure and temperature measurements are known. However, the concentrations are indirectly measured parameters. The concentrations are calculated with the measured density by a separate flowmeter combined with the measured pressure and temperature.

$$x = x(\rho, P, T) \tag{6.8}$$

To calculate the uncertainties in the concentrations Equation 6.2 is used.

At last, the isentropic enthalpy is a function of the entropy at the suction of the compressor. The uncertainties in the isentropic enthalpy and entropy are as well calculated with Equation 6.2.

$$h_{is} = h_{is}(P, s, x) \tag{6.9}$$

$$s = f(P, T, x) \tag{6.10}$$

UNCERTAINTY OF THE INDICATED POWER

In order to determine the isentropic efficiency, the indicated power is needed as well. The indicated power can be determined by the following equation:

$$\dot{W}_{ind} = \frac{\sqrt{3}nIV}{C60} \tag{6.11}$$

The compressor is set to a certain rotational speed, n. The voltage from the power grid, V, is known and the current, I, to the compressor can be directly measured. The measurement of the current can contain an uncertainty, U_I . The factor, C, is an empirical factor that depends on the compressor and is unknown at this point. Equation 6.1 can be applied.

UNCERTAINTY IN THE ISENTROPIC EFFICIENCY

Finally the uncertainty of the isentropic efficiency can be determined. The isentropic efficiency is the ratio between the isentropic power and the indicated power of the compressor.

$$\eta_{is} = \frac{\dot{W}_{is}}{\dot{W}_{ind}} \tag{6.12}$$

For the uncertainty in the isentropic efficiency Equation 6.1 is used as follows:

$$U_{\eta_{is}} = \sqrt{\left(\frac{\partial \eta_{is}}{\partial \dot{W}_{is}} U_{\dot{W}_{is}}\right)^2 + \left(\frac{\partial \eta_{is}}{\partial \dot{W}_{ind}} U_{\dot{W}_{ind}}\right)^2}$$
(6.13)

UNCERTAINTY IN THE INLET VAPOUR QUALITY

The vapour quality is an important parameter to keep an eye on during the experiments. It is therefore useful to know the uncertainty of this parameter. The vapour quality calculation depends on the measured pressure, temperature and concentration. The uncertainty is calculated again with Eq. 6.2.

$$q = q(T, P, x) \tag{6.14}$$

CONCLUSIONS AND RECOMMENDATIONS

7.1. CONCLUSIONS

One of the main objectives of this study is to develop a theoretical model of a screw compressor operating under wet conditions with $NH_3-H_2O-CO_2$ as a working fluid. The compressor model is used to study the performance of the compressor with the addition of CO_2 to an ammonia water working fluid. This study leads to the following conclusions:

- The compressor model operating with NH₃-H₂O-CO₂ predicts better performances of the compressor than for ammonia water. The effect of vapor quality, pressure ratio and amount of CO₂ addition have been investigated more extensively. For all investigated cases, the isentropic efficiency is predicted to be higher for NH₃-H₂O-CO₂. For 5 wt% CO₂ addition the isentropic efficiency improves by 3.5 % compared to ammonia water, where the pressure ratio and vapor quality are kept the same for both mixtures. For 10 wt% CO₂ addition, the isentropic efficiency is not significantly changed, compared to an addition of 5 wt% CO₂. This conclusion is valid as long the suction vapor quality is higher than 0.45.
- The compressor model operating with NH₃-H₂O-CO₂ is not able to predict the isentropic efficiency correctly for suction vapor qualities lower than 0.45. The model is significantly over predicting the isentropic efficiency, since values above 90 % are reached. For lower vapor qualities, it is observed that the isentropic enthalpy at the discharge is larger than the actual discharge enthalpy, which is physically not possible. The isentropic enthalpy is the only parameter in the model that is using the property entropy. One explanation can be that the entropy is determined incorrectly by the thermodynamic property model implemented in Aspen Plus. The other output parameters in the model are of the same order of magnitude compared to the values of the model with ammonia water, and as such are expected to be correct.
- For low suction vapor qualities, the indicated power can be used as a performance indicator instead of the isentropic efficiency. A lower indicated power can indicate a higher compressor performance, as long as the mass flow, pressure ratio and vapor quality are the same for both mixtures. When this is the case, the compressor model with NH₃-H₂O-CO₂ shows lower indicated powers than for ammonia water.

Another main objective of this study is to investigate the benefits that can be reached by the addition of CO_2 to an ammonia water working fluid in a CRHP. The compressor model enables to determine the isentropic efficiency of the compressor for the different working fluids integrated in the CRHP cycle for several applications. Since the operation conditions are different for each working fluid, the isentropic efficiency and indicated power from the compressor model should not be compared on its own. The focus lies on the final result of the efficiency of the compressor included in the COP calculation of the heat pump. The following conclusions can be made:

- The benefits of the addition of CO₂ to an ammonia water working fluid in CRHP is depending on the type of application.
- For a heat pump application, containing a cooling and heating requirement, the working fluid NH₃-H₂O-CO₂ is not beneficial for the performance of the CRHP. With the addition of CO₂, the COP of the heat pump decreases. Both mixtures, ammonia water and NH₃-H₂O-CO₂, show non linear temperature glides along the resorber and desorber. It is observed that the temperature glide of NH₃-H₂O-CO₂ is not able to fit as well to the temperature glide in the desorber as ammonia water. For ammonia concentrations around 40-50 wt% the temperature glide behaves closest to ideal for both mixtures and the highest COPs are reached for those ammonia concentrations.
- For the same heat pump application, containing a cooling and heating requirement, the performance of ammonia water and NH₃-H₂O-CO₂ in a CRHP are compared with several working fluids in a VCHP reported by Zühlsorf et al. [33]. During this analysis the isentropic efficiency of the compressor is assumed to be 75%. The CRHP operating with ammonia water is able to compete with many working fluids in a VCHP. However, a few working fluids, e.g. DME isopentane, in a VCHP are able to reach slightly higher COPs. The compressor model with ammonia water indicates a higher isentropic efficiency than 75% for the operation conditions of this application. With the isentropic efficiency from the model taken into account, the COP of a CRHP operating with ammonia water becomes higher than the best performing working fluid in a VCHP. The application was selected by Zühlsorf et al. for the analysis of VCHPs. More advantages for CRHPs are reached if larger temperature glide applications are considered.
- For a larger temperature glide application, containing only a heating requirement, the benefits of NH₃-H₂O-CO₂ in a CRHP can be observed. Two heating applications are considered. For both applications similar results are found. When the isentropic efficiencies are the same for ammonia water and NH₃-H₂O-CO₂, the COPs show an improvement around 1 % and 3 % for 5 wt% and 10 wt% of CO₂ addition, respectively. With the compressor model included in the heat pump calculations, improvements in the COPs are significantly higher. For the case of 5 wt% and 10 wt% CO₂ addition the COPs increase around 4% and 5-7%, respectively. The improvements in the COPs for both applications is partly caused by the significant increase in produced heat in the resorber and due to higher expected isentropic efficiencies for the addition of CO₂ determined by the compressor model. The vapor quality is chosen sufficiently high to obtain reliable values for the efficiencies of NH₃-H₂O-CO₂.

7.2. RECOMMENDATIONS

To finalize this work, a number of recommendations can be derived for further research.

- For further process simulations with NH₃-H₂O-CO₂ a thermodynamic property routine as a MEX is needed. Rattner and Garimella developed such a routine for the thermodynamic properties of ammonia water. The thermodynamic properties of NH₃-H₂O-CO₂ are currently collected from the thermodynamic model in Aspen Plus and implemented into the compressor model by the use of tables. In order to make the model work properly the tables need to be highly refined. Therefore, the tables become very large and generating the tables is time consuming. Each time a different pressure range, temperature range or mixture composition is of interest new tables need to be generated.
- The compressor model operating with ammonia water and NH₃-H₂O-CO₂ must be validated with experimental data. Several operation conditions have been simulated, such as different vapor qualities and pressure ratios. The compressor must be tested for these operation conditions to see if the predicted isentropic efficiencies can be reached.
- The compressor model operating with NH₃-H₂O-CO₂ must be improved for low suction vapor qualities. The model is determining physically incorrect isentropic efficiencies for vapor qualities lower than 0.45. One explanation is that the entropy determined by the thermodynamic model implemented in Aspen is incorrect. In the entropy calculations the heat capacity is used and assumed to be temperature independent. It must be investigated if this assumption is valid. The data from the experiments can be used to modify the model such that it predicts the isentropic efficiencies more realistically.
- In the compressor model the geometry of the compressor is described. The maximum volume per cavity is fixed and is therefore restricting the mass flow in the compressor. When a certain heat pump application imposes a heat duty of the heat sink or source, a certain mass flow is obtained from that. This mass flow is often not the same as the mass flow obtained by the compressor model. The compressor size needs to be scaled correctly to satisfy to the heat load of the heat pump cycle. The scaling of the compressor in the model must be further explored. For example, do all the parameters in the compressor scale linearly?



APPENDIX

In this appendix the enthalpy-pressure diagrams are given for different suction vapor qualities. The suction pressure is 1 bar and the discharge pressure 4.5 bar. The mixture composition is 20 wt% ammonia and 5 wt% $\rm CO_2$. In the diagram the suction and discharge enthalpies are given together with the isentropic enthalpy at the discharge for these conditions. In figure A.1 a detailed view of the discharge values are shown. The isentropic enthalpy at the discharge must be always lower than the actual discharge enthalpy. Otherwise, the compression process would create energy, which is physically incorrect. Figure A.1 shows that for a vapor quality of 30 % and 40%, the isentropic values are higher. For the vapor qualities of 50 %, 60%, 70 % and 85 % the isentropic values are lower. At a vapor quality of 45 % the discharge and isentropic values are equal. Only from vapor qualities higher than 45 % the compressor model obtains physical solutions.

94 A. APPENDIX

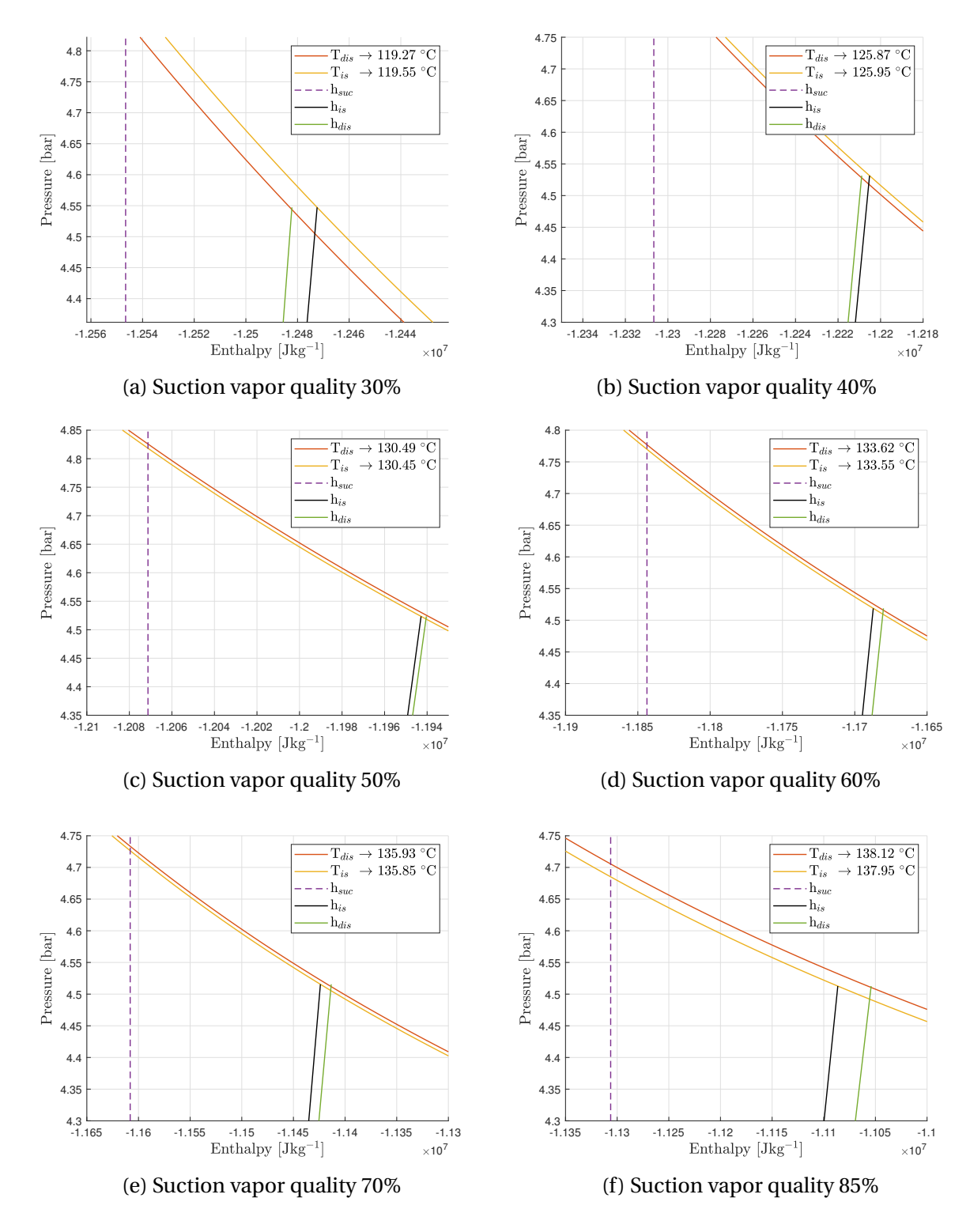


Figure A.1: Enthalpy-pressure diagram with the enthalpies at the inlet and outlet of the compression process for $NH_3-H_2O-CO_2$.

B

APPENDIX

In this appendix the sensor specifications for the temperature, pressure and flow sensors are listed. The uncertainties of the sensors are listed in the table specifications as well. These values are used in the error propagation to estimate the uncertainties in the indirectly measured parameters. A few temperature sensors have been calibrated. The relation between the measured and calibrated values is given by Equation B.1.

TEMPERATURE SENSORS

There are eleven temperature sensors placed throughout the set up. The specifications of the temperature sensors are listed in Table B.1. These type of sensors are known as resistance temperature detectors (RTD) that are based on a linear relationship between the change in electrical resistance and the temperature.

Five of these sensors are used to measure the local temperature of the working fluid in the setup. They are placed before and after the compressor, in the liquid line, vapour line and before the seperator. The other sensors are used to measure the temperature of the cooling water going in and out of the heat exchangers.

Nine of these temperature sensors have been calibrated by the production company at three different temperatures 60 °C, 120 °C and 180 °C. The accuracy of the sensors is given as ± 0.06 K. These sensors have been tested to see if the real measurements indeed matched with the calibration given by the company.

One heat exchanger is connected to the compressor to cool down the lubricant, needed for the gears, bearings and seals of the compressor. The cooling water lines going in and out this heat exchanger also contain temperature sensors. These two sensors were not calibrated by the production company. The calibration is done by using a thermostatic bath and a high precision temperature sensor with accuracy of ± 0.01 K. The range of the calibration is between 20 °C and 60 °C with an interval of 10 K. The relation for the measured value and the calibrated value is for both temperature sensors the following:

$$T_{cali} = T_{meas} - 1.57 \tag{B.1}$$

For the uncertainty of these sensors the same value as the other temperature sensors is taken, since the calibration method causes some uncertainties as well and this must be

96 B. APPENDIX

added to the accuracy of ± 0.01 K of the high precision temperature sensor. The uncertainty of ± 0.06 K has been validated by tests in the setup.

Table B.1: Specifications of the temperature sensors.

Sensor	PT-100
Type	1/10 DIN Element
Range	-50 250 °C
Uncertainty	$\pm 0.06~\mathrm{K}$

PRESSURE SENSORS

There are four gauge pressure sensor installed in the setup. The specifications of the pressure sensors are listed in Table B.2. The four pressure sensors are used to measure the local pressure of the working fluid in the liquid line, vapour line and before and after the compressor.

The parameter, r, in Table B.2 is denoted as the span ratio. The span ratio is defined as follows:

$$r = \frac{\text{maximum measuring span}}{\text{set measuring span}}$$
 (B.2)

For the current experiments, the span ratio is 4.

Table B.2: Specifications of the gauge pressure transmitters.

Sensor	SITRANS P DS III
Туре	7MF4033-1EA00-1AB6-Z A01+Y01
Range	-1 16 bar
Span ratio	4
Uncertainty	
Linear	$\pm (0.0029 \cdot r + 0.0071)\%$
Long-term drift	$\pm (0.25 \cdot r)\%$ per 5 years
Influence ambient temperature	$\pm (0.08 \cdot r + 0.01)\%$
Total	$\pm 1.348\%$

FLOW METERS

There are two flow meters placed in the setup to measure the flow of the working fluid. As mentioned earlier, the available two-phase flow meters are not suitable for the requirements of the setup. These flow meters can only measure low velocities. The flow is, therefore, measured separately in the liquid and vapor lines. To determine the total flow of the mixture these measured flows are summed. The specifications of the liquid flow meter are listed in Table B.3 and the specifications for the vapor flow meter are listed in Table B.4.

Table B.3: Specifications of the liquid flow meter.

Sensor	Cori-Flow
Type	IP-65
Range	1.575 kg/h
Uncertainty	$\pm 0.5\%$

Table B.4: Specifications of the vapor flow meter.

Sensor	Rheonik coriolis flow meter
Туре	RHM12
Range	30200 kg/h
Uncertainty at 200 kg/h	$\pm 0.75\%$

Then three flow meters are installed in the cooling water lines of the heat exchangers. The specifications of the flow meters are given in Table B.5. The flow meter in the cooling line of the heat exchanger after the compressor has a larger range to 900 l/h, the other two flow meters have a range to 300 l/h.

The last flow meter is placed in a parallel line before the seperator. Only a small part of the mixture is flowing through this line. This flow meter is able to measure the density of the mixture and can be used to calculate the concentration of the mixture. The specifications of this flow meter are listed in Table B.6.

Table B.5: Specifications of the flow meters for the cooling water.

Sensor	SITRANS F M MAGFLO
Sensor type	MAG 1100
Transmitter type	MAG 5000
Range	0300 l/h and 0900 l/h
Uncertainty	
$v \ge 0.5 \text{ m/s}$	$\pm~0.5\%$
v < 0.5 m/s	$\pm \frac{0.25}{v[m/s]}\%$

Table B.6: Specifications of the flow meter to measure the density.

mini Cori-Flow
M14
030 kg/h
$\pm 5 \text{ kg/m}^3$

C

APPENDIX

Aspen Plus [2] can be used to predict the conditions of NH_3 - H_2O - CO_2 in the setup. For the compressor model Aspen plus is only used to obtain the thermodynamic properties of NH_3 - H_2O - CO_2 . However, Aspen plus is developed as a process simulator and the processes in the setup can be simulated by Aspen. When the experimental setup is ready, this feature is an useful tool to develop a detailed experimental plan.

To start the process simulation of the setup in Aspen, the thermodynamic model of NH_3 - H_2O - CO_2 developed by Gudjonsdottir et al. [9] must be implemented in Aspen, as well. As mentioned, the thermodynamic model proposed by Que and Chen [18] is available in the Aspen Plus package. The new fit can be easily implemented in Aspen by changing the interaction parameters of Que and Chen to the values reported by Gudjonsdottir et al. Then, the simulation feature of the Aspen plus interface can be used to simulate the setup with NH_3 - H_2O - CO_2 . In the simulation feature many process equipment are built-in. Figure C.1 shows the experimental setup in Aspen, consisting of the separator, heater, coolers, control valves, mixer and the compressor.

For the process equipment in Aspen several options are available. An isentropic and mechanical efficiency of the compressor can be chosen. The compressor model can be used to find the isentropic efficiency of the compressor that is expected for the operating conditions of the experiments. In the example, Figure C.1, the isentropic efficiency is set to 0.70 and the mechanical efficiency to 1. The pressure ratio or the discharge pressure can be chosen as well in the compressor settings of Aspen. It is important to allow the working fluid to be in a two-phase sate in the compressor. This can be changed in the convergence criteria of the compressor settings. The simulation still gives a warning that the working fluid is in the two-phase regime during the compression process, see the yellow warning sign in Figure C.1. However, the aim is to have the working fluid in the two-phase regime, thus, this warning sign can be ignored.

For the heater and coolers the amount of superheating and subcooling can be varied in the setting options by giving the desired outlet temperature of the HEX.

100 C. APPENDIX

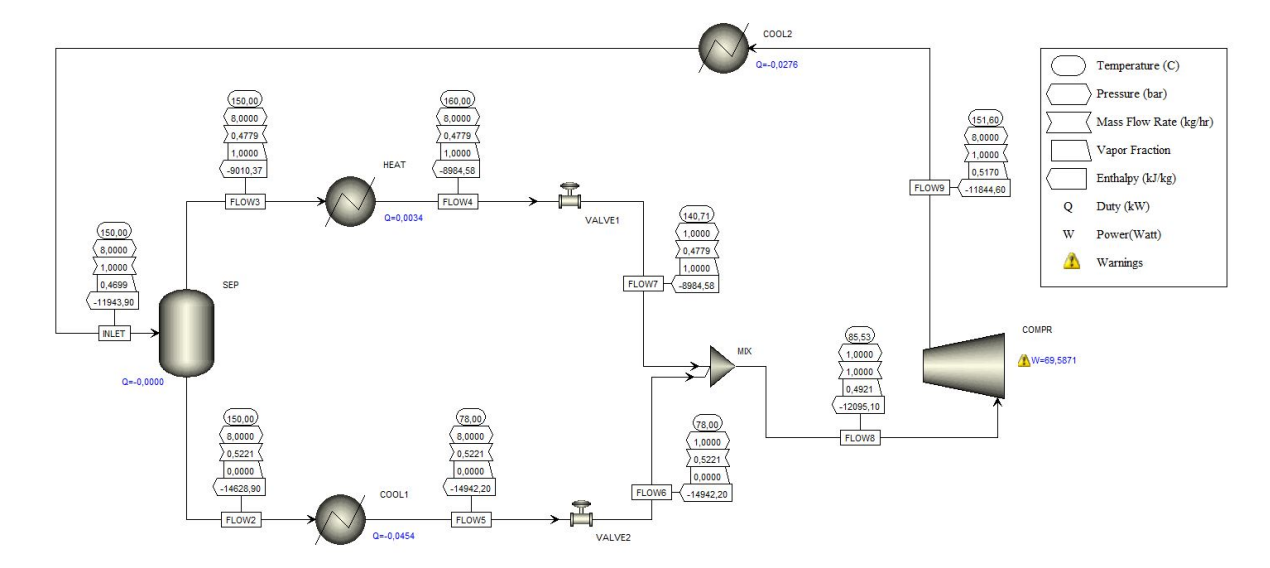


Figure C.1: Example of the experimental setup in Aspen plus with an NH_3 - H_2O - CO_2 working fluid. The composition of the mixture is 20 wt% ammonia and 5 wt% CO_2

At the inlet stream of the separator, the conditions of the working fluid can be set in terms of mass flow, mixture composition, temperature and pressure. For the settings of the separator the same pressure and temperature values are chosen, since it is assumed that these values stay the same during the separation process.

At last in the settings of the valves, the calculation type is set to adiabatic flash. This means that the enthalpy over the valves is constant. The pressure drop or outlet pressure can be chosen.

Then, Aspen plus calculates the conditions of the working fluid at several points in the setup and the condition of the working fluid at the inlet of the compressor can be analyzed.

Figure C.2 shows an example of changing the CO_2 concentration from 5 to 15 wt% CO_2 and keeping the rest of the operation conditions the same as in Figure C.1. The inlet vapor quality at the separator increases and, therefore, the inlet vapor quality at the compressor. The total increase of the vapor quality during the separation process is comparable for the different concentrations of CO_2 .

Figure C.3 shows the influence of increasing the amount of subcooling in the liquid line compared to Figure C.1. As expected, with an increased amount of subcooling, the vapor quality at the inlet of the compressor decreases.

At last, Figure C.4, shows an example of changing the inlet temperature of the separator. The inlet vapor quality of the compressor increases to 0.86 and the working fluid is getting superheated during the compression process. The outlet temperature at the compressor starts to rise rapidly. This operation condition must be avoided during the experiments. The inlet temperature of the separator must be decreased, or the amount of subcooling must be increased, or the superheating must be decreased.

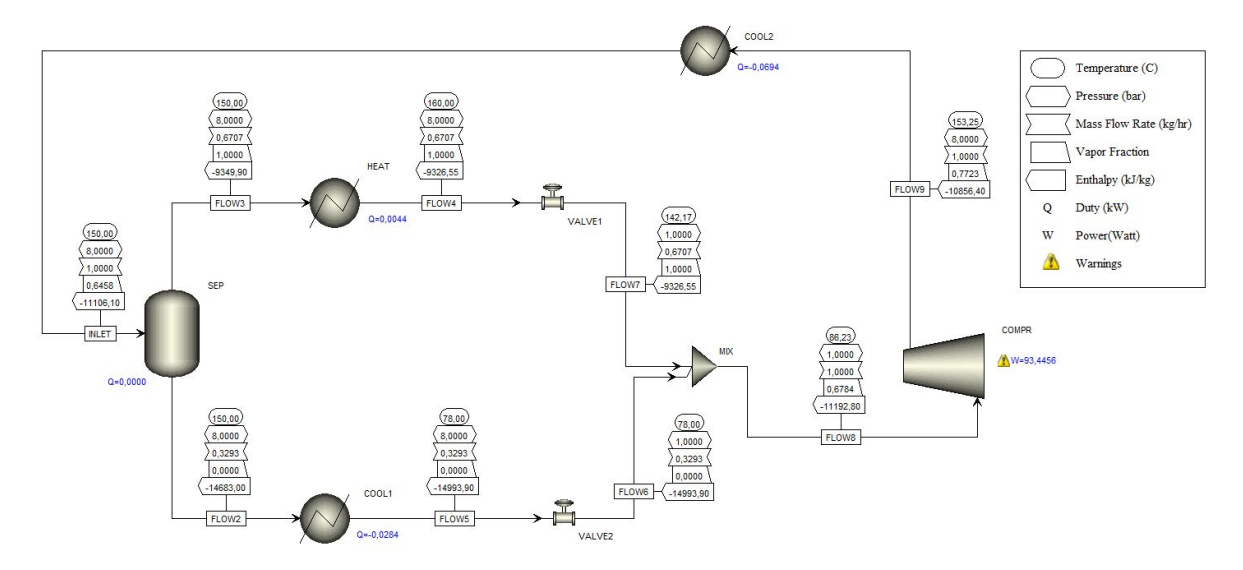


Figure C.2: Example of the experimental setup in Aspen plus with an NH_3 - H_2O - CO_2 working fluid. The composition of the mixture is 20 wt% ammonia and 15 wt% CO_2 .

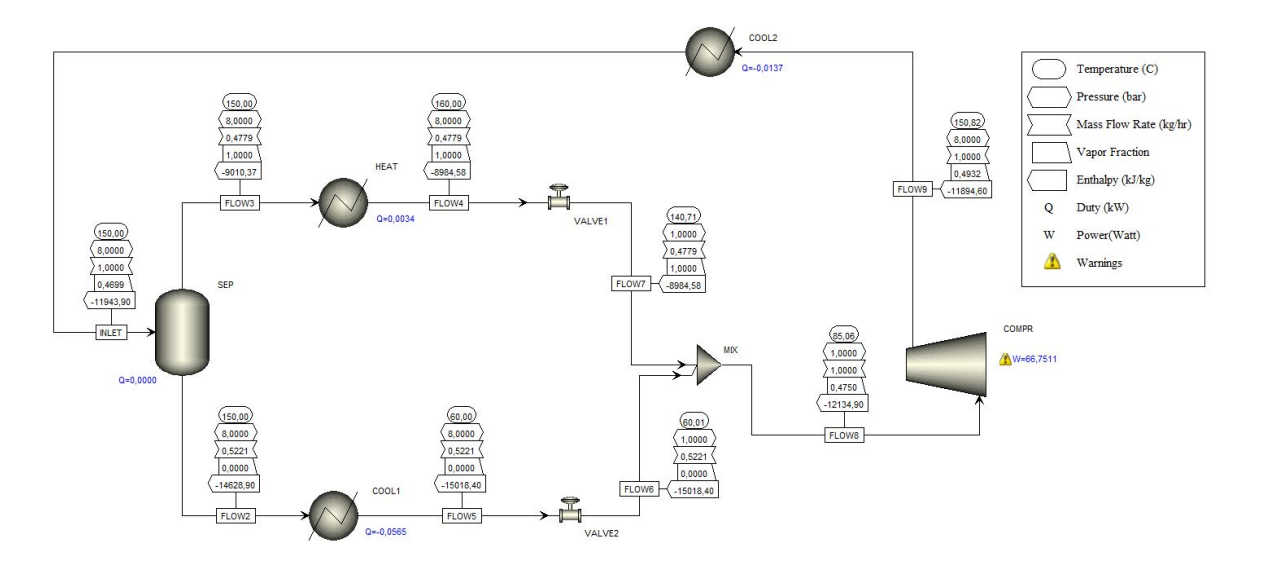


Figure C.3: Example of the experimental setup in Aspen plus with an NH_3 - H_2O - CO_2 working fluid. The composition of the mixture is 20 wt% ammonia and 5 wt% CO_2 . The outlet temperature of the cooler in the liquid line (COOL1) is decreased from 78 °C to 60 °C compared to Figure C.1.

C. APPENDIX

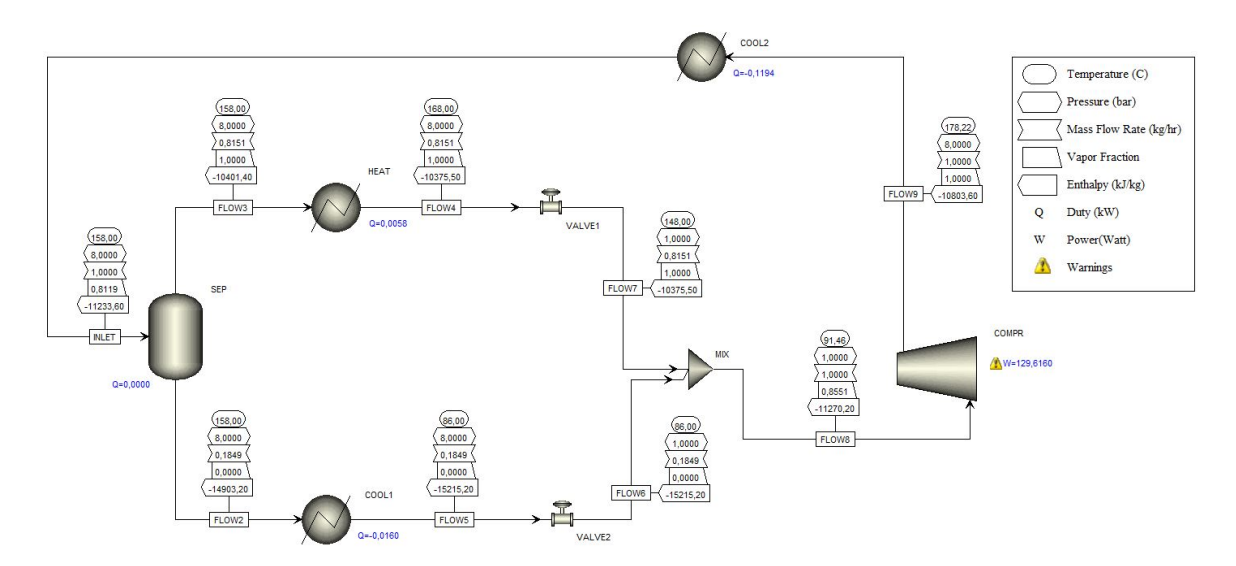


Figure C.4: Example of the experimental setup in Aspen plus with an NH_3 - H_2O - CO_2 working fluid. The composition of the mixture is 20 wt% ammonia and 5 wt% CO_2 . The inlet temperature of the separator is increased from 150 °C to 158 °C compared to Figure C.1.

BIBLIOGRAPHY

- [1] ARPAGAUS, C., BLESS, F., UHLMANN, M., SCHIFFMANN, J., AND BERTSCH, S. S. High temperature heat pumps: Market overview, state of the art, research status, refrigerants, and application potentials. *Energy* 152 (2018), 985 1010.
- [2] ASPEN PHYSICAL PROPERTY SYSTEM. Aspen Plus Version 8.8, Ma: Aspen Tech, 2015.
- [3] CHAMOUN, M., RULLIERE, R., HABERSCHILL, P., AND PEUREUX, J.-L. Modelica-based modeling and simulation of a twin screw compressor for heat pump applications. *Applied Thermal Engineering* 58, 1 (2013), 479 489.
- [4] DARDE, V., THOMSEN, K., VAN WELL, W. J. M., BONALUMI, D., VALENTI, G., AND MACCHI, E. Comparison of two electrolyte models for the carbon capture with aqueous ammonia. *International Journal of Greenhouse Gas Control* 8 (2012), 61 72.
- [5] DARDE, V., VAN WELL, W. J. M., STENBY, E. H., AND THOMSEN, K. Modeling of carbon dioxide absorption by aqueous ammonia solutions using the extended UNIQUAC model. *Industrial & Engineering Chemistry Research* 49, 24 (2010), 12663–12674.
- [6] Demirel, Y. Calculation of Excess Entropy for Binary Liquid Mixtures by the NRTL and UNIQUAC Models. *Industrial and Engineering Chemistry Researc* (1994).
- [7] FONTALVO, J. Using user models in Matlab within the Aspen Plus interface with an Excel link. *Ingenieria e Investigacion* 34 (08 2014), 39 43.
- [8] GUDJONSDOTTIR, V., INFANTE FERREIRA, C. A., GOETHALS, A., AND KISS, A. Measures to minimize entropy production in compresseion-resorption heat pumps. *13th IIR Gustav Lorentzen Conference, Valencia* (2018).
- [9] GUDJONSDOTTIR, V., INFANTE FERREIRA, C. A., REXWINKEL, G., AND KISS, A. A. Enhanced performance of wet compression-resorption heat pumps by using NH₃-CO₂-H₂O as working fluid. *Energy 124* (2017), 531 542.
- [10] GUÖMUNDSDÓTTIR, K. Wet compression with a twin screw compressor prototype. Master's thesis, Delft University of Technology, (2018).
- [11] Infante Ferreira, C. A., Zamfirescu, C., and Zaytsev, D. Twin screw oil-free wet compressor for compression-absorption cycle. *International Journal of Refrigeration* 29, 4 (2006), 556–565.
- [12] ITARD, L. C. M. Wet compression versus dry compression in heat pumps working with pure refrigerants or non-azeotropic mixtures. *International journal of refrigeration 18*, 7 (1995), 495–504.
- [13] ITARD, L. C. M. Wet compression-resorption heat pump cycles: thermodynamic analysis and design. PhD thesis, Delft University of Technology, (1998).

104 Bibliography

[14] LEMMON, E. W., HUBER, M. L., AND MCLINDEN, M. O. NIST Standard Reference Database 23: Reference Fluid Thermodynamic and Transport Properties-REFPROP, Version 9.0, National Institute of Standards and Technology, (2010).

- [15] LIANG, S. Absorption of ammonia-water and NH₃-CO₂-H₂O mixture in mini-channel heat exchangers. Master's thesis, Delft University of Technology, (2017).
- [16] MATLAB. version 9.3.0 (R2017b). The MathWorks Inc., Natick, Massachusetts, (2017).
- [17] MORAN, M. J., AND SHAPIRO, H. N. *Fundamentals of Engineering Thermodynamics*, sixth ed. John Wiley and Sons, 2010.
- [18] QUE, H., AND CHEN, C. Thermodynamic modeling of the NH₃-CO₂-H₂O system with electrolyte NRTL model. *Industrial & Engineering Chemistry Research* 50, 19 (2011), 11406–11421.
- [19] RATTNER, A. S., AND GARIMELLA, S. Fast, stable computation of thermodynamic properties of ammonia-water mixtures. *International Journal of Refrigeration 62* (2016), 39 59.
- [20] SEADER, J. D., AND HENLEY, E. J. *Separation Process Principles*, third ed. John Wiley and Sons, 2010.
- [21] TANG, Y. *Computer aided design of twin screw compressors*. PhD thesis, University of Strathclyde, 1995.
- [22] TEN ASBROEK, N., AND REXWINKEL, G. Improved heat pump and process of heat pumping. *Frames Renewable Energy Solutions BV*, Patent application number N2016303.
- [23] THOMSEN, K., AND RASMUSSEN, P. Modeling of vapor–liquid–solid equilibrium in gas–aqueous electrolyte systems. *Chemical Engineering Science* 54, 12 (1999), 1787–1802.
- [24] TIAN, Y., YUAN, H., WANG, C., WU, H., AND XING, Z. Numerical investigation on mass and heat transfer in an ammonia oil-free twin-screw compressor with liquid injection. *International Journal of Thermal Sciences* 120 (2017), 175–184.
- [25] VAN DE BOR, D., INFANTE FERREIRA, C. A., AND KISS, A. A. Low grade waste heat recovery using heat pumps and power cycles. *Energy* 89 (2015), 864–873.
- [26] VAN DE BOR, D. M., AND INFANTE FERREIRA, C. A. Quick selection of industrial heat pump types including the impact of thermodynamic losses. *Energy 53* (2013), 312 322.
- [27] VAN DE BOR, D. M., INFANTE FERREIRA, C. A., AND KISS, A. A. Optimal performance of compression–resorption heat pump systems. *Applied Thermal Engineering 65*, 1 (2014), 219 225.
- [28] Vuik, C., van Beek, P., Vermeulen, F., and van Kan, J. *Numerical Methods for Ordinary Differential Equations*, second ed. Delft Academic Press, February 2015.

BIBLIOGRAPHY 105

[29] Wang, M., and Infante Ferreira, C. A. Absorption heat pump cycles with NH₃ – ionic liquid working pairs. *Applied Energy 204* (2017), 819 – 830.

- [30] ZAYTSEV, D. Development of wet compressor for application in compression-resorption heat pumps. PhD thesis, Delft University of Technology, (2003).
- [31] ZAYTSEV, D., AND INFANTE FERREIRA, C. A. Profile generation method for twin screw compressor rotors based on the meshing line. *International Journal of Refrigeration* 28, 5 (2005), 744–755.
- [32] ZIEGLER, B., AND TREPP, C. Equation of sate for ammonia-water mixtures. *International Journal of Refrigeration* (1984).
- [33] ZÜHLSDORF, B., JENSEN, J. K., AND ELMEGAARD, B. Heat pump working fluid selection—economic and thermodynamic comparison of criteria and boundary conditions. *International Journal of Refrigeration* 98 (2019), 500–513.